Evaluation of *RAGE* polymorphisms and glycated albumin peptides for the risk prediction of type 2 diabetes and diabetic nephropathy

by

Arvindkumar Chaurasiya
10BB16A26042

A thesis submitted to the
Academy of Scientific & Innovative Research
for the award of the degree of
DOCTOR OF PHILOSOPHY
in
SCIENCE

Under the supervision of
Dr. Mahesh J. Kulkarni

CSIR-National Chemical Laboratory, Pune

Academy of Scientific and Innovative Research
AcSIR Headquarters, CSIR-HRDC campus,
Sector 19, Kamla Nehru Nagar,
Ghaziabad, Uttar Pradesh-201002, India

2023

CERTIFICATE

This is to certify that the work incorporated in this Ph.D. thesis entitled ***"Evaluation of RAGE polymorphisms and glycated albumin peptides for the risk prediction of type 2 diabetes and diabetic nephropathy"***, submitted by ***Arvindkumar Chaurasiya*** to the Academy of Scientific and Innovative Research (AcSIR), in fulfillment of the requirements for the award of the Degree of ***Doctor of Philosophy in Science***, embodies original research work carried-out by the student. We further certify that this work has not been submitted to any other University or Institution in part or full for the award of any degree or diploma. Research materials obtained from other sources and used in this research work have been duly acknowledged in the thesis. Images, illustrations, figures, tables, *etc*., used in the thesis from other sources, have also been duly cited and acknowledged.

Mr. Arvindkumar Chaurasiya
Research Student
Date: 03/08/2023

Dr. Mahesh J. Kulkarni
Research Supervisor
Date: 03/08/2023

STATEMENT OF ACADEMIC INTEGRITY

I, Arvindkumar Chaurasiya, a Ph.D. student of the Academy of Scientific and Innovative Research (AcSIR) with Registration No. 10BB16A26042 hereby undertake that, the thesis entitled "Evaluation of *RAGE* polymorphisms and glycated albumin peptides for the risk prediction of type 2 diabetes and diabetic nephropathy" has been prepared by me and that the document reports original work carried out by me and is free of any plagiarism in compliance with the *UGC* Regulations on *"Promotion of Academic Integrity and Prevention of Plagiarism in Higher Educational Institutions (2018)"* and the CSIR Guidelines for "*Ethics in Research and in Governance (2020)".*

Signature of the Student

Mr. Arvindkumar Chaurasiya

Date: 03/08/2023

Place: CSIR-NCL, Pune

It is hereby certified that the work done by the student, under my/our supervision, is plagiarism-free in accordance with the UGC Regulations on *"Promotion of Academic Integrity and Prevention of Plagiarism in Higher Educational Institutions (2018)"* and the CSIR Guidelines for "*Ethics in Research and in Governance (2020)".*

Signature of the Supervisor

Dr. Mahesh J. Kulkarni

Date: 03/08/2023

Place: CSIR-NCL, Pune

DEDICATED TO MY BELOVED FAMILY & TO EVERYONE WHO INSPIRED ME

Acknowledgment

It has been quite a long journey for me as a Ph.D. scholar at CSIR-NCL. I would like to express my sincere gratitude to all those who have contributed to the completion of this thesis and during this journey filled with sweet and sour memories.

First and foremost, I would like to express my heartfelt thanks to my supervisor Dr. Mahesh J. Kulkarni, for his invaluable guidance, constant support, motivation, and funding that kept me going in my research work. His expertise in the subject matter and insightful feedback gave direction to this study. I am highly grateful for the liberty and flexibility rendered by him in designing and executing the research that made me work stress-free in the laboratory.

I am thankful to my Doctoral Advisory Committee (DAC) members Dr. H. V. Thulasiram, Dr. Dhanasekaran Shanmugam, and Dr. B. Santhakumari, for spending their valuable time monitoring the progress of my research work at DAC meetings. Their constructive criticisms, support, and guidance kept me on track in the right direction to complete my research work. I express my special thanks to Dr. Dhanasekaran Shanmugam; the discussions with him and his expert views were truly scientific, which encouraged me to read, think, write, and work meticulously and helped me complete the research work in an organized way. I am also very grateful to Dr. B. Santhakumari for her guidance and support for the mass spectrometry facility.

I acknowledge the contribution of our collaborator Dr. Abdulrahaman Momin from Bharati Vidyapeeth (DTU) Medical College, Pune, for providing clinical samples and helping with statistical and biochemical analysis. I would also like to thank our collaborators, Dr. Ambika G. Unnikrishnan and Dr. Shalbha Tiwari from Chellaram Diabetes Institute, Pune, for providing clinical samples. I extend my gratitude to Shweta Kahar, who coordinated for clinical sample collection at Chellaram Diabetes Institute, Pune. I am grateful to all the participants who voluntarily gave their blood samples for this research. I am also thankful to University Grants Commission for the financial assistance in the form of regular fellowship and contingency.

I would like to thank our past director Prof. Ashwini Kumar Nangia, and present director, Dr. Ashish Lele; our past chairs of the Biochemical Sciences Division, Dr. Archana Pundle and Dr. Ashok Giri; and present chair, Dr. Narendra Kadoo, for providing all necessary

infrastructure and facility. I recognize the tough time faced by the director and HODs in framing rules and regulations for ensuring the safety of all staff members and students during the Covid pandemic while at the same time trying to manage the execution of essential research activities.

Working at the workplace won't be enjoyable without friends. I would like to express my heartwarming thanks to all my seniors Dr. Arati Deshmukh, Dr. Reema Banarjee, Dr. Rubina Kazi, Sharda, Dr. Kedar Batkulwar, Dr. Jagadeeshaprasad, Dr. Shankuntala Kolewar, Dr. Gouri Patil, Dr. Rajeshwari Rathore, Dr. Prachi Walke, Dr. Vaibhav Pandya, and Dr. Sneha Bansode for their care and guidance. I am also grateful to all my current and past labmates, Shabda, Babasaheb, Yugendra, Akshay, Rashmi, Vinashya, Meera, Shiva, Preeti, Nikita, Sneha M., Amreen, Monika, Swaraj, Rajesh, and Rashda. Thank you for making the work environment comfortable, friendly, and caring. The encouragement and support on the professional front and the moments we cherished together on the personal front at the lab, tea breaks, parties, and trips occupy a deep place inside my heart. A special mention goes to Shakuntala and Rajeshwari, who taught me mass spectrometry so well, and I immensely benefitted from the discussions we had. It's not possible to mention the contributions of each of them, but I recognize the support of all of them. I also thank my friend Ajinkya for introducing me to nanopore sequencing and teaching me sample preparation.

It's impossible to excel at a profession without family support. I owe a lot to my family, who encouraged and helped me at every stage of my personal and academic life. I am incredibly grateful to my wife, Meera, who helped me immensely in my wet-lab work. Also, she looked after home so well that I could spend additional time at the lab and with the writing work. Without her support, finishing the research work faster wouldn't have been possible. I thank my parents for giving me emotional support and courage to pursue my dreams. I also thank my brothers and sisters, Pradeep, Neeraj, and Poonam, who stood by me on the personal front during this journey. I also owe my gratitude to my sister-in-law and mother-in-law for their help. I am blessed to have my cute little son Rudransh, whose mere presence motivates me and makes me smile.

I convey my heartfelt thanks to all those who helped me in my journey directly or indirectly. Lastly, I am thankful to Almighty God for blessings with good health and patience that led to the successful completion of this piece of work.

Table of Contents

List of Figures

List of Tables

Abbreviations

ADA	American Diabetes Association
GDM	Gestational diabetes mellitus
GAD	Glutamic acid decarboxylase
ZnT8	Zinc transporter 8
FPG	Fasting plasma glucose
PPG	Postprandial plasma glucose
OGTT	Oral glucose tolerance test
AGE	Advanced glycation end product
DFL	Deoxyfructosyl-lysine
CML	Carboxymethyl-lysine
CEL	Carboxyethyl-lysine
MOLD	Methylglyoxal-lysine dimer
GOLD	Glyoxal-lysine dimer
GO	Glyoxal
MGO	Methylglyoxal
3-DG	3-deoxyglucosone
RAGE	Receptor for advanced glycation end products
HMGB1	High mobility group protein B1
N-RAGE	N-truncated RAGE
sRAGE	Soluble RAGE
esRAGE	Endogenous secretory RAGE
JAK/STAT	Janus kinase/signal transducer and activator of transcription
MAPK	Mitogen-activated protein kinase
Ras/MEK/ERK1/2	Ras/mitogen-activated protein kinase/ERK1/2
SAPK/JNK	Stress-activated protein kinase/c-Jun amino-terminal kinase
GSK-3β	Glycogen synthase kinase 3β
NF-κB	Nuclear factor kappa B
AP-1	Activator protein 1
Egr-1	Early growth response-1
IκB	Inhibitor of κB
IL-1β	Interleukin-1β
IL-6	Interleukin-6
TNF-α	Tumor necrosis factor-α
BMI	Body mass index
ESRD	End-stage renal disease
eGFR	Estimated glomerular filtration rate
MS	Mass spectrometry
PTM	Post-translational modification
MRM	Multiple Reaction Monitoring
PRM	Parallel Reaction Monitoring
MRM-HR	High-resolution multiple reaction monitoring
Q-TOF	Quadrupole time-of-flight

SNP	Single nucleotide polymorphism
RFLP	Restriction fragment length polymorphism
ddNTPs	Dideoxyribunucleotides
dNTPs	Deoxynucleotides
NGS	Next-generation sequencing
CCD	Charge-coupled device
TGS	Third-generation sequencing
SMRT	Single molecule real-time
HSA	Human serum albumin
DTT	Dithiothreitol
IAA	Iodoacetamide
FA	Formic acid
ACN	Acetonitrile
DM	Type 2 diabetes subjects without nephropathy
DN	Type 2 diabetes subjects with nephropathy
ROC	Receiver operating characteristic
FBG	Fasting blood glucose
PPBG	Postprandial blood glucose
LC-MS	Liquid chromatography-mass spectrometry
AUC	Area under curve
ANOVA	One-way analysis of variance
PCR-RFLP	Polymerase chain reaction-restriction fragment length polymorphism
ONT	Oxford nanopore technology
MDA	Malondialdehyde
HOMA-IR	Homeostatic model assessment for insulin resistance
CRP	C-reactive protein
UACR	Urinary albumin-to-creatinine ratio
HDL	High-density lipoprotein
SD	Standard deviation
OR	Odds ratio
CI	Confidence interval

Chapter 1

Introduction

Chapter 1 : Introduction

1.1 Diabetes

Diabetes mellitus, commonly known as diabetes, is a set of diverse metabolic diseases in which patients have chronic high blood sugar levels. Diabetes is manifested when the body cannot produce adequate insulin or efficiently respond to insulin. The β-cells in the pancreatic islets of Langerhans synthesize and secrete insulin, a major anabolic hormone. Insulin promotes the internalization of blood glucose by various insulin-sensitive cells for energy generation and storage. When there is reduced insulin secretion or resistance to insulin action, blood glucose is not sufficiently utilized, and the accumulation of blood glucose results in hyperglycemia.[1] Increased appetite, increased thirst, frequent urination, and weight loss are the prominent symptoms of diabetes.[2] Diabetes is a global health concern as diabetes-associated morbidity and mortality burden the health infrastructure and economy.

1.1.1 Epidemiology

Diabetes and its complications are a leading cause of death in non-communicable diseases. Diabetes and diabetic complications accounted for 6.7 million, corresponding to 12.2% of adult deaths in 2021 globally.[1, 3] The American Diabetes Association (ADA) reports that the prevalence of diabetes has been rising rapidly. The number of diabetes cases climbed from 151 million in 2000 to 537 million in 2021 and is expected to increase further at a rapid pace (Figure 1.1). China and India have the maximum number of diabetic adults. 74.2 million or 9.6% adult population of India was diabetic in 2021 and is estimated to increase to about 125 million in 2045. Diabetes and its complications claimed 0.6 million lives in India in 2021. More than half of the diabetic cases (39.4 million) in India remained undiagnosed.[1] Therefore, there is an urgent need to control the menace of diabetes by creating awareness that will enable early detection and prevention of diabetes. Also, cheap and improved healthcare access will help mitigate the implications of diabetes and its complications.

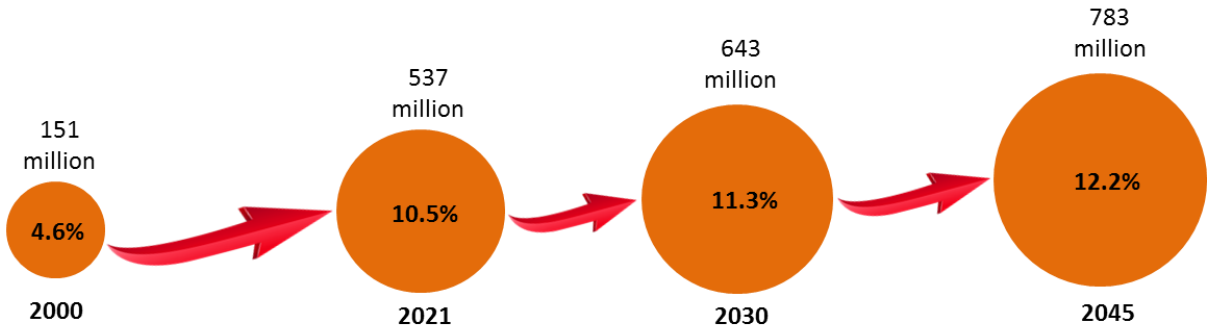

Figure 1.1 Past and predicted future prevalence of diabetes worldwide
The prevalence of diabetes has increased rapidly worldwide and will continue to increase in the future.[1]

1.1.2 Classification of diabetes

According to ADA, diabetes is categorized into four types: type 1 diabetes, type 2 diabetes, gestational diabetes mellitus (GDM), and other specific types of diabetes.[4]

1.1.2.1 Type 1 diabetes

Type 1 diabetes, or insulin-dependent diabetes, comprises about 5-10 % of all diabetes cases.[5] It results from insufficient or no insulin secretion, which causes high blood sugar levels. In type 1 diabetes, the autoimmune system destroys the β-cells in the pancreatic islets of Langerhans, resulting in decreased insulin secretion. The autoimmune markers for type 1 diabetes are autoantibodies to islet cells, insulin, glutamic acid decarboxylase (GAD), tyrosine phosphatases IA-2 and IA-2β, and zinc transporter 8 (ZnT8).[6] Due to the fact that type 1 diabetes typically occurs in childhood and adolescence, it is also referred to as juvenile-onset diabetes. However, it can also happen at any age.[5] Environmental factors and genetic predisposition significantly contribute to developing type 1 diabetes.[2] Type 1 diabetes cannot be prevented, and individuals with type 1 diabetes require exogenous insulin administration to compensate for the low insulin level in the blood.[1]

1.1.2.2 Type 2 diabetes

Most cases of diabetes are type 2, and it comprises about 90-95 % of all diabetes cases. It is also referred to as adult-onset or insulin-independent diabetes. Insulin resistance is the primary causal factor that results in a decreased response of body cells to insulin. Notably, most type 2 diabetic people also have insulin deficiency.[5] Insulin insufficiency in type 2 diabetes is attributed to a reduction in β-cell mass and β-cell function.[7] The development of hyperglycemia is slow, and it takes years to develop noticeable symptoms. Hence, type 2 diabetes often remains undetected for years.[5] Therefore, the condition may keep worsening

and heighten the risk of diabetic complications development. Environmental factors immensely contribute to the development of type 2 diabetes. Diabetes is a lifestyle-associated disease, and a poor lifestyle is mainly attributed to the development of diabetes, which includes an unhealthy diet and lack of physical exercise. Old age, prediabetes, hypertension, dyslipidemia, history of GDM, familial diabetes history, obesity, smoking, and drinking alcohol are the major risk factors for developing type 2 diabetes.[1, 5, 8] Though it is well known that genetic predisposition plays a significant role in type 2 diabetes development, the complex causal genetic factors are yet to be fully understood.[5] The development of type 2 diabetes is preventable, or it can be delayed, unlike type 1 diabetes.[1] It is typically treated by weight reduction, exercise, and hypoglycemic agents, lowering blood glucose levels.[5]

1.1.2.3 Gestational diabetes mellitus

Gestational diabetes mellitus (GDM) is characterized by hyperglycemia developed during pregnancy and complicates about 16.7% of all pregnancies.[1] GDM poses serious health risks to both mother and child. Macrosomia is one of the most typical adverse consequences of GDM. Gestational diabetes is also associated with congenital malformation, birth injuries, preterm birth, shoulder dystocia, cesarean delivery, preeclampsia, and neonatal hypoglycemia.[9-11] Though GDM generally gets resolved after delivery, it can still have adverse consequences in the future; for example, both the mother and the child become more susceptible to developing type 2 diabetes and cardiovascular diseases.[1] Older maternal age, obesity, history of GDM, familial diabetes history, polycystic ovary syndrome, and sedentary lifestyle are risk factors for GDM.[2] Insulin resistance induced by hormonal changes during pregnancy is the primary cause of GDM.[12] GDM is diagnosed at the 24-28th week of gestation by oral glucose tolerance test.[2]

1.1.2.4 Other specific types of diabetes

Other specific diabetes types include diabetes developed due to genetic defects of β-cell (maturity-onset diabetes of the young characterized by the onset of hyperglycemia before 25 years of age), genetic defects in insulin action, exocrine pancreas disease (any condition that damages the pancreas), endocrinopathies (caused by an overproduction of hormones counteracting insulin activity) and infections (viral infections that cause β-cell damage such as congenital rubella, coxsackievirus B, cytomegalovirus, adenovirus, and mumps), drug or chemical-induced diabetes (that affect insulin secretion), rare types of immune-mediated diabetes and other genetic syndromes occasionally associated with diabetes.[4, 6]

1.1.3 Diagnosis of diabetes

The diagnosis of diabetes is clinically made by measuring plasma glucose (fasting plasma glucose or postprandial plasma glucose) or HbA_{1c} (glycated hemoglobin), as shown in Table 1.1. In order to diagnose diabetes, plasma glucose has long served as the gold standard. Fasting plasma glucose (FPG) is measured after at least an 8 h overnight fast. Measurement of FPG is not expensive and is widely used for diabetes diagnosis. However, there is a lack of reproducibility in this test. Also, FPG can change in an individual from day to day and can be altered due to diet, prolonged fasting, exercise, and stress.[13]

Postprandial plasma glucose (PPG) is measured by measuring plasma glucose concentration 2 h after meals. The other test is the oral glucose tolerance test (OGTT), in which an overnight fast of 10 to 16 h is necessary, and the glucose concentration is measured in the plasma sample collected 2 h after the consumption of 75 g glucose. It is a sensitive indicator of the risk of diabetes as 2 h plasma glucose increases before the increase in FPG. However, similar to FPG, 2 h plasma glucose has poor reproducibility, and there is a high intraindividual variability which is more than FPG. Therefore, due to inconvenience, cost, and lack of reproducibility, FPG is preferred to OGTT for diagnosis of diabetes.[5, 13]

HbA_{1c} is formed when glucose is non-enzymatically attached to the valine at the N-terminus of the hemoglobin β-chain. While plasma glucose reflects instantaneous glycemic status, HbA_{1c} shows the average glycemic status of the past 2-3 months because erythrocytes have a life span of 120 days. HbA_{1c} strongly correlates with microvascular complications and predicts the risk of their development. HbA_{1c} is regarded as the current gold standard for evaluating glycemic control. Unlike plasma glucose, HbA_{1c} is not affected by recent diet, exercise, or stress. It has better reproducibility than plasma glucose, and subjects need not be fasting. However, HbA_{1c} has a few limitations as well. It is affected by conditions that change erythrocyte lifespan, such as hemolytic disease, recent blood loss or transfusion, and iron deficiency anemia. Pregnancy, HIV infection, and some hemoglobin variants also affect HbA_{1c}. Also, HbA_{1c} measurement is costlier than plasma glucose measurements.[6, 13, 14]

Table 1.1 ADA criteria for the diagnosis of diabetes

Diagnostic criterion	Healthy	Prediabetes	Diabetes
Fasting plasma glucose (mg/dL)	≤ 99	100-125	≥ 126
Postprandial plasma glucose (mg/dL)	≤ 139	140-199	≥ 200
OGTT (mg/dL)	≤ 139	140-199	≥ 200
HbA_{1c} (%)	≤ 5.6	5.7-6.4	≥ 6.5

[Table adapted from[5]]

1.2 Glycation reaction, advanced glycation end product (AGE) formation, and interaction with ligand

1.2.1 Glycation and advanced glycation end product formation

AGEs are a group of heterogeneous compounds produced by the non-enzymatic reaction between reducing sugars and amino groups of proteins. Louis Camille Maillard was the first to describe this non-enzymatic reaction, wherein the heating of amino acids in the presence of reducing sugars resulted in the formation of brown-colored compounds. Hence this reaction is also known as the Maillard reaction or non-enzymatic browning.[15, 16] The Maillard reaction is vital in the food industry as it produces several compounds that contribute to odors and flavors but reduce nutritional value. Later in the 1960s, a Maillard reaction-like process was discovered under physiological conditions when an increased level of glycated hemoglobin was observed in diabetic patients, and this reaction is commonly known as glycation. Since then, a number of AGEs and their harmful physiological effects have been described.[16]

A schematic illustration of the glycation reaction is depicted in Figure 1.2. The non-enzymatic reaction between the free amino group of proteins (particularly lysine and arginine residues and free amino terminal of proteins) and the carbonyl group of reducing sugars form an unstable Schiff's base, which goes through structural rearrangement to generate relatively stable early glycation product, chemically known as deoxyfructosyl-lysine (DFL). DFL is widely known as an Amadori product that reacts with proteins to cross-link them. The protein cross-links then undergo numerous reactions, including oxidation, dehydration, cyclization, and breakdown, to form stable advanced glycation end products, known as AGEs.[15-17] The physiological presence of several AGEs, such as carboxymethyl-lysine (CML), carboxyethyl-lysine (CEL), methylglyoxal-lysine dimer (MOLD), glyoxal-lysine dimer (GOLD),

pentosidine and pyrraline has been described.[18, 19] Amadori products can also undergo dehydration and rearrangement to form dicarbonyl compounds, e.g., glyoxal (GO), methylglyoxal (MGO), and 3-deoxyglucosone (3-DG), which are highly reactive. GO and MGO are also formed as a by-product of glycolysis. These dicarbonyl compounds are AGE precursors, which react with proteins to form various AGEs. The reactive dicarbonyl compounds can also be formed by other pathways, e.g., the oxidative fragmentation of Schiff's base (Namiki pathway) and auto-oxidation of glucose (Wolff pathway). Since diabetic patients have persistent hyperglycemia, glycation occurs at a faster pace in diabetic patients. Thus, glycated proteins and AGEs increasingly form and accumulate in hyperglycemic conditions.[16] AGEs' accumulation on various plasma proteins has been reported,[20] especially long-lived proteins such as hemoglobin, tissue collagen, and lens crystalline.[15, 17] On the other hand, glycated albumin has the largest share of glycated plasma proteins due to the highest plasma concentration and a large number of glycation-sensitive lysine and arginine residues.[20, 21] AGEs also cross-link the proteins, adversely affecting their functions or rendering them functionally inactive.[16] Also, AGEs can interact with their receptors present on the cell surface, i.e., receptor for advanced glycation end products (RAGE), and this interaction initiates a downstream signaling pathway that results in various deleterious outcomes (described later in section 1.2.3).

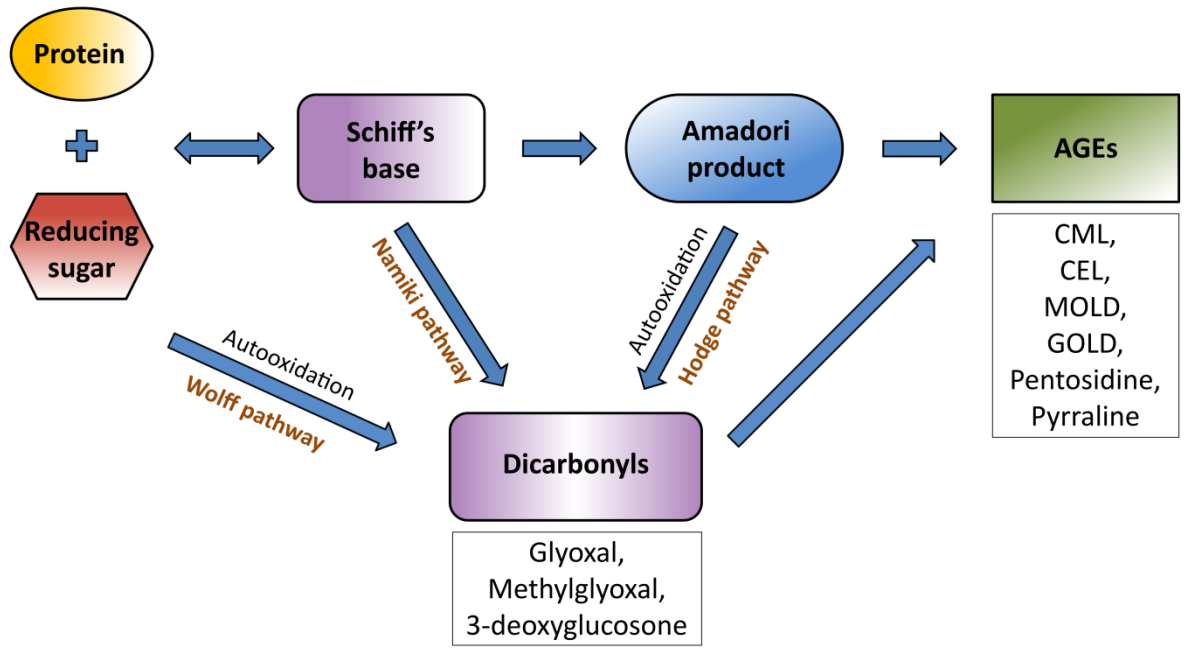

Figure 1.2 Formation of AGEs through glycation

The reaction of reducing sugars with free amino groups of proteins leads to the formation of early and several advanced glycation end products through a series of non-enzymatic reactions. Several reactive dicarbonyl compounds can be formed from reducing sugars or early glycation products by different

pathways which serve as AGE precursors.

1.2.2 RAGE

RAGE is a transmembrane receptor found on the membrane of nearly all cells at low levels. However, it has a high expression level in the lung. RAGE belongs to the immunoglobulin superfamily and can bind to several ligands. RAGE was first described as a receptor for AGEs.[22] Besides AGEs, RAGE can also bind to several ligands, e.g., S-100/cangrulins, high mobility group protein B1 (HMGB1), β-amyloid peptides, Mac-1, lysophosphatidic acid, complement protein C1q, phosphatidylserine and mitochondrial transcription factor A.[19, 23-25]

The *RAGE* gene, coding for the RAGE protein, is highly polymorphic and is located within the major histocompatibility complex III locus on chromosome 6. Twelve alternatively spliced transcripts coding for different RAGE isoforms and one non-coding variant have been reported (ncbi.nlm.nih.gov/genbank, Oct 2022). The longest isoform of RAGE is composed of 420 amino acids. In contrast, the most predominant isoform of RAGE comprises 404 amino acids. RAGE contains an extracellular variable domain, two extracellular constant domains, one transmembrane domain, and one intracellular domain. The extracellular variable domain of RAGE interacts with its ligands.[23]

Figure 1.3 shows the schematic representation of full-length RAGE and the generation of soluble RAGE isoforms. Three major RAGE isoforms are also expressed in addition to full-length RAGE. The N-RAGE (N-truncated RAGE) is membrane-bound, like full-length RAGE; however, it lacks the extracellular variable domain and cannot bind to ligands. The other two isoforms are C-truncated RAGE, lacking the transmembrane and cytoplasmic domains. One of the C-truncated RAGE, sRAGE (soluble RAGE), is produced when the proteolytic enzymes, such as matrix metalloproteinases, cleave the full-length RAGE, whereas esRAGE (endogenous secretory RAGE) is encoded by alternatively spliced full-length RAGE transcript. sRAGE and esRAGE freely circulate in the blood and can bind to AGEs but cannot induce intracellular signaling as they lack transmembrane and intracellular domains. Thus sRAGE and esRAGE act as decoy receptors of AGEs and competitively inhibit the binding of AGEs with RAGE.[26]

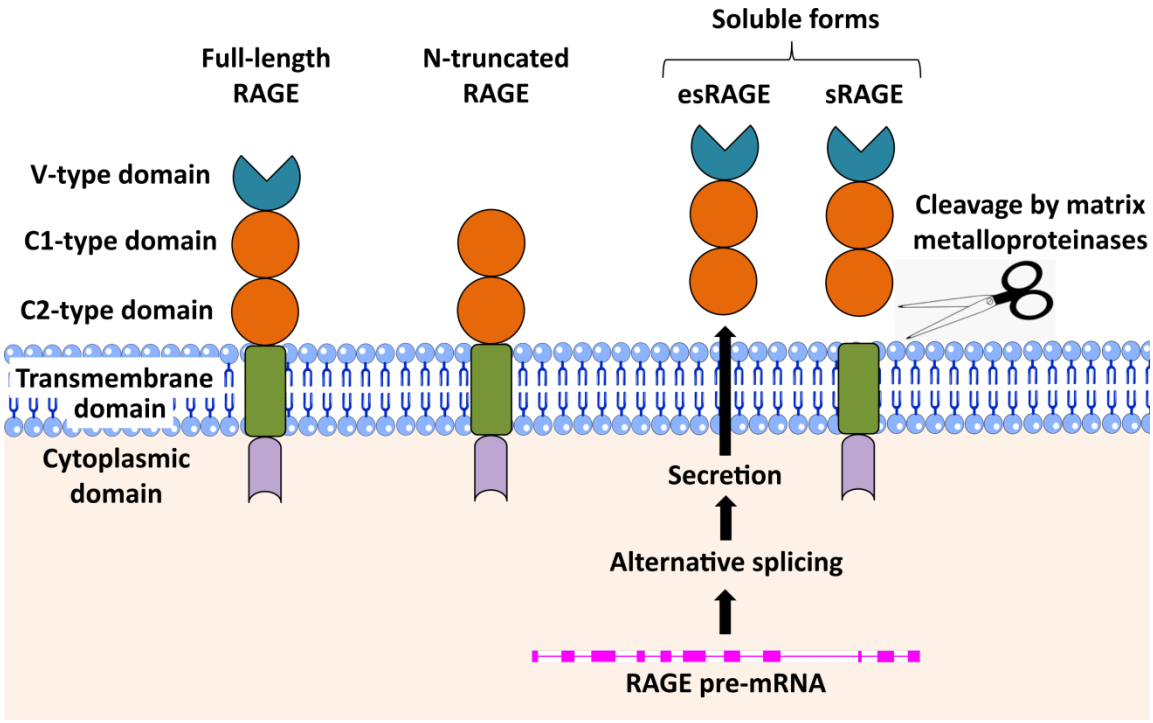

Figure 1.3 Structure of full-length RAGE and its isoforms
A full-length RAGE receptor consists of one V-type extracellular, two C-type extracellular, one transmembrane, and one cytoplasmic domain. N-truncated RAGE isoform is devoid of a V-type domain, whereas C-truncated RAGE isoforms, esRAGE (formed by alternative splicing of RAGE transcript) and sRAGE (formed by proteolytic cleavage of the extracellular domains), are devoid of transmembrane and cytoplasmic domains. C-truncated RAGE isoforms are not membrane-bound. [Figure modified and adapted from[26]]

RAGE expression is increased in many inflammatory diseases.[25, 27] Similarly, *RAGE* gene polymorphisms have been reported to be linked with the risk of developing various diseases such as autoimmune disease, diabetes, cancer, chronic obstructive pulmonary disease, and Crohn's disease.[23]

1.2.3 AGE-RAGE interaction and signaling pathways

Interaction of RAGE with its different ligands triggers different downstream signaling pathways depending on the ligand type and the cell type. Therefore, the RAGE network is very complex. RAGE-ligand interaction induces diverse cellular signaling cascades, e.g., janus kinase/signal transducer and activator of transcription (JAK/STAT), PI3K/AKT, NADPH oxidase, mitogen-activated protein kinase (MAPK)/P38, Ras/mitogen-activated protein kinase/ERK1/2 (Ras/MEK/ERK1/2), stress-activated protein kinase/c-Jun amino-terminal kinase (SAPK/JNK), small GTPase Cdc42/Rac1 and glycogen synthase kinase 3β (GSK-3β). After that, these pathways activate many transcription factors, including nuclear factor kappa B (NF-κB), STAT3, activator protein 1 (AP-1), and early growth response-1

(Egr-1), which in turn, increase the expression of many genes.[25]

Figure 1.4 depicts the AGE-RAGE interaction and the activated downstream signaling pathways. The downstream signaling activated by AGE-RAGE interaction is mediated via four pathways, namely, JAK2/STAT1, PI3K/AKT, MAPK/ERK, and NADPH oxidase/ROS.[15] All of these signaling pathways activate transcription factor NF-κB. In the inactivated state, NF-κB is located in the cytosol through binding to its inhibitory protein called inhibitor of κB (IκB). RAGE-mediated signaling activates the enzyme IκB kinase, which phosphorylates IκB, leading to ubiquitin-mediated degradation of the inhibitor. Once activated, NF-κB gets translocated into the nucleus, where it induces the expression of target genes of oxidative stress and proinflammatory cytokines, e.g., interleukin-1β (IL-1β), interleukin-6 (IL-6), and tumor necrosis factor-α (TNF-α).[28] This downstream signaling also increases the expression of RAGE, creating a positive feedback loop.[29] The adverse consequences of AGE-RAGE signaling play a significant role in developing diverse diseases such as diabetes and its complications, cardiovascular disease, neurodegenerative diseases, inflammation, and cancer.[15]

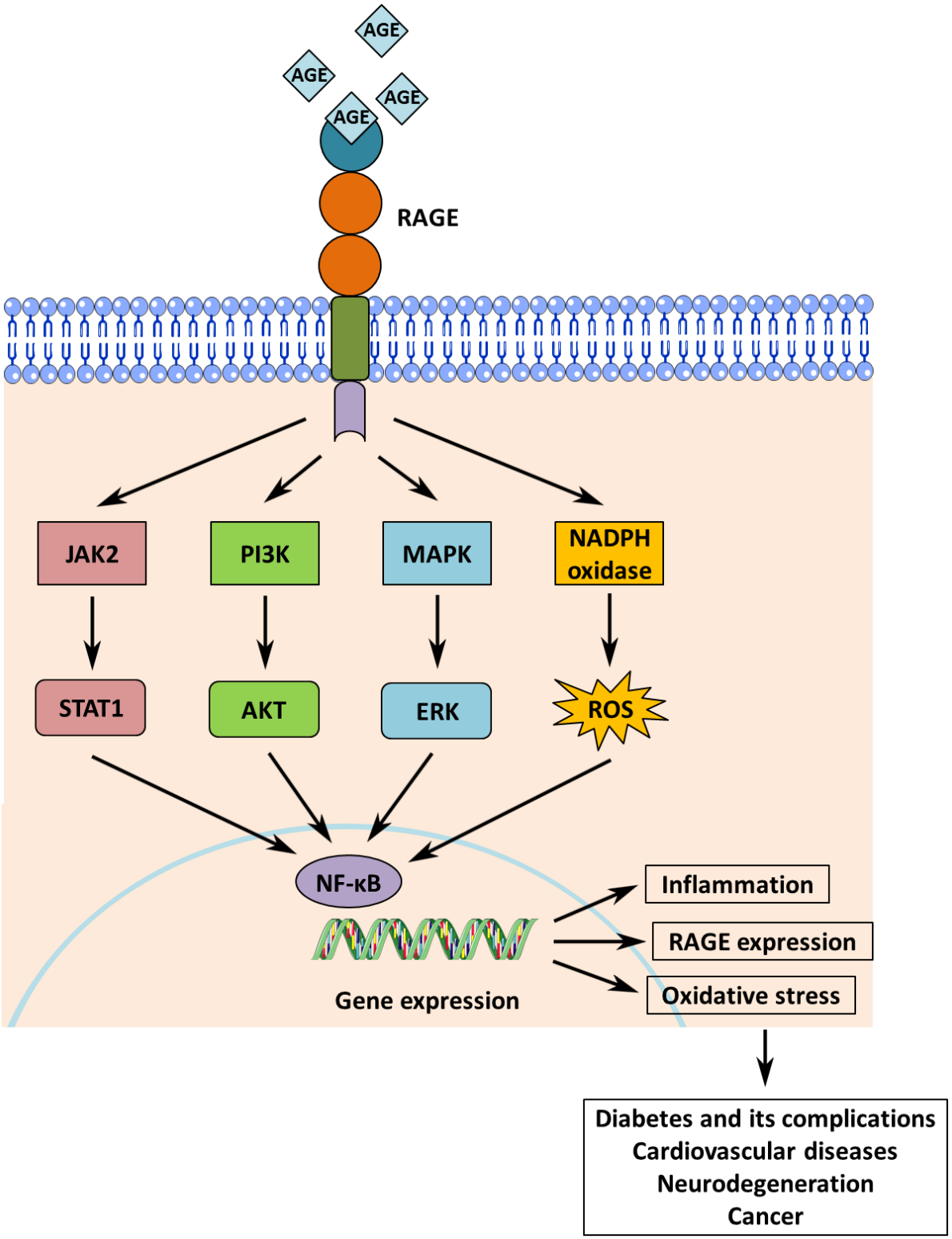

Figure 1.4 Schematic representation of AGE-RAGE interaction and signaling pathways
Interaction of AGEs with RAGE induces several downstream signaling pathways that activate transcription factor NF-κB and ROS production. Activated NF-κB translocates to the nucleus, where it activates the transcription of its target genes that increase inflammation, oxidative stress, and RAGE expression resulting in the pathogenesis of several diseases, especially diabetes and its complications. [Figure modified and adapted and modified from[15]]

Given that RAGE is crucial to the pathogenesis of several diseases, targeting RAGE to block the AGE-RAGE axis, e.g., by using soluble forms of RAGE or anti-RAGE antibodies, could be one of the preventive and therapeutic strategies to prevent the development and progression of these diseases.[19, 30-32]

1.3 Diabetic complications

Chronic hyperglycemia in diabetes increases the generation and buildup of AGEs, which plays a significant role in the development and progression of several diabetic complications.[33] AGEs are known to induce insulin insensitivity and impaired β-cell function, thus further worsening diabetic conditions. AGE modification of cellular proteins and cross-linking adversely affects their structures and functions, thereby damaging the cells directly.[34] Also, AGE-RAGE interaction-induced inflammation and oxidative stress are principal pathogenic factors that damage tissues and thereby promote the onset of several diabetic complications.[16]

The prevalence of diabetic complications is rising concurrently with the prevalence of diabetes. These complications are broadly divided into microvascular and macrovascular complications.

1.3.1 Microvascular complications

Microvascular complications arise due to damage to small blood vessels.[35] There are three prominent microvascular complications, namely, diabetic retinopathy, diabetic neuropathy, and diabetic nephropathy, which damage the eyes, nervous system, and renal system, respectively.

1.3.2.1 Diabetic retinopathy

Diabetic retinopathy is the principal causal factor for impaired vision and blindness in people aged 20-74 years.[36] Diabetic retinopathy develops in over half of diabetic patients in their lifetime.[37, 38] Chronic hyperglycemia leads to oxidative stress, protein kinase C activation, inflammation, accumulation of AGEs and sorbitol, and elevated renin-angiotensin system. These biochemical and physiological changes are primarily responsible for microvascular damage that causes diabetic retinopathy. A longer diabetes duration, hyperglycemia, and hypertension increase the risk of developing diabetic retinopathy. Controlling blood pressure and glucose levels lowers the risk and severity of diabetic retinopathy.[39] Additional factors

increasing the risk of developing diabetic retinopathy are dyslipidemia, smoking, higher body mass index (BMI), ethnicity, pregnancy, sex (female), and puberty.[8, 36, 40] Diabetic retinopathy also increases the likelihood of macrovascular complication development.[36] Non-proliferative and proliferative diabetic retinopathy are the two main types of diabetic retinopathy. The first clinical sign of non-proliferative diabetic retinopathy is the formation of small bulges in the retinal capillary walls, or microaneurysms.[40] Non-proliferative diabetic retinopathy can gradually progress from mild to severe with characteristic changes in the eye, including ischemia. New blood vessels are formed (neovascularization) in the retina to compensate for ischemia-induced hypoxia, and this stage is known as proliferative diabetic retinopathy. Neovascularization is followed by hemorrhage and other pathological changes that cause retinal detachment, resulting in blindness.[39, 40] Fundus photography and optical coherence tomography are commonly used for the diagnosis of diabetic retinopathy.[36, 41] Most blindness cases due to diabetic retinopathy can be prevented if detected and treated early.[8] ADA recommends annual screening for diabetic retinopathy in individuals with type 2 diabetes.[41]

1.3.2.2 Diabetic neuropathy

Diabetic neuropathy is characterized by the loss of sensory functions in the extremities of the limbs due to damage to the peripheral and autonomic nervous systems. Loss of senses begins distally in the lower limbs. Diabetic neuropathy develops in over half of diabetic patients in their lifetime, and about 30-50 % of diabetic neuropathy patients experience neuropathic pain in the feet.[42] Diabetic neuropathy can cause foot ulceration, followed by gangrene and limb amputation.[43, 44] Diabetic neuropathy is responsible for 50-75 % of non-traumatic amputations,[42] most of which are preventable.[44] Diabetic neuropathy is associated with erectile dysfunction, impaired wound healing, and cardiovascular diseases observed in diabetic patients.[43, 45] Duration of diabetes and glycemic level are the main risk factors for diabetic neuropathy. Other risk factors include hypertension, dyslipidemia, obesity, smoking, alcohol consumption, and advanced age. Diabetic neuropathy symptoms include numbness, tingling, burning, pain, weakness, and unsteadiness, starting in the digits of the lower and upper limbs and progressing proximally over the years.[42, 45] Diabetic neuropathy may remain asymptomatic for years after the onset of diabetes.[44, 46] Diabetic neuropathy is diagnosed by testing for a decreased sensation of the pinprick, temperature, and vibration. ADA recommends to screen for diabetic neuropathy at diagnosis and annually in type 2 diabetic patients.[41] Glycemic control and exercise help in the prevention and halting of the

progression of diabetic neuropathy.[42, 45]

1.3.2.3 Diabetic nephropathy

Diabetic nephropathy is a major diabetic complication, and it affects about 20-40 % of diabetic people globally.[47] Glomerular capillaries in the nephron (a filtration unit of the kidney) are responsible for the filtration of blood.[48] In diabetic nephropathy, the glomerular filtration rate is gradually decreased, and therefore urinary blood proteins are excreted at a higher rate, called proteinuria.[49, 50] Microalbuminuria is the earliest sign of diabetic nephropathy, in which a slight increase in urinary protein excretion (urinary albumin excretion of 30-299 mg/24 h) is observed. It is diagnosed in three ways, as shown in Table 1.2. 24 h urine collection is considered the gold standard for urinary albumin assessment. However, the albumin to creatinine ratio in random spot urine samples is commonly used for diagnosing diabetic nephropathy as it is cost-effective, easy to measure, and has similar diagnostic accuracy as the 24 h urine collection.[51, 52] Further progress in diabetic nephropathy leads to an advanced stage called macroalbuminuria, characterized by an abnormal increase in urinary protein excretion (≥ 300 mg/24 h) and is also known as overt nephropathy.[53] If the renal function further worsens, the kidneys can no longer support adequate blood filtration. This stage is known as end-stage renal disease (ESRD), and the patient needs renal dialysis or a transplant to survive at this stage.[54]

Table 1.2 Diagnosis of diabetic nephropathy

Category	Spot collection (µg/mg creatinine)	24 h collection (mg/24 h)	Timed collection (µg/min)
Normal	< 30	< 30	< 20
Microalbuminuria	30-299	30-299	20-199
Macroalbuminuria	≥ 300	≥ 300	≥ 200

[Table adapted from[50]]

The pathogenesis of diabetic nephropathy involves several pathological changes in the kidneys. Nearly all cell types of the kidney are affected by hyperglycemia.[43, 55] There is mesangial cell proliferation and hypertrophy, an increase in extracellular mesangial matrix produced by the mesangial cells, thickening of glomerular basement membrane, inflammatory cell recruitment in glomerulus and tubulointerstitium, tubular hypertrophy, and tubulointerstitial fibrosis.[55, 56] Loss of podocytes, a component of the filtration slit, and

abnormal changes in the shape of podocytes adversely affect glomerular filtration.[57]

In part, hyperglycemia and the resultant elevation in the level of AGEs cause an increase in the extracellular matrix.[55] Various pathways, including oxidative stress, the rennin-angiotensin-aldosterone system, and inflammation, are involved in developing and progressing diabetic nephropathy.[58] Additional factors that increase diabetic nephropathy risk are hypertension, obesity, advanced age, race, dyslipidemia, insulin resistance, and smoking.[56, 58, 59] Genetic predisposition also contributes to developing diabetic nephropathy.[56, 59] Maintaining blood pressure below 130/80 mmHg, HbA_{1c} below 7 %, treating dyslipidemia (LDL < 100 mg/dL), and renin-angiotensin-aldosterone system blockage using drugs can prevent the onset of diabetic nephropathy or delay the progression to advanced stages.[56, 58, 59] ADA recommends annual screening for urinary albumin and estimated glomerular filtration rate (eGFR) in type 2 diabetic patients and twice annually for macroalbuminuria patients.[41]

1.3.2 Macrovascular complications

In diabetic macrovascular complications, large blood vessels are affected.[35] Diabetic people are at four-times likelihood of developing cardiovascular disease. Atherosclerosis, myocardial infarction, and stroke are the major disorders associated with cardiovascular disease.[60] Cardiovascular disease accounts for up to 65 % of deaths of diabetic patients.[8] Diabetic patients are at a greater risk of heart attack, which is a major reason for death due to cardiovascular events in people with diabetes. Diabetes also increases the risk of stroke, another significant reason for mortality in diabetic people.[35] Though it is unclear how hyperglycemia is associated with cardiovascular disease in diabetic people,[8] atherosclerosis is quite common in diabetic patients.[61] The pathophysiology of diabetic macrovascular complications is largely driven by atherosclerosis which causes constriction of the artery walls.[60] The significant risk factors for cardiovascular disease are hyperglycemia, hypertension, obesity, dyslipidemia, and smoking.[35, 62]

1.4 Importance of early detection of diabetes and its complications

Just like diabetes, diabetic complications develop slowly, often taking years to manifest clinically .[1] Without preventive measures and treatment, diabetic complications can progress and lead to advanced stages that can result in severe consequences, such as the loss of vision,

limbs, kidneys, or even death. However, if diabetes and its complications are appropriately managed, their adverse outcomes can be prevented or delayed.[1] Therefore, detecting diabetes and diabetic complications at an early stage is very important.

1.5 Risk prediction of type 2 diabetes and diabetic nephropathy

Besides early detection, risk prediction of type 2 diabetes and its complications would help resort to early preventive measures. Diabetic nephropathy causes the progressive loss of kidney functions over the years. Even though microalbuminuria is the earliest sign of diabetic nephropathy development, the complication is already established, causing kidney damage during the asymptomatic initial stages.[53] Similarly, type 2 diabetes often remains undetected for several years due to a lack of symptoms.[5] Hence there is a need for markers that can predict the risk of type 2 diabetes and diabetic nephropathy. Since hyperglycemia is the root cause of the development of several diabetic complications, including diabetic nephropathy, early measurement of glycemic change may help in predicting their development. Plasma is a rich source of disease markers. Hence, the glycation level on different plasma proteins, mainly albumin, may be helpful in measuring glycemic status[20] and further evaluating them for diabetic nephropathy risk prediction. Recently, glycated albumin has been increasingly evaluated for predicting the risk of diabetic nephropathy due to the advantages it has over other glycated proteins.[63, 64] Albumin is the most prevalent plasma protein having a half-life of 19 days; hence glycated albumin reflects the glycemic status of the past 2-3 weeks.[65] Thus, glycated albumin can be a good marker to assess type 2 diabetes risk and diabetic nephropathy.

There is ample evidence that some individuals are genetically prone to the onset of type 2 diabetes and its complications. This genetic predisposition can be due to expression level changes of certain genes, epigenetic changes, or polymorphisms in specific genes.[66, 67] Polymorphisms can affect the translated protein's structure or gene expression in various ways.[68, 69] Therefore certain gene polymorphisms may alter the disease susceptibility in the mutant population for developing type 2 diabetes and diabetic nephropathy. If the genetic cause of the differential vulnerability to type 2 diabetes and diabetic nephropathy is established precisely, it can be used as a risk prediction marker. Such risk prediction markers can be highly useful in identifying individuals at high risk of developing type 2 diabetes and diabetic nephropathy, which can, in turn, help to resort to early preventive measures by susceptible individuals to prevent or slow the development of type 2 diabetes and diabetic

nephropathy.

1.6 Mass spectrometry for the quantification of PTMs and glycated peptides

Mass spectrometry (MS) is an analytical technique to detect and identify molecules by measuring their mass-to-charge ratio with high sensitivity and specificity. Typically, mass spectrometers have three major components, i.e., ion source, mass analyzer, and detector. The ion source converts the analyte molecules into ionic form, followed by separation according to their mass-to-charge ratio by the mass analyzer and detection by the detector. Most mass spectrometers used nowadays are tandem mass spectrometers which have an additional mass analyzer. The first mass analyzer in tandem MS allows for the selection of specific precursor ions. The selected precursor ions get fragmented in the collision cell upon collision with an inert gas. The fragment ions generated are then analyzed by the second mass analyzer. This approach leads to the accurate identification of analytes. Mass spectrometers are widely used in the research milieu for the detection, identification, and quantification of proteins and metabolites in diverse sample types. In fact, in recent years, MS has found applications in clinical diagnosis.[70]

Post-translational modification (PTM) of proteins refers to any modifications of the protein after its biosynthesis. Post-translational modifications on proteins orchestrate a diverse biological function. Phosphorylation, acetylation, methylation, glycosylation, and ubiquitination are among the most common PTMs in an organism. PTMs are involved in regulating numerous cellular processes such as aging, cell signaling, and modulation of protein-protein interaction.[71-73] The modification states of proteins and the site of PTM modification determine the specific tasks, e.g., gene expression can be either activated or repressed depending upon the methylation state and the site of lysine methylation in H3 histone.[74] Thus, overall modification states of proteins and PTM cross-talk determine the fate of cellular processes in the cell. Therefore, any perturbation in PTM can affect normal functioning and even result in the manifestation of the disease. Several diseases are associated with a perturbation in the PTMs in terms of the type of PTM, the site of PTM occupancy, or the level of PTM modification. Changes in PTM pattern or extent of modification, including phosphorylation, glycosylation, acetylation, methylation, and ubiquitination, are associated with numerous diseases, e.g., cancer, cardiovascular diseases, and neurodegenerative diseases.[75-78] Similarly, the hyperglycemic condition in diabetes leads

to increased glycation reaction, which causes increased accumulation of advanced glycation end product (AGE)-modified proteins in cells as well as in plasma proteins, and this accumulation of AGEs is one of the major causes for the development of diabetic complications.[79] Since the changes in PTM pattern or level may lead to the manifestation of specific clinical conditions, PTMs can be potential biomarkers for that particular disease diagnosis, monitoring, or risk prediction.

PTMs can be detected and quantified by several approaches. Antibody-based techniques such as immunofluorescence, Western blot, and ELISA can be used for detecting and quantifying specific proteins and PTMs.[80-82] In fact, ELISA is one of the most sensitive and high-throughput techniques.[78, 82] However, antibody-based approaches have limitations in that only one specific analyte can be quantified at a time. Also, antibodies must be available for the quantification of particular proteins or PTMs. In several cases, commercial antibodies against the target analytes may not be available or may not be possible to generate. Antibody-based methods are also limited by non-specific antibody binding, especially in complex samples.[83]

PTMs can also be detected by mass spectrometry. Mass spectrometry is a powerful tool that has revolutionized the field of proteomics, and it is one of the most widely used techniques for the accurate detection and quantification of PTMs. With the advancement in mass spectrometry instrumentation, workflows, and sample preparation methods, especially in the last two decades, it has become one of the most preferred techniques for the characterization and quantification of PTMs. Its current sensitivity, resolution, accuracy, and scan speed allow the quantification of hundreds of analytes in a single run. This high multiplexity is not possible in antibody-based techniques. Unlike antibody-based approaches, mass spectrometry does not depend upon the availability of target-specific antibodies, and virtually any PTM can be detected and quantified.[84] The identification of the PTMs by mass spectrometry is done by detecting the change in the mass of the precursor ions compared to their unmodified counterpart. In tandem mass spectrometry, fragmentation of the PTM-modified precursors ions generates a series of fragment ions. The modification site in a protein can be detected by comparing the fragment ions bearing the mass of PTM to the fragment ions from corresponding unmodified precursors.[85] Mass spectrometers can detect the presence and localization of PTMs on proteins by untargeted MS approaches[86] whereas targeted MS approaches are particularly useful for quantifying the PTMs.[78]

A few targeted MS approaches have been developed that can precisely and sensitively

quantify the target analytes. Multiple Reaction Monitoring (MRM) using stable isotope-labeled standard peptides is considered a gold standard approach for the quantification by MS using triple quadrupole mass spectrometers.[87] Parallel Reaction Monitoring (PRM) is a quantification approach that quantifies analytes with high resolution using a hybrid Quadrupole-Orbitrap mass spectrometer.[88] High-resolution multiple reaction monitoring (MRM-HR) refers to PRM experiments performed on a Quadrupole time-of-flight (Q-TOF) mass spectrometer.[89] In the MRM approach, prior information on precursor and fragment ion masses is required. Also, the optimum collision energy for each of the fragments needs to be determined beforehand.[87] Unlike the MRM approach, no fragment ions are selected by the second mass analyzer, i.e., Orbitrap or TOF, in the PRM approach, and all fragment ions generated are analyzed with high resolution. In PRM experiments, the selection of fragment ions for analytes' quantification is made after sample acquisition. Optimization of collision energy for each fragment ion is not required in the PRM approach. Instead, a normalized collision energy is used for the fragmentation of all precursor ions in the PRM approach. Therefore, PRM experiments are much easier to set up. Also, PRM experiments have sensitivity and dynamic range similar to that of SRM experiments. Therefore, PRM methods are extensively used for the quantification of target analytes.[88]

Glycation is associated with diabetes and its complications. Glycation occurs at the lysine, arginine, and N-terminus of protein. Different glycating moieties, e.g., carboxymethyl, carboxyethyl, and deoxyfructosyl, have been detected and very well characterized by MS.[61, 90] Thus, targeted MS approaches, such as PRM (or MRM-HR) can be used to detect the site and extent of glycation on a protein as a marker in diabetes and its complications.

1.7 Genetic polymorphisms

Genetic polymorphism refers to two or more variant forms of a specific DNA sequence among different individuals. The most frequent type of genetic polymorphism is single nucleotide polymorphism (SNP), a single nucleotide difference in a DNA sequence.[91] The other types of DNA polymorphism are insertion or deletion (indels) of a specific stretch of DNA.[92] Polymorphism differs from mutation in that it is present at a population frequency of $\geq$ 1%.[93] Most of the genetic polymorphisms are silent as they cannot change the gene expression level.[94] However, some genetic polymorphisms may increase disease susceptibility in various ways. Non-synonymous SNPs in a gene's exonic region result in the replacement of one amino acid by a different amino acid. This non-synonymous replacement

may alter the structure and function of the protein.[94] The SNPs present in the intronic region of the gene may affect the pre-mRNA alternative splicing and thereby affect the protein structure. SNPs present in the gene's promoter region may alter gene expression.[69] Several SNPs have been found to be linked with a number of diseases. Therefore, SNPs are being widely investigated for their association with various diseases. SNPs have been found to increase the risk of various diseases, including cancer, diabetes, coronary heart disease, and neurological disorders.[23, 93, 95-97]

1.8 Conventional tools for detecting gene polymorphisms

Several tools such as TaqMan fluorescent probe,[98] pyrosequencing,[99] cycle sequencing with dye-labeled terminators,[100] and restriction fragment length polymorphism (RFLP)[91] can be used to detect polymorphisms in DNA. PCR, followed by RFLP, is the most extensively used SNP detection method as it is highly specific, fast, cost-effective, easy to perform, and requires simple instruments.[91, 101] Figure 1.5 illustrates SNP detection by PCR-RFLP. In PCR-RFLP, the region of DNA spanning the polymorphic site is amplified by PCR, and a specific restriction enzyme is used that cuts the DNA at or near its restriction site. Because of the polymorphism, a new restriction site may be created, or the existing restriction site may be abolished. Thus, the presence or absence of restriction sites results in DNA fragments of varying lengths upon restriction digestion of wild-type and mutated allele.[102] The restriction fragments are separated in a gel by electrophoresis and visualized to determine their size. Thus the polymorphisms are detected.[101] However, there are limitations to the use of PCR-RFLP for SNP detection. It is a laborious and time-consuming method.[102] It is not a high-throughput method. Since the PCR-RFLP method is based on the detection of restriction sites, a specific restriction enzyme is required to detect a particular SNP. Detection of more than one SNP, therefore, requires many restriction enzymes and the separate digestion of the PCR-amplified products. Thus it won't be cost-effective.[101] The absence of a suitable restriction enzyme for many polymorphic sites restricts the use of PCR-RFLP for detecting such SNPs. Also, the disadvantage of PCR-RFLP is that it cannot detect unknown polymorphisms.[103]

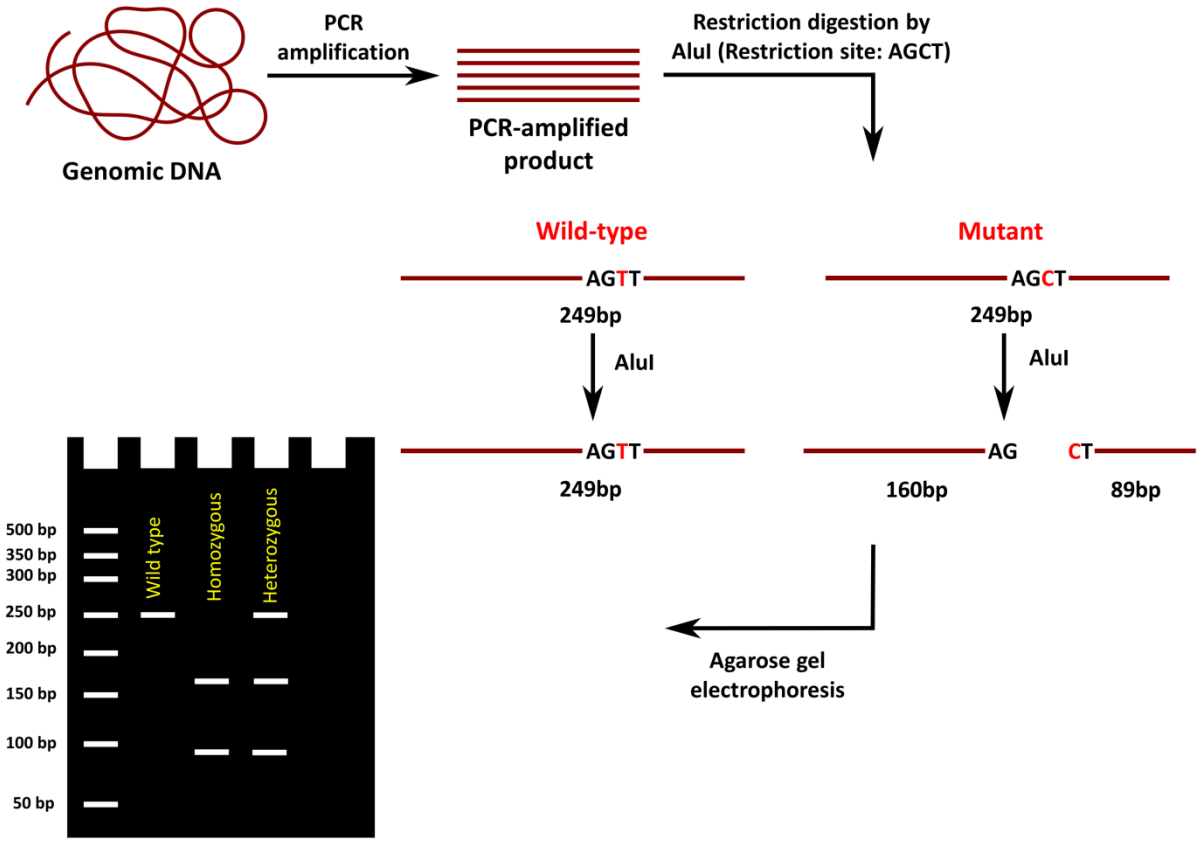

Figure 1.5 Schematic representation of PCR-RFLP
A short stretch of DNA harboring the polymorphic site is PCR amplified and digested using a restriction enzyme. In the illustration, AGTT in the wild-type allele is converted to AGCT (restriction site for AluI) in the mutant allele because of T>C polymorphism. AluI cannot cut the wild-type allele, but it cuts the mutated allele resulting in two short DNA fragments. Upon electrophoresis of the restriction digested products, wild-type, homozygous mutant, and heterozygous mutant can be identified.

1.9 DNA sequencing-based tools for detecting gene polymorphisms

1.9.1 First-generation sequencing

DNA sequencing-based approaches are typically based on the amplification of a stretch of the DNA using PCR and then sequencing the nucleotides of the amplified PCR products. Thus the exact determination of the nucleotide sequence empowers the detection of polymorphisms in the sequenced region of DNA. Two DNA sequencing methods were developed in 1977 and widely adopted, namely, the 'chain termination method' of Sanger and the 'chemical degradation' method of Maxam and Gilbert.[104, 105]

1.9.1.1 Maxam and Gilbert method

Maxam and Gilbert sequencing was the first widely used DNA sequencing method. In this method, a particular type of nucleotide in the ^{32}P-end-labeled DNA is modified by a specific chemical agent and cleaved by piperidine at the modified sites.[106] Four different reaction mixtures for four different nucleotides are set up that generates a series of ^{32}P-end-labeled DNA fragments. The length of the DNA fragments can be deduced by electrophoresis of the fragments of the four reactions in separate lanes on a polyacrylamide gel, and this allows the nucleotide sequence to be determined. However, due to the complexity and the use of hazardous chemicals in the Maxam and Gilbert method, Sanger sequencing was increasingly adopted.[104]

1.9.1.2 Sanger's method

Sanger's chain termination method is a sequencing-by-synthesis method in which radiolabeled dideoxyribunucleotides (ddNTPs) are mixed at low concentrations with the normal deoxynucleotides (dNTPs) in a small fraction for DNA synthesis. Because ddNTPs lack the 3'OH group, they cannot make the phosphodiester bond with the 5' phosphate of the next nucleotide during DNA synthesis. Thus, upon random incorporation of ddNTPs, the DNA synthesis terminates at the incorporated radiolabeled ddNTP, and DNA fragments of varying lengths are produced. By setting up four separate reaction mixtures with different ddNTPs and separating products on four separate lanes of polyacrylamide gel by electrophoresis, the nucleotide sequence of DNA can be determined. There have been a number of improvements in the Sanger sequencing method, such as the replacement of the radiolabeled ddNTPs with four different fluorescently labeled ddNTPs and nucleotide detection by capillary electrophoresis. The use of hazard-free chemicals, very high accuracy, and automation have made Sanger sequencing a widespread method of DNA sequencing for DNA fragments less than 1 kb.[105, 107]

1.9.2 Second-generation sequencing

Second-generation sequencing is also referred to as next-generation sequencing (NGS). The massively parallel sequencing of the DNA by all of the second-generation DNA sequencing technologies made sequencing of DNA high-throughput and overall cost-effective than Sanger sequencing.[104]

1.9.2.1 Roche 454 sequencing

Roche 454 sequencing is based on pyrosequencing. This method involves the attachment of single fragments of DNA to the surface of capture beads via adapter sequences, and beads are emulsified in a water-in-oil emulsion containing reagents for PCR. The template DNA is PCR amplified in the emulsion droplet to generate millions of copies of amplified DNA attached to the capture beads, and then DNA-coated beads are transferred to the picotiter plate, where each well can accommodate only a single bead. As the pyrosequencing reagents are washed over the plate, the addition of dNTP causes the release of pyrophosphate. Pyrophosphate is used by the enzyme to generate luminescence, and a charge-coupled device (CCD) camera detects it. Sequentially flowing the four nucleotide bases, the sequencing is done in over one million wells for a read length of 400-500 bp.[104, 105]

1.9.2.2 Illumina sequencing

In the Illumina sequencing method, adapters are ligated to both ends of the DNA fragments and flown over the flow cell having adapter-complementary oligonucleotides bound to it. Subsequent solid phase PCR cycles result in 'bridge amplification,' and copies of template DNA are created around the original DNA strand. The clusters of single-strand DNA fragments are then sequenced. All four fluorescently labeled 'reversible terminator' dNTPs and reagents for polymerization are added. The blocking moiety at the 3'OH of the incorporated dNTP prevents further binding of the nucleotides. Laser excitement emits the light characteristic to the fluorescent nucleotide and is detected by the CCD camera. The next polymerization cycle is performed after the cleavage of the fluorescent label and enzymatic removal of the blocking moiety at the 3'OH.[104, 105] The read length in Illumina sequencing is approximately 100 bp.

1.9.2.3 SOLiD sequencing

SOLiD sequencing approach uses emulsion PCR to prepare the library, similar to Roche 454 sequencing. However, in this method, the beads coated with amplified DNA are enriched, and the DNA templates on the beads are attached to the solid phase of the flow cell. A fluorescently labeled dinucleotide probe is passed over the flow cell, and the correct complementary dinucleotide is ligated to the primer on the solid phase. After washing, the fluorescence is recorded, which is characteristic of the dinucleotide probe. After that, the fluorescent dye is removed, and the next cycle of ligation is started. This method generates over 1 billion reads of approximately 50 bp. [104, 108]

1.9.3 Third-generation sequencing

Unlike NGS, single molecules of DNA can be sequenced by third-generation sequencing (TGS) methods, i.e., without requiring PCR amplification of the DNA strand to be sequenced. Third-generation sequencing methods can generate longer reads with lower cost and high throughput.[104] The two most commonly used TGS methods are single molecule real-time (SMRT) sequencing from Pacific Biosciences and nanopore sequencing from Oxford Nanopore Technologies.

1.9.3.1 SMRT sequencing

In SMRT sequencing, single DNA polymerase molecules are immobilized in nano chambers (zero-mode waveguide chambers). Single-strand DNA library and four different fluorescently labeled dNTPs are flown over the nano chambers. As the fluorescent nucleotide is incorporated, the fluorescence of only the incorporated nucleotide is detected, and the fluorescent tag is then cleaved. It can generate read lengths up to 10 kb. Since the error rate of SMRT sequencing is high (approximately 85 % accuracy), it has a very limited application in SNP discovery.[104, 105]

1.9.3.2 Nanopore sequencing

Nanopore sequencing is a widely used third-generation sequencing tool to sequence DNA. Nanopore sequencing was conceptualized in the 1980s, and through multiple improvements, it was released commercially for the first time in 2014 by Oxford Nanopore Technologies.[109, 110] Nanopore sequencing can sequence extremely long read lengths. A read length of approximately 2.3 Mb has been reported recently.[111] In fact, the read length for nanopore sequencing is not restricted by the technology but by getting extremely long read lengths of sufficient quality. The nanopore sequencing tool is high-throughput, cost-effective, and provides real-time data.[109, 110]

Figure 1.6 shows the schematic representation of nanopore sequencing. Nanopore sequencing uses protein nanopores embedded in an electro-resistant synthetic membrane. An electrolyte solution is present on both sides of the membrane, and a voltage application across the membrane causes the ions to pass through the nanopore across the membrane, generating a stable current. When the prepared DNA library is loaded onto the flow cell for sequencing, motor protein docks onto the pore, unwinds the double-stranded DNA, and the negatively charged single-stranded DNA is driven through the nanopore under an electric field. While

the single-stranded DNA molecule moves through the nanopore, it blocks the passage of a certain amount of ions which causes a disruption in the current. Each different nucleotide of DNA gives a characteristic fluctuation in the current that is measured and decoded to determine the DNA sequence.[109, 110] The steps involved in nanopore sequencing are schematically represented in Figure 1.6

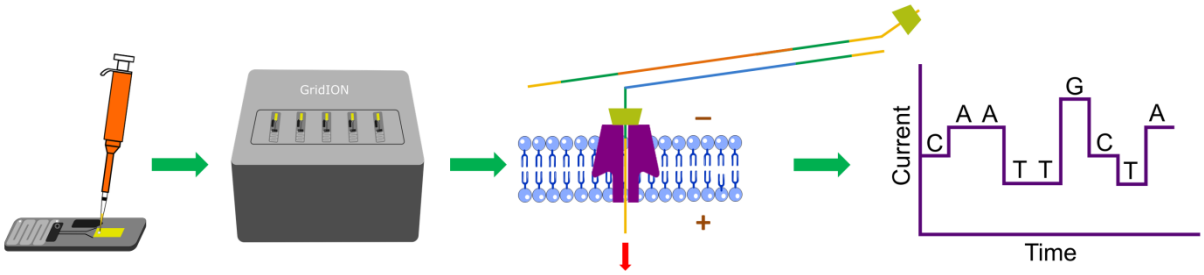

Figure 1.6 Schematic representation of the nanopore sequencing
The prepared DNA library is loaded onto the flow cell and sequenced by the sequencer. As the nucleotides of the single-strand DNA pass through the nanopore, the characteristic current fluctuations are recorded and decoded into nucleotides by base calling.

Nanopore sequencing had an error rate of approximately 15 % which has been brought down to 3 % by using an adapter that promotes entry of the second DNA strand after the first DNA strand has passed through.[112] Further, a read coverage of 40X is sufficient to make the sequencing virtually error-free.[30] Nanopore sequencing has diverse applications, including whole genome sequencing, detection of epigenetic modification, infectious disease detection, metagenomics analysis, direct RNA sequencing, and SNP detection.[107, 109, 110, 112]

MinION, the first sequencer launched in 2014, is a tiny-sized portable nanopore sequencer suitable for field applications. GridION sequencer can perform sequencing in up to five flow cells in parallel. PromethION sequencer allows for very high-throughput sequencing as it can hold up to 48 flow cells. The sequencing cost using PromethION is the lowest among all sequencing tools.[112]

1.10 Scope of the work and research problem

Diabetes is a metabolic disorder with a very high prevalence. The prevalence of diabetes has been rapidly increasing and is projected to continue to increase rapidly as a consequence of, at least partly, changing socio-economic status and lifestyle. A poor lifestyle is closely associated with type 2 diabetes. Type 2 diabetes has a prevalence of approximately 90 % in the Indian population. Over half of the diabetes cases in India are undiagnosed. Poor diabetes management facilitates the development of diverse vascular complications. Diabetic

nephropathy is a diabetic complication that progressively damages the kidneys. It may ultimately lead to renal failure, which can be life-threatening. Thus it becomes crucial to detect type 2 diabetes and diabetic nephropathy early to facilitate early preventive and therapeutic measures. On the other hand, asymptomatic initial phases of type 2 diabetes and diabetic nephropathy make early detection even more challenging. Therefore, it's important not only to detect them early but also to predict the risk of their development.

In this context, glycated albumin can be a good marker for predicting diabetic nephropathy risk, as it shows a short-term glycemic status of 19 days. Moreover, glycation measurement may be even more sensitive if measured at the glycation-sensitive lysine residues of human serum albumin (HSA). Type 2 diabetes and diabetic nephropathy are strongly correlated with genetic makeup. In particular, considering the involvement of RAGE in the etiology of type 2 diabetes and diabetic nephropathy, SNPs of the *RAGE* gene may be associated with the risk of developing type 2 diabetes and diabetic nephropathy. Although numerous studies have evaluated *RAGE* SNPs association with diabetes and its complications, the results have been contradictory. Racial differences in the subject cohorts could be one of the reasons for the discrepancies reported. Also, barely any such studies have been performed on Indian subjects. Hence, there is a need to have a comprehensive picture of all *RAGE* SNPs present in the Indian population and their association with type 2 diabetes and diabetic nephropathy. The *RAGE* SNPs that increase the risk of type 2 diabetes and diabetic nephropathy can help screen individuals vulnerable to these diseases.

With this background, the following objectives were designed for the thesis.

1. To evaluate glycated HSA peptides for the risk prediction of diabetic nephropathy.

2. To detect *RAGE* gene polymorphisms and their association with type 2 diabetes and diabetic nephropathy.

Chapter 2

Evaluation of glycated HSA peptides for the risk prediction of diabetic nephropathy

The contents of this chapter have been published in *ACS Omega*, 2023, 8(23):20654-20660

Chapter 2 : Evaluation of glycated HSA peptides for the risk prediction of diabetic nephropathy

2.1 Background

Diabetic nephropathy is a major diabetic complication that affects about 20-40 % of patients with diabetes. Due to glomerular damage, diabetic nephropathy patients have a progressive decrease in renal function.[47] In diabetic nephropathy, there is an accumulation of nitrogenous waste in the blood, such as urea nitrogen and creatinine,[47, 113] and increased excretion of blood proteins in the urine.[114] Diabetic nephropathy is typically diagnosed by measuring albumin concentration in the urine. Microalbuminuria is the earliest clinical sign of diabetic nephropathy.[50] Diabetic nephropathy develops and progresses through different stages.[53, 115] The initial stages of diabetic nephropathy, before the development of microalbuminuria, are subclinical. Therefore, there remains a risk of diabetic nephropathy onset even when the urinary albumin concentration is within the normal range. Thus, early detection of diabetic nephropathy is crucial for starting timely preventive measures. However, the currently used diagnostic markers may not be sensitive enough for early-stage detection of diabetic nephropathy. Therefore, there is an urgent need of a marker for predicting diabetic nephropathy development risk.

Increased glycation is known for promoting the onset of several complications in diabetes patients, including diabetic nephropathy. Due to the causal link of glycation with diabetic complications,[47] glycated proteins could be useful markers for risk prediction of diabetic nephropathy. Numerous studies have evaluated the ability of well-established glycemic markers like glycated hemoglobin (HbA_{1c}) and other markers, such as glycated albumin, to predict diabetic nephropathy.[47, 63, 116-118] In a longitudinal study involving 449 type 2 diabetes subjects, glycated albumin levels were found to predict diabetic nephropathy development better than HbA_{1c} levels.[63] In another longitudinal study conducted on 154 participants, glycated albumin could predict the progression of diabetic nephropathy, but HbA_{1c} could not.[64] Similarly, another study reported superior performance of glycated albumin over HbA_{1c} for the prediction of diabetic nephropathy. Therefore, it is worth evaluating the diabetic nephropathy risk prediction performance of glycated albumin.

The half-life of HSA is about 19 days;[65] hence it represents a short-term glycemic status. HSA is directly exposed to reducing sugars in plasma, and it is the most abundant plasma

protein containing 59 lysine and 24 arginine residues, many of which can be glycated[119]. Therefore, glycated albumin represents a large share of glycated plasma proteins, and measuring glycated albumin could be more sensitive than other glycated plasma proteins.

Glycated albumin has been increasingly investigated in recent years for its involvement in diabetic complications onset and for its prediction.[47, 120, 121] Several reports have found an association between glycated albumin and diabetic nephropathy.[47, 64, 117, 120] However, most of the reports on the association of albumin glycation and diabetic nephropathy have focused on the quantification of total glycated albumin, but it has been reported previously that the lysine residues of albumin vary in their glycation sensitivity.[20, 122, 123] Therefore, quantifying glycation-sensitive peptides rather than overall glycated HSA can make the analysis more sensitive. Mass spectrometry (MS) is being increasingly used for the discovery and quantification of disease biomarkers.[124] MS is the best tool to characterize and quantify glycated peptides by bottom-up proteomics. It offers great sensitivity and resolution to measure protein and peptides level accurately. In this context, targeted mass spectrometry-based approaches, such as MRM-HR, offer accurate and sensitive quantification of target peptides with the ease of the mass spectrometry acquisition method setup. Herein, we selected three glycation-sensitive HSA peptides, namely FKDLGEENFK, KQTALVELVK, and KVPQVSTPTLVEVSR, corresponding to sites K36, K549, and K438, respectively, based on previous literature;[20, 21, 90, 123, 125, 126] quantified these peptides in unmodified and DFL-modified (Amadori-modified) form by MRM-HR approach in a study group comprising healthy and type 2 diabetes subjects with and without nephropathy; and evaluated if these glycated peptides can be good predictors for diabetic nephropathy.

2.2 Materials and methods

2.2.1 Materials

All chemicals, including ammonium bicarbonate, dithiothreitol (DTT), iodoacetamide (IAA), formic acid (FA), and proteomics grade trypsin, were procured from Sigma-Aldrich (St. Louis, MO, USA). Bradford reagent was obtained from Bio-Rad Laboratories Inc. (Hercules, CA, USA). LC-MS grade water and acetonitrile (ACN) were purchased from JT Baker (PA, USA). Sep-Pak C18 cartridges were procured from Waters (Waters Corporation, MA, USA). Eksigent micro-LC column (ChromXP C18, 100 X 0.3 mm, 3 µM, 120 Å) was procured from SCIEX (Framingham, MA, USA).

2.2.2 Study design

This cross-sectional study was designed to assess three glycated HSA peptides as a marker for the risk prediction of diabetic nephropathy. Peripheral blood samples from healthy, type 2 diabetes subjects without nephropathy (DM) and type 2 diabetes subjects with nephropathy (DN) were collected, and the plasma was separated. Plasma samples were digested by trypsin, and the tryptic peptides were analyzed by targeted mass spectrometry for the quantification of deoxyfructosyl-lysine (DFL)-modified HSA peptides, namely FKDLGEENFK, KQTALVELVK, and KVPQVSTPTLVEVSR. Statistical analysis was performed to check if these glycated peptides were significantly elevated in DM and DN groups. The accuracy of these glycated peptides in differentiating between healthy, DM, and DN groups was evaluated using receiver operating characteristic (ROC) curve analysis.

2.2.3 Subjects

Five ml of blood samples were collected from 25 healthy, 25 DM, and 25 DN subjects in EDTA-coated vacutainers. Subjects without a history of known diabetes having HbA_{1c} < 5.7% were categorized as healthy, while those having $HbA_{1c} \geq 6.5\%$ and spot urine microalbumin < 2mg/dL were categorized as type 2 diabetes subjects without nephropathy. Subjects with $HbA_{1c} \geq 6.5$ % and spot urine microalbumin ≥ 2 mg/dL were grouped as subjects with diabetic nephropathy. Subjects with chronic disease, inflammation, thyroid disorder, cardiovascular disease, and pregnancy were excluded from the study. All participants in the study provided their written informed consent before blood sample collection, and the study was performed adhering to the guidelines of the Declaration of Helsinki. The institute ethics committee of Chellaram Diabetes Institute, Pune, approved the study. Clinical characteristics of the subjects, including fasting blood glucose (FBG) level, 2 h postprandial blood glucose (PPBG) level, HbA_{1c}, total cholesterol, triglycerides, HDL, LDL, VLDL, serum creatinine, serum albumin, and urine microalbumin were measured. Plasma was separated from erythrocytes by centrifuging the blood samples at 1000 rpm at 4 °C for 15 min. Plasma in the supernatant was collected in a fresh collection tube, and cellular contaminants and debris were separated by centrifugation at 14000 rpm at 4 °C for 20 min. The clear plasma was collected and stored at minus 80 °C until further analysis.

2.2.4 Sample preparation for MS analysis

Plasma protein concentration was estimated by Bradford's method. 50 mM ammonium bicarbonate buffer of pH 8.0 was used for diluting 50 µg of the protein from each sample to

get the final protein concentration of 1 mg/mL in 50 µL reaction volume. It was heated for 15 min at 80 °C to denature proteins. 2.5 µL of 100 mM DTT was added to the solution and heated at 60 °C for 15 min for disulphide bond reduction. Alkylation of the sulfhydryl group was performed by the addition of 2.5 µL of 200 mM IAA and incubating the solution at RT in dark condition for 30 min. Trypsin at 1:25 (w/w) trypsin to protein ratio was added, and the digestion was performed at 37 °C for 16 h. Trypsin was inactivated by the addition of 1 µL FA and incubating at 37° C for 20 min. The tryptic peptides were desalted using Sep-Pak C18 cartridges. The desalted tryptic peptide solution was dried by vacuum concentrator and stored at minus 80 °C until MS analysis.

2.2.5 Liquid chromatography-mass spectrometry (LC-MS) analysis

HSA peptides were resuspended in 2% ACN with 0.1 % FA. NanoDrop 2000 spectrophotometer (Thermo Scientific) at 205 nm was used for estimating the peptide concentration, and 0.6 µg of peptides were loaded onto Eksigent C18-RP HPLC column using an Eksigent Ekspert MicroLC 200 system (SCIEX, Framingham, MA, USA) coupled to Triple TOF 5600 mass spectrometer (SCIEX). The column temperature was maintained at 40 °C. Peptides were separated using a mixture of mobile phase A (water with 0.1 % FA) and mobile phase B (ACN with 0.1 % FA) at a flow rate of 7 µL/min and two linear LC gradient segments, i.e., 2 to 20 % mobile phase B for 20 min followed by 20 to 40 % mobile phase B for 14 min, were used. MRM-HR approach was used for the data acquisition. The m/z values of the unmodified and DFL-modified HSA peptides FKDLGEENFK, KQTALVELVK, and KVPQVSTPTLVEVSR and their corresponding collision energies were specified in the acquisition method (Appendix 1) with a collision energy spread as 10 eV. The temperature of the ESI source was kept at 200 °C and voltage at 5500 V. Nebulizer gas, heater gas, and curtain gas were set at 25 psi each. Declustering potential was set to 80 V. Accumulation time was set to 0.25 s for the TOF MS scan over the mass range 350-1250 Da and 0.6 s for the fragment ion scan over the mass range 100-1200 Da.

2.2.6 Data analysis

The MS data generated were analyzed using Skyline version 22.2.0.255 (MacCoss Lab, University of Washington, WA, USA). The proteolytic enzyme was specified as trypsin, and the missed cleavage was set to 1. The fixed modification was set as carbamidomethylation at cysteine (57.021464 Da), whereas DFL modification at lysine (162.052795 Da) was specified as variable modification. Target HSA peptides for quantification were specified as

FKDLGEENFK, KQTALVELVK, and KVPQVSTPTVEVSR. The resolution was specified as 30000. Skyline-generated theoretical precursor and fragment ion masses based on the specified parameters served as the spectral library for precursor quantification. The retention times of the peptides were manually corrected wherever necessary. High-intensity b and y fragment ions of each precursor detected in all samples were selected, and their areas under curve (AUC) were integrated to calculate the AUC of the respective precursor. The AUC of DFL-modified peptides was normalized with the AUC of corresponding unmodified peptides to quantify the respective glycated peptides in each sample.

2.2.7 Statistical analysis

One-way analysis of variance (ANOVA) followed by a *post hoc* Tukey's test was used for the comparison of the glycated HSA peptide level among different subject groups. Correlation analysis of DFL-modified peptides with all the recorded clinical parameters was performed using Pearson's correlation method. The ROC curve analysis was done using MedCalc version 20.0.1 (MedCalc Software Ltd., Ostend, Belgium) to assess and compare the accuracy of glycated HSA peptides as a marker to detect diabetic nephropathy. *p*-values < 0.05 were considered as significant.

2.3 Results

2.3.1 Quantification of glycated HSA peptides by MRM-HR approach

The site of glycation-sensitive lysine residues in HSA focused in this study, m/z values of glycated HSA peptides, and their corresponding unmodified peptides are shown in Table 2.1. The DFL-modified peptides are characterized by a mass increase of 162 Da. The MS output data were analyzed using Skyline. Representative chromatograms depicting coeluting fragment ions of DFL-modified HSA peptides are shown in Figure 1. Fragment ions present in all samples with good intensity were used for precursor quantification (Table 2.1). The b ions bearing DFL modification were considered as qualifier ions for glycation. The precursor AUC was derived by integrating the AUC of selected fragment ions, and the DFL-modified precursor AUC was normalized with the respective unglycated precursor AUC. The normalized AUC of DFL-modified HSA peptides and HbA_{1c} were compared by one-way ANOVA between healthy, DM, and DN groups (Figure 2.1).

Table 2.1 Details of precursor ions and their corresponding fragment ions used for quantification

Modification site	Peptide	Precursor m/z	Precursor Charge state	Fragment ions used for precursor quantification (m/z)
K36	FKDLGEENFK	613.8062	2	$y6^{+}$ (723.3308), $y7^{+}$ (836.4149), $y8^{+}$ (951.4418), $y9^{++}$ (540.272) , $b2^{+}$ (276.1707), $b3^{+}$ (391.1976), $b8^{+}$ (933.4312)
K36	F***K(DFL)***DLGEENFK	694.8326	2	$y2^{+}$ (294.1812), $y6^{+}$ (723.3308), $y7^{+}$ (836.4149), $y8^{+}$ (951.4418), $b3^{+}$ (553.2504), $b4^{+}$ (666.3345), $b5^{+}$ (723.3559)
K549	KQTALVELVK	564.853	2	$y4^{+}$ (488.3079), $y7^{+}$ (771.4975), $y8^{+}$ (872.5451), $y9^{+}$ (1000.6037), $b7^{+}$ (770.4407), $b8^{+}$ (883.5247), $b9^{+}$ (982.5932)
K549	***K(DFL)***QTALVELVK	645.8794	2	$y2^{+}$ (246.1812), $y7^{+}$ (771.4975), $y8^{+}$ (872.5451), $y9^{+}$ (1000.6037), $b6^{+}$ (803.4509), $b7^{+}$ (932.4935), $b8^{++}$ (523.2924)
K438	KVPQVSTPTLVEVSR	547.3174	3	$y4^{+}$ (490.262), $y5^{+}$ (589.3304), $y6^{+}$ (702.4145), $y8^{+}$ (900.5149), $b7^{+}$ (740.4301), $b9^{+}$ (938.5306), $b10^{+}$ (1051.6146)
K438	***K(DFL)***VPQVSTPTLVEVSR	601.335	3	$y5^{+}$ (589.3304), $y6^{+}$ (702.4145), $y7^{+}$ (803.4621), $y8^{+}$ (900.5149), $b4^{+}$ (615.3348), $b5^{+}$ (714.4032), $b7^{+}$ (902.4829)

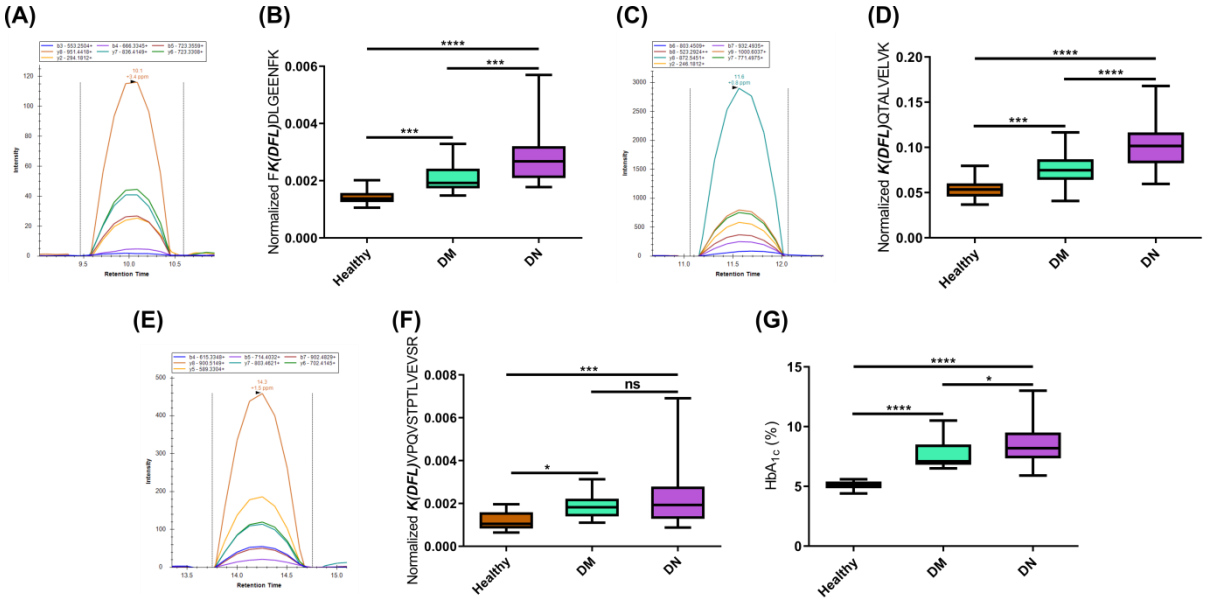

Figure 2.1 Representative DFL-modified peptide chromatograms and their quantification in healthy, type 2 diabetes without nephropathy (DM) and diabetic nephropathy (DN) groups
Chromatogram showing coeluting fragment ion peaks of F***K(DFL)***DLGEENFK (A); DM group showed an increased normalized AUC of F***K(DFL)***DLGEENFK than the healthy group. DN group had significantly elevated normalized AUC of F***K(DFL)***DLGEENFK compared to the healthy and DM group (B); Chromatogram showing coeluting fragment ion peaks of ***K(DFL)***QTALVELVK (C); DM group had an increased normalized AUC of ***K(DFL)***QTALVELVK than the healthy group. DN group had significantly elevated normalized AUC of ***K(DFL)***QTALVELVK compared to the healthy and DM group (D); Chromatogram showing coeluting fragment ion peaks of ***K(DFL)***VPQVSTPTLVEVSR (E); DM and DN groups had significantly elevated normalized **K(DFL)**VPQVSTPTLVEVSR compared to the healthy group, but there was no difference in its level between DM and DN group (F); DM group had significantly elevated HbA_{1c} compared to the healthy group, whereas the DN group had elevated HbA_{1c} compared to both healthy and DM groups (G). ns: nonsignificant, * $p < 0.05$, ** $p < 0.01$, *** $p < 0.001$, **** $p < 0.0001$.

An increase in DFL modification of HSA peptides was observed from healthy to type 2 diabetes and further to diabetic nephropathy condition. DM group had significantly elevated levels of F***K(DFL)***DLGEENFK, ***K(DFL)***QTALVELVK, and ***K(DFL)***VPQVSTPTLVEVSR compared to the healthy group. Similarly, when compared to the healthy and DM groups, the DN group had higher levels of F***K(DFL)***DLGEENFK, and ***K(DFL)***QTALVELVK. However, the DN group showed a significantly elevated level of ***K(DFL)***VPQVSTPTLVEVSR compared to the healthy group but not when compared to the DM group. ***K(DFL)***QTALVELVK level showed a relatively higher significant difference ($p < 0.0001$) between DM and DN groups than F***K(DFL)***DLGEENFK ($p = 0.0006$). Although HbA_{1c} also could differentiate between DM and DN groups, it had a lesser statistically significant difference ($p = 0.0163$) than observed with F***K(DFL)***DLGEENFK and ***K(DFL)***QTALVELVK for detecting diabetic nephropathy. The increase in DFL modification

of HSA peptides in DM and DN groups compared to the healthy group is represented in terms of fold change and compared to that of HbA_{1c} in Figure 2.2. While HbA_{1c} showed only a 1.69 fold increase in the DN group, F***K(DFL)***DLGEENFK and ***K(DFL)***QTALVELVK were increased by 1.93 and 1.94 fold, respectively, in the DN group while comparing to healthy subjects.

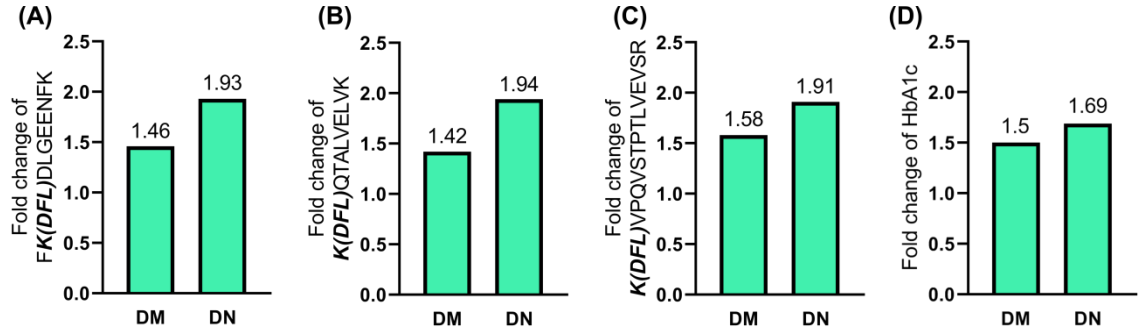

Figure 2.2 Fold-change in DFL-modified HSA peptide levels and HbA_{1c} in different subject groups

Compared to the healthy group, an increase in the level of F***K(DFL)***DLGEENFK (A), ***K(DFL)***QTALVELVK (B), ***K(DFL)***VPQVSTPTLVEVSR (C), and HbA_{1c} (D) was observed in both DM and DN groups.

2.3.2 ROC curve analysis for comparing diabetic nephropathy detection accuracy

ROC curve analysis was done to evaluate the diabetic nephropathy detection accuracy of glycated HSA peptides F***K(DFL)***DLGEENFK, ***K(DFL)***QTALVELVK, and ***K(DFL)***VPQVSTPTLVEVSR, and compared to that of HbA_{1c} (Figure 2.3). The sensitivity, specificity, and AUC of these peptides and HbA_{1c} are summarized in Table 2.2. ROC plot for ***K(DFL)***VPQVSTPTLVEVSR indicated that it was not useful as a marker for diabetic nephropathy detection (p = 0.6256). Among the other two DFL-modified peptides, the area under the ROC curve of ***K(DFL)***QTALVELVK was more (AUC: 0.81, 95% CI: 0.674-0.907) than that of F***K(DFL)***DLGEENFK (AUC: 0.752, 95% CI: 0.610-0.863) for diabetic nephropathy detection. However, the difference between the AUCs of ***K(DFL)***QTALVELVK and F***K(DFL)***DLGEENFK was insignificant (Appendix 2). Similarly, the AUC of the ROC curve for both F***K(DFL)***DLGEENFK and ***K(DFL)***QTALVELVK was more than that of HbA_{1c}, though not statistically significant.

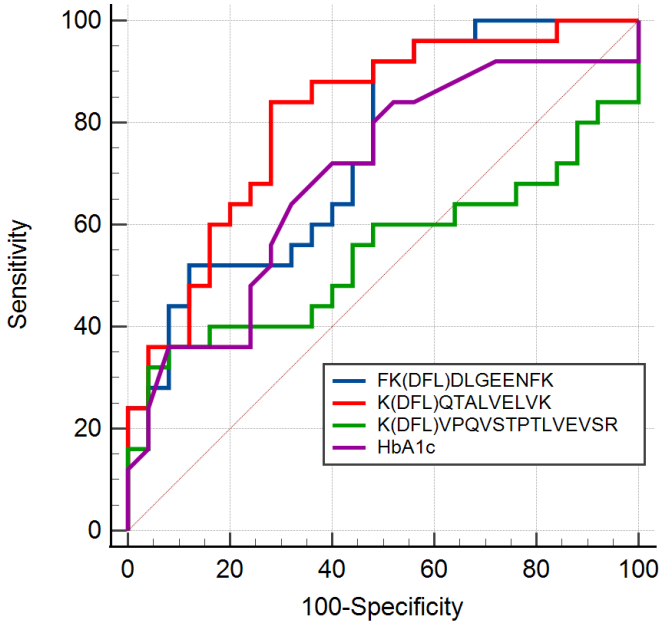

Figure 2.3 ROC curve analysis for DFL-modified HSA peptides and HbA_{1c} in the detection of diabetic nephropathy

K(DFL)QTALVELVK showed higher accuracy in detecting diabetic nephropathy, followed by F***K(DFL)***DLGEENFK and HbA_{1c}.

Table 2.2 Summary of ROC curve analysis for assessing the accuracy of DFL-modified HSA peptides and HbA_{1c} for detecting diabetic nephropathy

Peptide	DM vs. DN			
	Sensitivity	**Specificity**	***p*-value**	**AUC (95% CI)**
F***K(DFL)***DLGEENFK	92	52	0.0002**	0.752 (0.610-0.863)
K(DFL)QTALVELVK	84	72	<0.0001***	0.81 (0.674-0.907)
K(DFL)VPQVSTPTLVEVSR	36	92	0.6256	0.542 (0.396-0.684)
HbA_{1c}	82	52	0.0101*	0.696 (0.550-0.818)

* $p < 0.05$, ** $p < 0.001$, *** $p < 0.0001$

2.3.3 Correlation of glycated HSA peptides and HbA_{1c} with clinical parameters

A correlation analysis of several clinical parameters with glycated HSA peptides and HbA_{1c} levels was performed using Pearson's correlation method, and the results are summarized in Table 2.3. F***K(DFL)***DLGEENFK, ***K(DFL)***QTALVELVK, and ***K(DFL)***VPQVSTPTLVEVSR showed a strong positive correlation with fasting and postprandial blood glucose level and HbA_{1c}. ***K(DFL)***QTALVELVK had a stronger positive correlation with urine microalbumin (r = 0.429***) than F***K(DFL)***DLGEENFK (r = 0.333**) and HbA_{1c} (r = 0.351**), while all these three markers showed a negative correlation with serum albumin. Only ***K(DFL)***QTALVELVK showed a significant positive correlation with serum creatinine (r = 0.326**). ***K(DFL)***VPQVSTPTLVEVSR was not found to be associated with urine microalbumin or serum creatinine levels.

Table 2.3 Correlation of DFL-modified HSA peptides and HbA_{1c} with clinical parameters

Clinical parameters	Correlation coefficient (r)			
	F***K(DFL)***DLGEENFK	***K(DFL)***QTALVELVK	***K(DFL)***VPQVSTPTLVEVSR	HbA_{1c}
FBG (n = 75)	0.606****	0.635****	0.574***	0.788****
PPBG (n = 74)	0.7****	0.656****	0.578***	0.783****
HbA_{1c} (n = 75)	0.727****	0.787****	0.558***	1****
Total cholesterol (n = 75)	-0.107	-0.127	-0.098	-0.026
Triglycerides (n = 75)	0.06	0.088	0.046	0.189
HDL (n = 75)	-0.116	-0.09	-0.027	-0.157
LDL (n = 75)	-0.158	-0.193	-0.111	-0.105
VLDL (n = 75)	0.061	0.098	0.043	0.194
Serum creatinine (n = 74)	0.161	0.326**	-0.091	0.221
Serum albumin (n = 74)	-0.28*	-0.356**	-0.107	-0.449****
Urine microalbumin (n = 63)	0.333**	0.429***	0.152	0.351**

2.4 Discussion

Diabetic nephropathy is a major diabetic complication. With the increasing prevalence of diabetes, the burden of diabetic nephropathy will also increase in parallel. At the last stage of diabetic nephropathy (ESRD), the patients must undergo dialysis or renal transplant.[127] Therefore, it is vital to predict and detect diabetic nephropathy early to resort to early preventive and therapeutic measures to delay or stop the progression to ESRD. However, the currently used markers, based on urinary albumin concentration measurement, may not be efficient in detecting diabetic nephropathy at early stages; and it can be detected only when there is increased albumin excretion in urine, a condition called microalbuminuria. At this stage, the kidneys are already damaged.[53] Hence, there is an urgent need of a marker for predicting diabetic nephropathy.

Plasma proteins with different half-lives can reflect the glycemic status of varying periods.[20] Among these, there has been a growing interest in glycated albumin as a marker for monitoring glycemic status and predicting diabetic complications.[47, 120, 121] Glycated albumin has several advantages as a marker. Being the most abundant plasma protein with many glycation-sensitive lysine and arginine residues directly exposed to plasma, HSA is prone to extensive glycation.[119] It has a half-life of 19 days, which is sufficient for glycation reactions. Therefore, glycated albumin could be a potential candidate marker for the risk prediction of diabetic nephropathy. Also, since different lysine and arginine residues of albumin have different propensities for glycation,[123, 128] measuring the glycation on glycation-sensitive residues can be more sensitive for diabetic nephropathy prediction instead of measuring total glycation on albumin. In this context, we evaluated the level of glycation of the three glycation-sensitive HSA peptides, namely, FKDLGEENFK, KQTALVELVK, and KVPQVSTPTLVEVSR, in healthy, type 2 diabetes and diabetic nephropathy subjects using a targeted mass spectrometry approach, MRM-HR, to assess the utility of glycated HSA peptides as marker for risk prediction of diabetic nephropathy.

Significantly higher levels of all three DFL-modified HSA peptides, namely, F***K(DFL)***DLGEENFK, ***K(DFL)***QTALVELVK, and ***K(DFL)***VPQVSTPTLVEVSR, were observed in type 2 diabetes subjects than in the healthy group. Hence, all three DFL-modified HSA peptides were able to differentiate between healthy and type 2 diabetes subjects. But, for diabetic nephropathy detection, only F***K(DFL)***DLGEENFK, and ***K(DFL)***QTALVELVK were useful. Type 2 diabetes and diabetic nephropathy group did not show a significantly

different ***K(DFL)***VPQVSTPTLVEVSR level; hence this peptide could not detect diabetic nephropathy. ***K(DFL)***QTALVELVK detected diabetic nephropathy with a greater statistically significant difference, followed by F***K(DFL)***DLGEENFK and HbA_{1c}. A similar trend in DFL-modified HSA peptide level and HbA_{1c} was observed when the increase in DFL modification in the type 2 diabetes and diabetic nephropathy group was represented as fold-change and compared to the healthy controls. ***K(DFL)***QTALVELVK and F***K(DFL)***DLGEENFK showed a greater fold-change compared to HbA_{1c}. This finding indicates that F***K(DFL)***DLGEENFK, and ***K(DFL)***QTALVELVK are more sensitive than HbA_{1c} and may better predict diabetic nephropathy risk. The higher DFL modification of HSA peptides in the DN group could be attributed to the faster DFL modification of albumin than hemoglobin.[47] Also, since albumin has a short half-life than hemoglobin, glycated albumin can reflect glycemic changes faster than HbA_{1c}.[117] Therefore, DFL-modified HSA peptides may detect diabetic nephropathy sensitively and earlier than HbA_{1c}. Thus, the faster increase in DFL modification of albumin compared to hemoglobin translates into higher glycated albumin to HbA_{1c} ratio observed in diabetic nephropathy.[117]

Glycated albumin has previously been assessed for the risk prediction of diabetic nephropathy and has been compared with HbA_{1c} .[47, 120, 121] Our results are in agreement with the earlier reports that glycated albumin predicts early diabetic nephropathy development than HbA_{1c} .[63, 117] This can be explained by the fact that the glycation of albumin changes faster than glycated hemoglobin in response to the serum glycemic index, i.e., albumin is more sensitive to glycation than hemoglobin.[129, 130] Different plasma proteins get glycated to different extents, and the degree of glycation increases with the increase in glycemia.[17] Glycated albumin level also increases with the severity of diabetes.[118] Thus, being the most abundant plasma protein with a large number of lysine and arginine residues, the DFL-albumin accumulates in patients with diabetes and later promotes diabetic complications onset, including diabetic nephropathy.[47] While previous studies mostly quantified total albumin glycation using an enzymatic assay, quantification of glycation-sensitive HSA peptides by mass spectrometry could be more sensitive.

A ROC curve analysis was done to assess the accuracy of glycated HSA peptides and HbA_{1c} for detecting diabetic nephropathy. While ***K(DFL)***VPQVSTPTLVEVSR could not differentiate between type 2 diabetes and diabetic nephropathy, ***K(DFL)***QTALVELVK, F***K(DFL)***DLGEENFK and HbA_{1c} could differentiate the two groups. The AUC of

K(DFL)QTALVELVK was greater, followed by F***K(DFL)***DLGEENFK and HbA_{1c}, though this difference was not statistically significant between them. Thus among the three DFL-modified HSA peptides, ***K(DFL)***QTALVELVK and F***K(DFL)***DLGEENFK could be useful markers for predicting diabetic nephropathy.

Pearson's correlation analysis was performed to check for the association of DFL-modified HSA peptides and HbA_{1c} with clinical parameters, especially with diabetic nephropathy-associated parameters, i.e., urine microalbumin and serum creatinine. Urine microalbumin represents the extent of urinary albumin excretion, a parameter used in diabetic nephropathy diagnosis. Urine microalbumin was more strongly associated with ***K(DFL)***QTALVELVK than F***K(DFL)***DLGEENFK and HbA_{1c}. Also, only ***K(DFL)***QTALVELVK was significantly associated with serum creatinine, a nitrogenous waste elevated in diabetic nephropathy. Therefore, ***K(DFL)***QTALVELVK showed the best association with diabetic nephropathy-associated markers.

Thus based on mass spectrometry, ROC curve, and correlation analysis, it can be concluded that ***K(DFL)***QTALVELVK could be a better risk prediction marker for diabetic nephropathy, followed by F***K(DFL)***DLGEENFK and HbA_{1c}.

2.5 Conclusion

Currently, there are no markers in clinical practice that can detect diabetic nephropathy at very early stages. Therefore, in the search for a potential marker, we evaluated the glycated HSA peptides for the risk prediction of diabetic nephropathy. ***K(DFL)***QTALVELVK and F***K(DFL)***DLGEENFK could detect diabetic nephropathy better than HbA_{1c}. ***K(DFL)***QTALVELVK was better correlated with diabetic nephropathy-associated clinical parameters, i.e., serum creatinine and urine microalbumin, than F***K(DFL)***DLGEENFK. Absolute quantification and determining the range and cutoff value in a large cohort would help in developing ***K(DFL)***QTALVELVK peptide as a marker for predicting the risk of diabetic nephropathy.

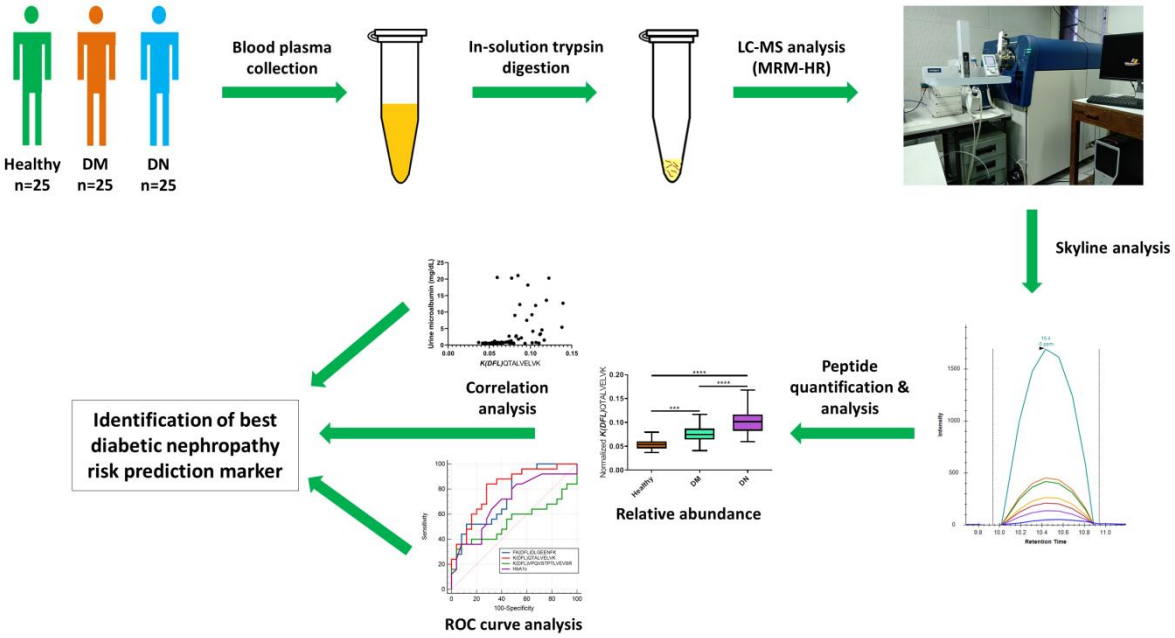

Figure 2.4 Summary figure

Chapter 3

Detection of *RAGE* gene polymorphisms and their association with type 2 diabetes and diabetic nephropathy

The contents of this chapter have been published in *ACS Omega*, 2023.
doi.org/10.1021/acsomega.3c00297

Chapter 3 : Detection of *RAGE* gene polymorphisms and their association with type 2 diabetes and diabetic nephropathy

3.1. Background

Diabetes is a complex metabolic disorder that results from inadequate secretion of insulin, as in type 1 diabetes mellitus, or insulin resistance, as in type 2 diabetes mellitus. According to the projection of the International Diabetes Federation, global adult diabetes cases will increase from 537 million in 2021 to 783 million by 2045. Chronic hyperglycemic condition in people with diabetes promotes the development of several microvascular and macrovascular complications, such as diabetic retinopathy, diabetic nephropathy, diabetic neuropathy, and cardiovascular diseases.[131] Amongst these, diabetic nephropathy is a major diabetic complication, and 20-40 % of diabetic people develop diabetic nephropathy in their lifetime.[114, 132] It is a leading cause of end-stage renal disease.[133]

Several etiological factors, including lifestyle, genetics, environment, and ethnicity, are among the major factors responsible for developing diabetes and its complications.[134-136] Amongst these, genetic factors are responsible for differential susceptibility to diabetes and its complications. Differential expression of specific genes and certain gene polymorphisms are reported to be associated with diabetes and its complications, such as *PPARG*, *IRS-1*, *IRS-2*, *IL-1β*, *SLC2A2*, *PI3KR1*, *VEGF*, *ELMO1*, *ADIPOQ*, and *RAGE*.[23, 137-140] The *RAGE* gene is highly polymorphic, and *RAGE* polymorphisms are among the most investigated for their association with numerous diseases.[23] The *RAGE* gene encodes for a protein called receptor for AGEs. It is a membrane-bound receptor belonging to the immunoglobulin superfamily and can bind to numerous ligands. It consists of an extracellular variable domain, two extracellular constant domains, one transmembrane domain, and one cytosolic domain. RAGE binds to AGEs, and this AGE-RAGE interaction activates the nuclear transcription factor NF-κB, which increases cytokine production, oxidative stress, and inflammation and contributes to the pathogenesis of diabetes and its complications.[131, 141, 142]

The involvement of RAGE in diabetes and diabetic nephropathy has been well established.[23] The single nucleotide polymorphisms (SNPs) present in the exonic regions of the *RAGE* gene can cause non-synonymous replacement of the amino acids that can alter the RAGE structure.[143] Alteration in the RAGE structure can potentially affect its binding with its

ligands and downstream signaling. Also, SNPs present in the promoter region of *RAGE* can affect the transcriptional activity of *RAGE*, hence affecting its expression.[144] Although SNPs in the intron region may not directly affect the RAGE structure, they might affect the splicing of RAGE mRNA, leading to the expression of different RAGE isoforms.[23] The sequences for 13 different splice variants of RAGE have been reported and are available in GenBank (ncbi.nlm.nih.gov/genbank, Oct 2022).

Polymerase chain reaction-restriction fragment length polymorphism (PCR-RFLP) is routinely used for SNP detection. However, it is not a high-throughput method as it detects only one SNP at a time and is time-consuming.[102] Moreover, by PCR-RFLP, one can interrogate only previously reported mutations. On the other hand, DNA sequencing facilitates the identification of all variations associated with the locus of interest. Oxford Nanopore Technology (ONT) (nanoporetech.com) based DNA sequencing is a third-generation nucleic acid sequencing technology that has recently gained attention for rapid and high-throughput sequencing of DNA and RNA. The ONT approach generates long-read sequences with high accuracy and is increasingly used for high-throughput *de novo* sequencing and SNP detection.[145, 146]

Several studies have reported the association of *RAGE* polymorphisms with diabetes and its complications;[23] however, the reported findings are often contradictory and may have missed many mutations due to reliance on techniques such as PCR-RFLP. In this study, nanopore sequencing of the *RAGE* gene was performed to detect all *RAGE* polymorphisms (known and novel) in a cohort population from Pune, India, and to evaluate the possibility of establishing this technique as a robust and routine diagnostic method for SNP detection. To compare and cross-validate the findings from nanopore sequencing, we used the PCR-RFLP method to interrogate the four most commonly reported SNPs of the *RAGE* gene, i.e., rs3134940, rs1800624, rs1800625, and rs2070600 from the samples. Statistical tests were performed to check whether the detected *RAGE* SNPs were associated with type 2 diabetes and diabetic nephropathy. Further, we quantified diabetes-associated biochemical markers, such as FBG and HbA_{1c}. We also measured plasma fructosamine, glycated albumin, an inflammatory cytokine, i.e., TNF-α, malondialdehyde (MDA), fasting insulin, homeostatic model assessment for insulin resistance (HOMA-IR) and C-reactive protein (CRP). Finally, we assessed these clinical and biochemical parameters to check whether these parameters were associated with type 2 diabetes-associated *RAGE* SNPs. Since diabetes and its complications

remain asymptomatic until the appearance of the first symptoms or diagnosis,[114, 147] it is crucial to detect them early to reverse, stop, or regress diabetes and its complications' advancement. Any association of SNPs with diabetes or diabetic nephropathy onset can serve as a disease risk biomarker, enabling the screening of individuals vulnerable to disease development at a much earlier stage for early preventive measures.

3.2. Materials and Methods

3.2.1 Study design

We designed a case-control study to investigate the association between *RAGE* SNPs and type 2 diabetes. Some type 2 diabetes subjects had diabetic nephropathy, and hence *RAGE* SNPs were also evaluated for their association with diabetic nephropathy. DNA was extracted from the blood samples of healthy, type 2 diabetes subjects without nephropathy (DM) and type 2 diabetes subjects with nephropathy (DN). The full-length *RAGE* gene was PCR amplified from each sample, and the amplicons were sequenced by ONT for the purpose of identifying all genetic variations associated with the gene (such as SNPs and indels). This approach enabled us to determine the genotype and allele frequencies of the detected *RAGE* SNPs in each subject group and the possibility of detecting any novel *RAGE* gene polymorphisms in our cohort group. Appropriate statistical tests were performed to investigate the association of specific genotypes and alleles with type 2 diabetes and diabetic nephropathy. Four previously reported SNPs (rs3134940, rs1800624, rs1800625, and rs2070600), which were also detected by nanopore sequencing in the samples used in this study, were cross-validated by the PCR-RFLP method in all of the samples. To evaluate the impact of SNPs associated with type 2 diabetes, the levels of diabetes-associated biochemical markers such as FBG, HbA_{1c}, fructosamine, glycated albumin, TNF-α, MDA, fasting insulin, HOMA-IR, and CRP were compared between the wild-type and carrier genotype subjects.

3.2.2 Subjects

A total of 128 subjects who were confirmed as type 2 diabetic, with or without diabetic nephropathy, and 71 unrelated healthy subjects were recruited in this study at Bharati Vidyapeeth (DTU) Medical College, Pune, India. Subjects having FBG ≥126 mg/dL were diagnosed as type 2 diabetic according to the 2003 ADA diagnostic criteria for diabetes.[148] Type 2 diabetic subjects were further divided into two subgroups, i.e., without diabetic nephropathy (n = 86), having a urinary albumin-to-creatinine ratio (UACR) < 30 mg/g, and with diabetic nephropathy (n = 42), having a UACR ≥ 30 mg/g. Type 2 diabetes subjects with

diabetic complications other than diabetic nephropathy, type 1 diabetic subjects, pregnant women, subjects with angina or heart failure, and patients suffering from severe concurrent illness were not included in the study. The ethics committee of Bharati Vidyapeeth (DTU) Medical College, Pune, approved the study, and each participant gave written informed consent before participating.

3.2.3 Biochemical analysis

Clinical and biochemical parameters such as age, sex, FBG, HbA_{1c}, blood urea, serum creatinine, cholesterol, triglyceride, high-density lipoprotein (HDL), fasting insulin, and CRP were measured for each participating subject at Bharati Vidyapeeth (DTU) Medical College, Pune. Besides these parameters, the plasma concentration of total protein (estimated by Bradford's method), fructosamine (using the fructosamine assay kit from Abbexa Ltd, Cambridge, UK), albumin (using bromocresol green albumin assay kit MAK124 from Sigma-Aldrich), glycated albumin (using the Human glycated albumin ELISA kit, CSB-E09599h, Cusabio, China), and MDA (using lipid peroxidation assay kit from Sigma-Aldrich), were determined. The plasma fructosamine concentration was normalized to the total plasma protein concentration and was expressed as µM/g of plasma protein. To determine the plasma glycated albumin concentration, a four-parameter logistic regression curve was plotted using the web tool GainData ELISA data calculator (Arigo Biolaboratories, Hsinchu City 300, Taiwan). Glycated albumin concentration was normalized with respective plasma albumin concentrations and expressed in µM/g of albumin. The calculation of HOMA-IR was done using the following formula.[149]

HOMA-IR = [fasting glucose (mmol/L) X fasting insulin (mIU/L)] / 22.5

3.2.4 Nanopore DNA sequencing of *RAGE* gene

3.2.4.1 DNA isolation from blood and PCR amplification of *RAGE* gene

The genomic DNA was extracted from whole blood collected from subjects enrolled in the study using a DNA isolation kit (Qiagen, Hilden, Germany) and used as template DNA to amplify the *RAGE* gene. The nucleotide sequence of the *RAGE* gene was retrieved from NCBI with gene ID-177 (Oct 2022). Forward and reverse primers were designed such that the complete *RAGE* gene could be amplified along with promoter region and 5' UTR and 3' UTR regions. The nucleotide sequence of the forward primer was 5'-GGGCAGTTCTCTCCTCACTT-3', and that of the reverse primer was 5'-

GCAAAGTTCCCTCTGACTCTTCC-3'. All PCR amplifications were performed in 25 µL reaction volume using the LongAmp Taq 2X master mix PCR reactions (New England BioLabs Inc, Ipswich, MA, USA) with the addition of 25 ng of genomic DNA as a template and 0.2 µmol/L of each primer. The PCR reactions were performed using a Veriti 96-well thermal cycler (Applied Biosystems, Foster City, California, USA) using the following protocol: initial heating of the reaction mixture at 95 °C for 10 min, 35 cycles of denaturation at 95 °C for 30 s, primer annealing at 61 °C for 30 s, and extension at 65 °C for 5 min. The last extension step was carried out at 65 °C for 10 min, after which the reaction mixture was cooled to 4 °C.

3.2.4.2 Oxford nanopore DNA sequencing library preparation

For sequencing the DNA amplicons, the sequencing library was prepared using the ONT Ligation Sequencing (SQK-LSK109) and Native Barcoding (EXP-NBD196) Kits. The *RAGE* amplicons were first purified using 1X AMPure XP beads (Beckman Coulter, USA), and DNA concentration was measured using Qubit dsDNA BR Assay Kit (Invitrogen, USA) on a Qubit 2.0 fluorometer (Invitrogen, USA). A total of 200 fmol of each amplicon, i.e., 517 ng, was taken forward for the end-repair step, where the 3' end was A tailed using NEBNext Ultra II End Prep Enzyme Mix (New England BioLabs Inc, USA). The reaction mixture was kept at 20 °C for 10 min and then heated at 65 °C for 10 min. Following the end-repair step, the amplicons were attached with barcodes available from the EXP-NBD196 kit (Oxford Nanopore Technologies, UK) using the 1X Blunt/TA ligase reaction (New England BioLabs Inc, USA). The reaction mixture was kept at RT for 20 min and then heated at 65 °C for 10 min to denature the enzyme and stop the ligation reaction. The barcoded samples were kept in ice for 1 min and pooled, and the pooled barcoded library was purified by using the AMPure XP beads (0.4X of sample volume) from the SQK-LSK109 kit (Oxford Nanopore Technologies, UK). The washed library was eluted in 35 µl nuclease-free water and quantified by the Qubit 2.0 fluorometer. Next, the sequencing adapters were added to the ends of the barcoded DNA fragments by combining 200 fmol of the purified library with Adapter Mix II (Oxford Nanopore Technologies, UK) and Quick T4 ligase (New England BioLabs Inc, USA) and incubating this reaction mixture for 30 min at room temperature. The adapter-ligated library was purified using 1X AMPure XP beads according to the manufacturer's protocol for SQK-LSK109 kit (Oxford Nanopore Technologies, UK). The final adapter-ligated purified library (50 fmol) was loaded onto the FLO-MIN106D flow cell, and sequencing was done on the GridION MK1 sequencer (Oxford Nanopore Technologies,

UK) until at least 200 sequence reads were collected for each barcode.

3.2.4.3 Analysis of Oxford nanopore sequence reads and variant calling

While sequencing the samples, real-time base calling and demultiplexing were carried out using the Guppy v.5.0.14 program, which is part of the MinKNOW v21.05.12 operating software (Oxford Nanopore Technologies, UK), which runs the GridION sequencer. The super-accurate base calling model was selected for base calling, and demultiplexing was performed using the 'require barcodes at both ends' option. A bash script was written to perform all the steps required for further analysis, such as length filtering, variant calling, and generation of consensus assembly. The bash script can be accessed through the GitHub link https://github.com/ajinkyakhilari/ampvar. After the demultiplexing step, the read length and quality filtering was carried out using the NanoFilt software v2.5.0.[150] Minimap2 v2.24[151] was used to align the length and quality-filtered nanopore reads to the sequence of full-length human Chromosome 6 (where the *RAGE* gene is located) downloaded from GenBank (ncbi.nlm.nih.gov/genome/gdv/browser/gene/?id=7124, Oct 2022). The individual aligned reads were sorted according to genomic coordinates using the SAMtools v1.14[152] sort command, and variant calling was performed on the aligned and sorted reads using the Nanopolish v0.13[153] variant caller with the ploidy set to 2. Thereafter, *de novo* assembly and read polish were carried out using Canu v2.2,[154] Racon v1.4.3,[155] and Medaka v1.5[156] programs using their default parameter settings. Variant calling and annotation were performed using the SnpEff v4.3[157] from the Galaxy ToolShed,[158] and all *RAGE* SNPs detected were analyzed for linkage disequilibrium using the web tool SNPStats.[159]

3.2.5 Genotyping of the *RAGE* gene by PCR-RFLP

Four previously reported SNPs of the *RAGE* gene (rs3134940, rs1800624, rs1800625, and rs2070600) were detected by nanopore sequencing in the samples analyzed in this study, and these were verified using the PCR-RFLP method. Previously reported primers were used to amplify the regions of the *RAGE* gene containing these SNPs,[160-162] except the reverse primer for rs1800624. Table 3.1 shows the summary of the primer sequences employed for PCR amplification and the corresponding lengths for PCR products.

Table 3.1 PCR-RFLP primer pair used for the amplification of a region spanning the polymorphic site of the *RAGE* gene and the size of PCR-amplified product

SNP	Primer sequence	PCR product size (bp)
rs3134940	Forward primer: 5'-TAATTTCCTGCCCCATTCTG-3'	396
	Reverse primer: 5'-CATCGCAATCTATGCCTCCT-3'	
rs1800624	Forward primer: 5'-GGGGCAGTTCTCTCCTCACT-3'	502
	Reverse primer: 5'-CGTCTTGTCACAGGGAATGC-3'	
rs1800625	Forward primer: 5'-GGGGCAGTTCTCTCCTCACT-3'	249
	Reverse primer: 5'-GGTTCAGGCCAGACTGTTGT-3'	
rs2070600	Forward primer: 5'-GTAAGCGGGGCTCCTGTTGCA-3'	397
	Reverse primer: 5'-GGCCAAGGCTGGGGTTGAAGG-3'	

All PCR amplifications were carried out in a reaction volume of 15 µL by adding 10 ng of genomic DNA as a template and 0.3 µmol/L of each primer of primer pair in the master mix for PCR reactions (New England BioLabs Inc, USA). The PCR amplification protocol was the same as that used for amplifying the *RAGE* gene, except that the primer annealing temperature was set at 62 °C. The restriction digestion of the PCR amplicons was carried out using specific restriction enzymes (New England BioLabs Inc, USA) for each SNP, the details of which are shown in Table 3.2. The digested PCR products were separated on a 2.5% (w/v) agarose gel, and UV light was used to visualize DNA bands. The number and size of DNA bands enabled differentiation between homozygous wild-type, heterozygous, and homozygous mutant subjects for the particular SNP, as shown in Table 3.2.

Table 3.2 Restriction enzymes used for SNP detection by PCR-RFLP, restriction sites, and the size of restriction digestion products

SNP	Restriction enzyme	Restriction site	Sequence in wild-type allele	Sequence in mutant allele	Restriction digestion product size (bp)	
					Wild-type	Mutant
rs3134940	BsmF1	GGGAC (10/14)*	GG**A**AC	GG**G**AC	396	160 + 236 (RS creation)
rs1800624	Mfe1	C/AATTG	CAA**T**TG	CAA**A**TG	215 + 287	502 (RS deletion)
rs1800625	Alu1	AG/CT	AG**T**T	AG**C**T	249	89 + 160 (RS creation)
rs2070600	Alu1	AG/CT	**G**GCT	**A**GCT	248 + 149	181 + 67 + 149 (RS creation)

*BsmFI cuts ten nucleotides away from the restriction site in the same DNA strand and 14 nucleotides away in the complementary DNA strand.
The nucleotide at the polymorphic site is represented by bold font.
RS: Restriction site

3.2.6 Statistical analysis

GraphPad Prism for Windows version 8.0.2 (GraphPad Software Inc, California, USA) or SPSS version 17.0 (SPSS Inc. Chicago, IL, USA) was used to perform all statistical tests. The clinical characteristics of the subjects were presented as mean ± standard deviation (SD). The clinical characteristics and biochemical parameters across the groups were compared by one-way ANOVA followed by a *post hoc* Tukey's test. Biochemical parameters were compared between wild-type and carriers (heterozygous and homozygous mutants) using an unpaired Student's *t*-test. The Chi-square test was used to compare the intergroup genotype and allele distributions, but Fisher's exact test was used for comparing genotype and allele distribution in cases where the number of subjects in any of the groups being compared was less than five. The association of the *RAGE* SNPs with clinical parameters was investigated using logistic regression analysis. A p-value < 0.05 was considered significant. The odds ratio (OR) and 95 % confidence interval (CI) were also calculated.

3.3 Results

3.3.1 Clinical characteristics of healthy control, DM, DN, and DM+DN subjects

Table 3.3 presents a summary of the clinical characteristics of all the participating subjects. The age of the participants was not significantly different in different groups. The DM, DN, and DM + DN groups had significantly higher FBG, HbA_{1c}, and triglyceride levels than the healthy control group. FBG and triglycerides in the DN group were higher than in the DM group. Cholesterol levels were higher in the DN and DM + DN groups than in the healthy group. Blood urea and serum creatinine, which reflect the nitrogenous waste content in the blood, were significantly higher in the DN group than in the DM and healthy control groups. Similarly, in comparison to the healthy control group, the DM + DN group also had elevated levels of blood urea and serum creatinine. The DN and DM + DN groups had higher cholesterol and lower HDL levels than the healthy group.

Table 3.3 Clinical characteristics of healthy control, DM, DN, and DM + DN subjects

Clinical characteristics	Healthy	DM	DN	DM + DN
Age (years)	55.77 ± 10.16	56.4 ± 9.58	58.71 ± 11.27	57.16 ± 10.18
Sex (male/female)	37/34	43/43	27/15	70/58
Fasting blood glucose (mg/dL)	99.73 ± 8.28	218.9 ± 79.48†	251.5 ± 78.06†‡	229.6 ± 80.19†
HbA_{1c} (%)	5.54 ± 0.59	9.15 ± 2.16†	8.52 ± 1.91†	8.94 ± 2.1†
Blood urea (mg/dL)	22.93 ± 6.83	24.52 ± 7.85	87.71 ± 28.63†‡	45.26 ± 34.54†
Serum creatinine (mg/dL)	0.82 ± 0.14	0.88 ± 0.19	4.8 ± 1.99†‡	2.17 ± 2.17†
Cholesterol (mg/dL)	149.3 ± 35.28	159.7 ± 43.71	177.8 ± 44.24†	165.7 ± 44.54†
Triglyceride (mg/dL)	106.3 ± 34.92	138.9 ± 75.99†	187.1 ± 85.05†‡	154.7 ± 81.95†

Clinical characteristics	Healthy	DM	DN	DM + DN
HDL (mg/dL)	42.27 ± 9.18	38.81 ± 12.01	34.68 ± 11.18†	37.45 ± 11.86†
Normalized fructosamine (µM/g)	25.86 ± 10.06 (51)	38.26 ± 13.61† (64)	40.66 ± 15.00† (40)	39.19 ± 14.14† (104)
Normalized glycated albumin (µM/g)	0.77 ± 0.31 (51)	1.02 ± 0.39† (64)	1.18 ± 0.44† (40)	1.08 ± 0.41† (104)
TNF-α (pg/mL)	16.97 ± 22.00 (26)	18.97 ± 19.83 (22)	37.76 ± 54.28 (28)	29.50 ± 43.36 (50)
MDA (nM/mL)	39.18 ± 28.22 (29)	51.81 ± 33.8 (24)	46.18 ± 31.72 (31)	48.64 ± 32.46 (55)
Insulin (µM/mL)	17.38 ± 16.66 (59)	17.69 ± 17.3 (68)	20.19 ± 48.04 (36)	18.55 ± 31.31 (104)
HOMA-IR	4.23 ± 4.12 (59)	8.96 ± 7.68 (68)	14.01 ± 38.27 (36)	10.71 ± 23.28 (104)
CRP (mg/L)	16.33 ± 39.97 (53)	35.37 ± 60.31 (66)	53.15 ± 78.37 (36)	41.65 ± 67.39 (102)

Data are presented as mean ± SD or number of subjects
Number of subjects: healthy, n = 71; DM, n = 86; DN, n = 42; unless otherwise mentioned
Data in parentheses represent the number of subjects
†$p < 0.05$ vs healthy; ‡$p < 0.05$ vs DM
HDL: High-density lipoprotein; TNF-α: Tumor necrosis factor-α

Normalized fructosamine concentration, which reflects a measure of glycation of all plasma proteins, was significantly elevated in DM, DN, and DM + DN groups compared to the healthy control group. Similarly, the normalized glycated albumin concentration was higher in DM, DN, and DM + DN groups compared to the healthy control group. However, normalized fructosamine and normalized glycated albumin levels were not significantly different between the DM and DN groups. There were no significant differences observed in the plasma levels of inflammatory cytokine TNF-α, MDA, insulin, HOMA-IR, and CRP

among the subject groups.

3.3.2 PCR amplification and SNP detection by nanopore sequencing of the *RAGE* gene

PCR amplification of the *RAGE* gene was verified by agarose gel electrophoresis and confirmed to be in the expected size of ~4kb (Appendix 3). From nanopore sequencing of the *RAGE* gene amplicons, a total of 33 polymorphisms, including eight exon variants, 18 intron variants, five upstream variants, one 3 'UTR variant, and one downstream variant of the *RAGE* gene, were detected. During validation by PCR-RFLP analysis, we observed that there was a discrepancy in the detection of rs3134940 by nanopore sequencing for one healthy and one diabetic sample. To resolve this discrepancy, Sanger sequencing of the amplicons spanning the mutation was carried out for these two samples (Appendix 4). In this case, the results from Sanger sequencing agreed with the PCR-RFLP results, and based on this, the result of two discrepant cases was rectified in the SNP distribution detected by nanopore sequencing. The details of the *RAGE* polymorphisms and their distribution in healthy, DM, DN, and DM + DN groups are presented in Figure 3.1 and Table 3.4, respectively.

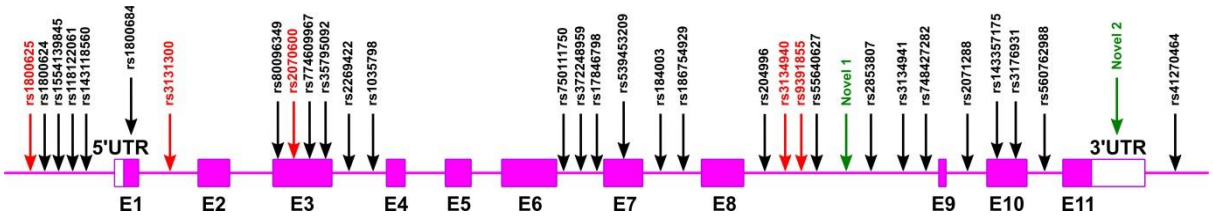

Figure 3.1 Schematic representation of the *RAGE* gene depicting the location of the polymorphisms detected

The locations of all the polymorphisms detected in this study are shown by arrows. Previously reported polymorphisms are shown by black arrows, whereas the two novel polymorphisms are indicated by green arrows. SNPs associated with type 2 diabetes are shown by red arrows.

Out of 33 *RAGE* polymorphisms detected, two SNPs are reported here for the first time, and these were not found in dbSNP (https://www.ncbi.nlm.nih.gov/snp, Oct 2022). One of these two novel variants is located on intron 8, causing a nucleotide change from G to A at position 32181834 of chromosome 6, and was detected in 0.5 % of the subjects. The other novel variant is a deletion mutation, causing the nucleotide change from CAG to G in the 3 'UTR of the *RAGE* gene at position 32181132 of chromosome 6 and was detected in 2.6 % of the subjects.

3.3.3 Association of the mutations with cohort groups

Due to the low frequency of homozygous mutant genotypes of the *RAGE* polymorphisms, we performed association analyses using the dominant inheritance model. For this, the subjects were grouped into homozygous wild-type and carrier populations (including both the heterozygous and homozygous mutant genotypes). The result of the association study is summarized in Table 3.5. The SNP rs1554139845 causes insertion/deletion of 63 bp stretch in the *RAGE* upstream region. Since rs1800624 is located within this 63 bp stretch, deletion of this 63 bp also causes the absence of the location at which the SNP rs1800624 occurs. Hence, 10 subjects in the present study carrying rs1554139845 were not considered while analyzing the genotype distribution and allele frequency of rs1800624. Among 33 *RAGE* polymorphisms detected, five SNPs were found to be linked with an elevated type 2 diabetes risk. The DM group showed a significantly greater frequency of SNP rs1800625 (OR = 2.104, p = 0.041) as compared to the healthy group. However, this SNP was not associated with the DN group. Similarly, when DM and DN groups were merged as a diabetic group (DM + DN) and compared to the healthy group, the extent of the association of rs1800625 with the merged diabetic group was reduced (OR = 1.823, p = 0.081). The SNP rs3134940 and rs3131300 were found to be in perfect linkage disequilibrium with rs1800625 (Appendix 5). Hence their association with DM and DN groups was the same as that of rs1800625.

The SNP rs2070600 was significantly associated with the DM group than the healthy group (OR = 2.235, p = 0.044). However, rs2070600 was not associated with the DN group compared to the healthy or DM group. When DM and DN groups were merged as a diabetic group, rs2070600 was associated with the merged diabetic group (DM + DN) compared to the healthy group (OR = 2.134, p = 0.0444). Thus, this SNP is more strongly associated with type 2 diabetes than the other three SNPs discussed earlier. The SNP rs9391855 was found in perfect linkage disequilibrium with rs2070600 (Appendix 5); hence, this SNP was also associated with DM and DM + DN group than the healthy group. The rest of the polymorphisms detected did not show any association with the DM or DM + DN group. When the DN group was compared with the DM group as a control, none of the 33 polymorphisms detected were associated with the DN group. Association analysis couldn't be performed for many low-frequency polymorphisms due to the absence of carrier genotypes in one or more subject groups. A few other SNPs were also found to be in perfect linkage disequilibrium with each other (Appendix 5 and Appendix 6). Wild-type major allele and mutated minor allele frequencies for *RAGE* polymorphisms were calculated and are presented

in Appendix 7. Appendix 8 presents the results of allele association with type 2 diabetes or diabetic nephropathy. We conclude that no association was found between any of the detected alleles from the *RAGE* gene and type 2 diabetes or diabetic nephropathy.

Table 3.4 SNPs detected in the *RAGE* gene, their position on chromosome 6, location on the gene, nucleotide change, and genotype distribution among healthy, DM, DN, and DM + DN groups

Polymorphism	Genomic position	Location	Wild-type allele/mutated allele	Healthy		DM		DN		DM + DN	
				Wild-type	Mutant	Wild-type	Mutant	Wild-type	Mutant	Wild-type	Mutant
rs1800625	32184665	Upstream	T/C	56	15	55	31	31	11	86	42
rs1800624	32184610	Upstream	T/A	50	16	64	20	28	11	92	31
rs1554139845	32184580	Upstream	63 bp deletion[#]	66	5	84	2	39	3	123	5
rs118122061	32184479	Upstream	G/A	70	1	83	3	41	1	124	4
rs143118560	32184478	Upstream	A/T	71	0	85	1	42	0	127	1
rs1800684	32184217	Exon 1	T/A	68	3	83	3	39	3	122	6
rs3131300	32184157	Intron 1	T/C	56	15	55	31	31	11	86	42
rs80096349	32183681	Exon 3	C/T	70	1	86	0	42	0	128	0
rs2070600	32183666	Exon 3	G/A	60	11	61	25	31	11	92	36
rs774609967	32183650	Exon 3	C/T	70	1	86	0	42	0	128	0
rs35795092	32183643	Exon 3	C/G	68	3	86	0	42	0	128	0
rs2269422	32183517	Intron 3	A/G	64	7	78	8	37	5	115	13

Polymorphism	Genomic position	Location	Wild-type allele/mutated allele	Healthy		DM		DN		DM + DN	
				Wild-type	Mutant	Wild-type	Mutant	Wild-type	Mutant	Wild-type	Mutant
rs1035798	32183445	Intron 3	C/T	52	19	66	20	31	11	97	31
rs750111750	32182808	Intron 6	G/A	71	0	86	0	41	1	127	1
rs372248959	32182728	Intron 6	T/C	71	0	84	2	42	0	126	2
rs17846798	32182721	Intron 6	C/T	66	5	84	2	39	3	123	5
rs539453209	32182697	Exon 7	G/C	70	1	86	0	42	0	128	0
rs184003	32182519	Intron 7	G/T	43	28	51	35	25	17	76	52
rs186754929	32182494	Intron 7	G/A	70	1	86	0	40	2	126	2
rs204996	32182106	Intron 8	G/A	58	13	76	10	36	6	112	16
rs3134940	32182039	Intron 8	A/G	56	15	55	31	31	11	86	42
rs9391855	32182024	Intron 8	G/A	60	11	61	25	31	11	92	36
rs55640627	32181979	Intron 8	G/A	67	4	81	5	41	1	122	6
Novel 1	32181834	Intron 8	G/A	70	1	86	0	42	0	128	0
rs2853807	32181795	Intron 8	C/T	58	13	76	10	36	6	112	16
rs3134941	32181760	Intron 8	G/C	56	15	58	28	31	11	89	39

Polymorphism	Genomic position	Location	Wild-type allele/mutated allele	Healthy		DM		DN		DM + DN	
				Wild-type	Mutant	Wild-type	Mutant	Wild-type	Mutant	Wild-type	Mutant
rs748427282	32181673	Intron 8	C/T	71	0	85	1	42	0	127	1
rs2071288	32181483	Intron 9	G/A	66	5	84	2	39	3	123	5
rs143357175	32181442	Exon 10	C/T	66	5	81	5	36	6	117	11
rs3176931	32181363	Exon 10	G/A	66	5	84	2	41	1	125	3
rs560762988	32181266	Intron 10	C/T	71	0	86	0	41	1	127	1
Novel 2	32181132	3' UTR	CAG/G	70	1	83	3	41	1	124	4
rs41270464	32180947	Downstream	G/A	66	5	79	7	38	4	117	11

[#]63 bp deletion: TTCCCCAGCCTTGCCTTCATGATGCAGGCCCAATTGCACCCTTGCAGACAACAGTCTGGCCTGA/A

Table 3.5 Association of polymorphisms detected in the *RAGE* gene with type 2 diabetes and diabetic nephropathy

Polymorphism	Healthy vs DM			Healthy vs DN			DM vs DN			Healthy vs DM + DN		
	χ^2	*p*	OR (95% CI)	χ^2	*p*	OR (95% CI)	χ^2	*p*	OR (95% CI)	χ^2	*p*	OR (95% CI)
rs1800625	**4.179**	**0.041**	**2.104 (1.039-4.396)**	0.382	0.537	1.325 (0.545-3.351)	1.243	0.265	0.63 (0.292-1.415)	3.051	0.081	1.823 (0.933-3.546)
rs1800624	0.004	0.951	0.977 (0.467-2.124)	0.202	0.654	1.228 (0.501-3.104)	0.273	0.601	1.257 (0.545-2.89)	0.021	0.884	1.053 (0.543-2.073)
rs1554139845	-	0.246	0.314 (0.061-1.547)	-	>0.999	1.015 (0.258-4.174)	-	0.33	3.231 (0.633-18.59)	0.941	0.332	0.537 (0.168-1.723)
rs118122061	-	0.627	2.53 (0.369-33.28)	-	>0.999	1.707 (0.088-32.84)	-	>0.999	0.675 (0.051-4.656)	-	0.657	2.258 (0.362-27.99)
rs143118560	-	-	-	-	-	-	-	-		-	-	-
rs1800684	-	>0.999	0.819 (0.187-3.602)	-	0.669	1.744 (0.39-7.713)	-	0.393	2.128 (0.477-9.38)	-	>0.999	1.115 (0.294-4.17)
rs3131300	**4.179**	**0.041**	**2.104 (1.039-4.396)**	0.382	0.537	1.325 (0.545-3.351)	1.243	0.265	0.63 (0.292-1.415)	3.051	0.081	1.823 (0.933-3.546)
rs80096349	-	-	-	-	-	-	-	-		-	-	-
rs2070600	**4.057**	**0.044**	**2.235 (1.042-4.773)**	1.926	0.165	1.935 (0.741-5.059)	0.116	0.734	0.866 (0.393-2.019)	**4.039**	**0.044**	**2.134 (1.035-4.667)**

Polymorphism	Healthy vs DM			Healthy vs DN			DM vs DN			Healthy vs DM + DN		
	χ^2	*p*	OR (95% CI)	χ^2	*p*	OR (95% CI)	χ^2	*p*	OR (95% CI)	χ^2	*p*	OR (95% CI)
rs774609967	-	-	-	-	-	-	-	-		-	-	-
rs35795092	-	-	-	-	-	-	-	-		-	-	-
rs2269422	0.014	0.906	0.938 (0.313-2.497)	0.116	0.733	1.236 (0.408-3.937)	0.209	0.647	1.318 (0.454-3.984)	0.004	0.947	1.034 (0.414-2.648)
rs1035798	0.256	0.613	0.829 (0.415-1.667)	0.004	0.947	0.971 (0.417-2.264)	0.132	0.716	1.171 (0.515-2.64)	0.157	0.692	0.875 (0.448-1.704)
rs750111750	-	-	-	-	-	-	-	-		-	-	-
rs372248959	-	-	-	-	-	-	-	-		-	-	-
rs17846798	-	0.246	0.314 (0.061-1.547)	-	>0.999	1.015 (0.258-4.174)	-	0.33	3.231 (0.633-18.59)	0.941	0.332	0.537 (0.168-1.723)
rs539453209	-	-	-	-	-	-	-	-		-	-	-
rs184003	0.026	0.873	1.054 (0.555-2.025)	0.012	0.913	1.044 (0.48-2.282)	0.001	0.981	0.991 (0.46-2.043)	0.027	0.87	1.051 (0.585-1.938)
rs186754929	-	-	-	-	0.554	3.5 (0.393-51.33)	-	-		-	>0.999	1.111 (0.127-16.31)

Polymorphism	Healthy vs DM			Healthy vs DN			DM vs DN			Healthy vs DM + DN		
	χ^2	*p*	OR (95% CI)	χ^2	*p*	OR (95% CI)	χ^2	*p*	OR (95% CI)	χ^2	*p*	OR (95% CI)
rs204996	1.389	0.239	0.587 (0.236-1.409)	0.306	0.58	0.744 (0.256-2.142)	0.182	0.669	1.267 (0.416-3.55)	1.238	0.266	0.637 (0.295-1.411)
rs3134940	**4.179**	**0.041**	**2.104 (1.039-4.396)**	0.382	0.537	1.325 (0.545-3.351)	1.243	0.265	0.63 (0.292-1.415)	3.051	0.081	1.823 (0.933-3.546)
rs9391855	**4.057**	**0.044**	**2.235 (1.042-4.773)**	1.926	0.165	1.935 (0.741-5.059)	0.116	0.734	0.866 (0.393-2.019)	**4.039**	**0.044**	**2.134 (1.035-4.667)**
rs55640627	-	>0.999	1.034 (0.294-3.478)	-	0.649	0.409 (0.033-2.632)	-	0.663	0.395 (0.033-3.084)	-	0.747	0.824 (0.211-2.663)
Novel 1	-	-	-	-	-	-	-	-		-	-	-
rs2853807	1.389	0.239	0.587 (0.236-1.409)	0.306	0.58	0.744 (0.256-2.142)	0.182	0.669	1.267 (0.416-3.55)	1.238	0.266	0.637 (0.295-1.411)
rs3134941	2.556	0.11	1.802 (0.874-3.805)	0.382	0.537	1.325 (0.545-3.351)	0.54	0.462	0.735 (0.338-1.677)	2.016	0.156	1.636 (0.829-3.203)
rs748427282	-	-	-	-	-	-	-	-		-	-	-
rs2071288	-	0.246	0.314 (0.061-1.547)	-	>0.999	1.015 (0.258-4.174)	-	0.33	3.231 (0.633-18.59)	0.941	0.332	0.537 (0.168-1.723)

Polymorphism	Healthy vs DM			Healthy vs DN			DM vs DN			Healthy vs DM + DN		
	χ^2	*p*	**OR (95% CI)**	χ^2	*p*	**OR (95% CI)**	χ^2	*p*	**OR (95% CI)**	χ^2	*p*	**OR (95% CI)**
rs143357175	0.098	0.754	0.815 (0.252-2.639)	1.576	0.209	2.2 (0.579-6.928)	2.578	0.108	2.7 (0.715-8.434)	0.149	0.7	1.241 (0.435-3.328)
rs3176931	-	0.246	0.314 (0.061-1.547)	-	0.409	0.322 (0.027-2.533)	-	>0.999	1.024 (0.069-9.004)	-	0.137	0.317 (0.082-1.255)
rs560762988	-	-	-	-	-	-	-	-		-	-	-
Novel 2	-	0.627	2.53 (0.369-33.28)	-	>0.999	1.707 (0.088-32.84)	-	>0.999	0.675 (0.051-4.656)	-	0.657	2.258 (0.362-27.99)
rs41270464	0.066	0.797	1.17 (0.383-3.405)	-	0.725	1.389 (0.405-5.045)	-	0.75	1.188 (0.37-4.1)	0.149	0.7	1.241 (0.435-3.328)

χ^2: Chi-square value; OR: Odds ratio; CI: Confidence interval, the text in the bold indicates significant association.

3.3.4 Validation of mutations identified in nanopore sequencing of the RAGE gene by PCR-RFLP

PCR-RFLP was used to detect the SNPs rs3134940, rs1800624, rs1800625, and rs2070600 to compare and validate the nanopore sequencing results. These four SNPs were chosen for the comparison as they have a relatively high frequency than most of the other SNPs in the *RAGE* gene and have been most investigated for their association with diabetes and diabetic complications.[163] The restriction enzymes used for the digestion of PCR-amplified products for detecting these SNPs, restriction sites, and the size of restriction-digested products for wild-type and mutant allele are summarized in Table 3.2. The nucleotide change caused by rs3134940, rs1800625, and rs2070600 results in the creation of a restriction site, whereas rs1800624 causes the deletion of the restriction site for the restriction enzymes, as mentioned in Table 3.2. A representative agarose gel image depicting DNA bands corresponding to undigested PCR-amplified products and restriction-digested products of different genotypes for the four SNPs is shown in Figure 3.2. The results of genotype distribution, allele frequencies, and their association with type 2 diabetes and diabetic nephropathy were the same, as shown in Tables 3.4-3.5 and Appendix 7-8. There was 99.75 % agreement between nanopore and PCR-RFLP genotyping results, with only two discrepant cases out of 199 samples for the four *RAGE* SNPs detected by the two methods (Appendix 4).

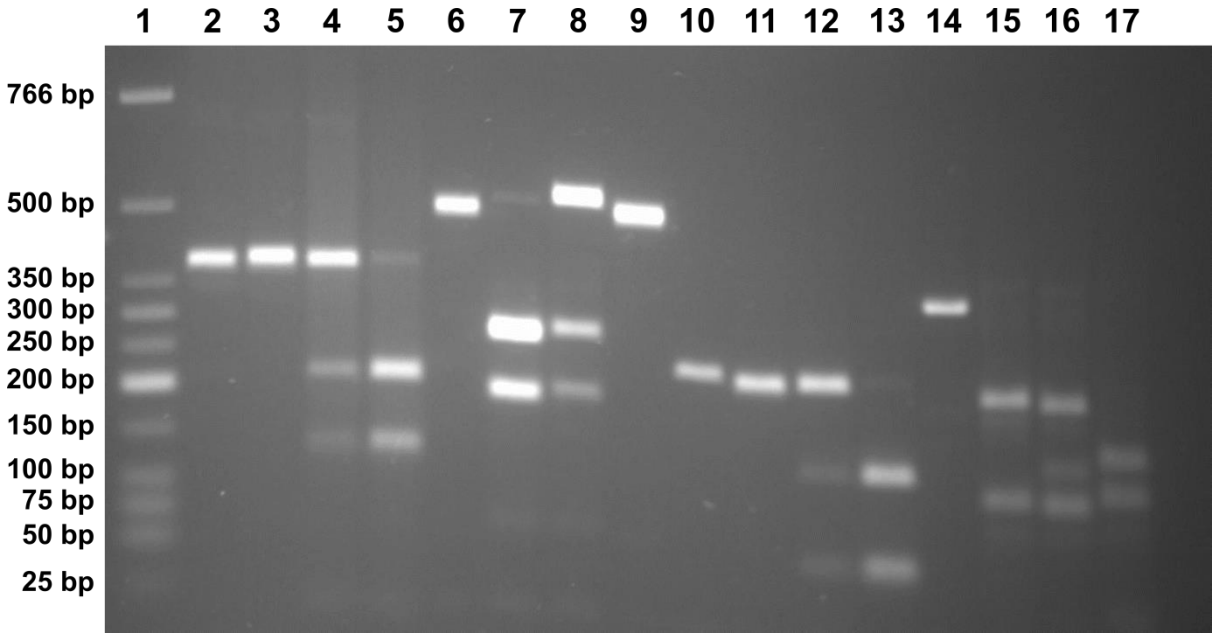

Figure 3.2 PCR-amplified and restriction-digested products for SNPs rs3134940, rs1800624, rs1800625, and rs2070600

Lane 1: Low molecular weight DNA ladder. Lane 2: PCR-amplified product for rs3134940. Lanes 3-5: Restriction digested products of wild-type (AA), heterozygous (AG), and homozygous mutant (GG) genotypes of rs3134940, respectively. Lane 6: PCR-amplified product for rs1800624. Lanes 7-9: Restriction digested products of wild-type (TT), heterozygous (TA), and homozygous mutant (AA) genotypes of rs1800624, respectively. Lane 10: PCR-amplified product for rs1800625. Lanes 11-13: Restriction digested products of wild-type (TT), heterozygous (TC), and homozygous mutant (CC) genotypes of rs1800625, respectively. Lane 14: PCR-amplified product for rs2070600. Lanes 15-17: Restriction digested products of wild-type (GG), heterozygous (GA), and homozygous mutant (AA) genotypes of rs2070600, respectively.

3.3.5 Association of diabetes-risk-associated SNPs with various clinical parameters

RAGE SNPs showing significant association with type 2 diabetes were checked to determine whether the carrier genotypes of these SNPs were associated with AGEs (fructosamine and glycated albumin), inflammatory cytokine (TNF-α), MDA, insulin, HOMA-IR, CRP and diabetes diagnosis markers (FBG and HbA_{1c}). Unpaired Student's *t*-test revealed that the carrier genotypes of none of these SNPs were associated with any of these clinical and biochemical parameters (Appendix 9). Appendix 10 displays the logistic regression analysis results examining if type 2 diabetes-associated *RAGE* SNPs were associated with any of the clinical parameters. While blood urea, insulin, and CRP were positively associated with rs1800625, rs3134940, and rs3131300, MDA and HOMA-IR were negatively associated. Similarly, HDL showed a negative association with rs2070600 and rs9391855.

3.4 Discussion

Diabetes is a multifactorial disease, and genetics plays a role in developing diabetes and its complications. Among various genes linked to diabetes and its complications, the *RAGE* gene is a potential candidate known to play a role in the pathogenesis of diabetes and its complications. AGE-RAGE signaling increases the expression of inflammatory cytokines and reactive oxygen species, which accelerate the development of diabetes and its complications. As a result, *RAGE* polymorphism may influence the outcomes of the AGE-RAGE interaction. In this study, we first detected all *RAGE* polymorphisms from the subjects by nanopore sequencing of the respective *RAGE* gene amplicons and studied their association with type 2 diabetes and diabetic nephropathy. PCR-RFLP was performed for four *RAGE* SNPs, i.e., rs3134940, rs1800624, rs1800625, and rs2070600, to assess the accuracy and utility of nanopore sequencing as a high-throughput method of SNP detection over conventional PCR-RFLP method.

Table 3.6 summarizes an overall comparison of the findings of this study with the previous reports of *RAGE* SNP association with diabetes and diabetic nephropathy. Earlier reports on the relationship between *RAGE* SNPs and diabetes and its complications have produced conflicting findings.[23] In this study, the SNP rs1800625 was linked to a higher type 2 diabetes risk but not diabetic nephropathy. While some reports conclude no association of rs1800625 with type 1 and type 2 diabetes,[164-167] diabetic nephropathy,[165, 168]and diabetic retinopathy,[169-171] other studies have found an increased type 1 diabetes[172] and diabetic nephropathy risk.[173] The SNP rs1800625 is present in the *RAGE* gene's promoter region. One in vitro study has illustrated a two-fold increase in the expression of the reporter gene caused by the mutant allele of rs1800625.[144] Thus, the increased RAGE expression may lead to increased AGE-RAGE interaction and downstream signaling, which may promote the development of diabetes and its complications.

Table 3.6 Comparison of the results of the present study with previous reports

SNP	Findings of this study	Previous supportive reports	Previous contradictory reports
rs1800625	Increased risk of type 2 diabetes	Increased type 1 diabetes risk[172]	No association with diabetes mellitus[166] and type 2 diabetes[164, 165, 167]
	No association with diabetic nephropathy	No association with diabetic nephropathy (in dominant model)[165, 168]	Increased risk of diabetic nephropathy[173]
rs3134940	Increased risk of type 2 diabetes		No association with diabetes[174] or type 2 diabetes[167]
	No association with diabetic nephropathy		Increased risk of diabetic nephropathy[175] and Decreased risk of diabetic nephropathy[160]
rs2070600	Increased risk of type 2 diabetes	Increased risk of diabetes[174] and type 1 diabetes[176]	No association with type 2 diabetes[164, 177]
	No association with diabetic nephropathy	No association with diabetic nephropathy[173, 175, 177-179]	

The intronic SNP rs3134940 was in perfect linkage disequilibrium with rs1800625. Hence, it was linked to an elevated type 2 diabetes risk but not diabetic nephropathy. However, contradictory to our finding, previous studies have reported that rs3134940 is not associated with type 2 diabetes [167, 174] and an increased[175] or decreased risk[160] of diabetic nephropathy. This SNP was also not associated with chronic kidney disease[180] and diabetic retinopathy.[169, 181, 182] During mRNA processing, introns are spliced from pre-mRNA; therefore, any SNPs in the intron region are least likely to affect the protein. The mechanism by which rs3134940 can increase the risk of diabetes or diabetic complications is unknown. It has been proposed by various groups that rs3134940 may affect the alternative splicing of RAGE mRNA involving the region between intron 7 and 9, which could affect the expression of endogenous secretory RAGE (esRAGE), one of the RAGE isoforms.[160, 181-184] Unlike RAGE, esRAGE is not involved in AGE-RAGE signaling as it lacks intramembrane and cytoplasmic domains. Thus esRAGE functions as a receptor decoy, binding to AGEs, and the physiological level of

esRAGE can affect the extent of AGE-RAGE signaling and the associated pathogenesis. However, no experimental evidence has shown the effect of rs3134940 on esRAGE production.

Compared to the SNPs rs1800625, a stronger association of rs2070600 with type 2 diabetes was observed, even though it was not associated with diabetic nephropathy. These results agreed with those of the previous studies, which reported that rs2070600 increases the risk of diabetes[174, 176] but not diabetic nephropathy.[173, 177-179] However, there are reports contradicting these results, which claim no association between rs2070600 and type 2 diabetes.[164, 177] No literature has reported a clear association between rs2070600 and diabetic nephropathy. The non-synonymous replacement of glycine by serine at the 82nd position of RAGE caused by rs2070600 induces changes in the structure of the variable domain of RAGE[143], which can potentially affect AGE-RAGE signaling. In vitro studies have elucidated that RAGE with rs2070600 has a higher binding affinity for amyloid-beta peptides (Aβ42) and prototypic S100/cangrulin, which upregulated inflammatory mediators.[185, 186] Substitution of glycine with serine at the 82nd position of RAGE promotes N-linked glycosylation of adjacent asparagine residue at the 81st position, which may also affect ligand binding and further downstream signaling initiated by AGE-RAGE interaction.[187] Several studies have also found a significantly lower plasma sRAGE level in the subjects carrying rs2070600,[169, 179, 188, 189] and the same has been elucidated using a cell culture model.[190] Decreased plasma sRAGE levels might fail to sufficiently clear the already elevated plasma AGEs in diabetics, resulting in increased AGE-RAGE signaling. In this study, sRAGE levels were not measured; hence, the contribution of rs2070600 to type 2 diabetes development via sRAGE stands obscure. The discrepancies in the results of *RAGE* SNP association with type 2 diabetes and diabetic nephropathy in this study and previous studies can be attributed to the different environments, lifestyles, genetics, ethnicity, and geography of the study population.

In this study, nanopore sequencing showed a high accuracy of 99.75 % compared to the result of PCR-RFLP. In fact, several studies have reported even up to 100 % concordance between the results of the nanopore and Sanger sequencing, a gold standard approach.[191-194] The high accuracy of the current nanopore sequencing approaches makes it a rapid, cost-effective, and high-throughput approach that can be used for SNP detection, including in clinical diagnostics.[191]

This study reports two novel polymorphisms in our population at positions 32181834 and

32181132 of chromosome 6, which are located in intron 8 and 3' UTR of the *RAGE* gene, respectively. These two SNPs were present at a very low frequency in our study population, and hence a large sample size would be required to sufficiently detect these novel polymorphisms and confidently check for their association with type 2 diabetes and diabetic nephropathy. We also found that none of the SNPs detected were associated with diabetic nephropathy, which could be due to the limited sample size of the diabetic nephropathy group; hence, a study involving a large population size is required.

Fructosamine and glycated albumin levels represent the extent of glycation, and a higher physiological level of AGEs is expected to promote both diabetes and diabetic complications.[131, 141] In this study, both DM and DN groups showed significantly elevated levels of fructosamine, glycated albumin, FBG, and, HbA_{1c}. Yet, these parameters were not associated with the carrier genotypes of the type 2 diabetes-associated SNPs. Hence, the carrier genotypes of type 2 diabetes-associated SNPs may not be involved in the observed disease-specific elevation of these biochemical parameters. These findings are similar to a previous report that found no association between rs1800625 or rs2070600 and AGEs.[195] The level of AGEs can be reasonably expected to be associated with glycemic status, which is elevated in diabetes, rather than gene polymorphisms. The TNF-α levels increase upon AGE-RAGE signaling, followed by NF-κB activation.[131] No association between rs1800625 or rs2070600 and the TNF-α level was observed in this study. Thus, despite the association of rs1800625 and rs2070600 with type 2 diabetes, the carrier genotypes of these SNPs may not have an impact on TNF-α levels. Also, in this study, TNF-α levels did not show an association with type 2 diabetes and diabetic nephropathy. This result is the same as previously found[196] but contradictory to several other reports.[197-199] Further, the carrier genotypes of rs1800625 and rs2070600 were not associated with FBG and HbA_{1c} despite being linked to type 2 diabetes. Also, MDA (a marker for oxidative stress), insulin, HOMA-IR, and CRP were neither elevated in any disease groups nor linked to any type 2 diabetes-associated SNPs assessed by one-way ANOVA and unpaired Student's *t*-test, respectively. Logistic regression analysis revealed that rs1800625 might increase fasting insulin level, and a higher fasting insulin level is linked to insulin resistance and type 2 diabetes.[200] In this study, HOMA-IR was found to be negatively associated with rs1800625, which could be due to the maintenance of blood glucose levels in subjects with high insulin levels undergoing oral hypoglycemic drug treatment. However, recent studies suggest that hyperinsulinemia is a causal factor for glucose intolerance.[200] Therefore, hyperinsulinemia could be a predictor of

future type 2 diabetes risk. CRP, an inflammatory marker, showed a weak positive association with rs1800625. It is reported that an increased CRP level is positively linked to type 2 diabetes risk.[201-203] While MDA showed a weak negative association and blood urea showed a weak positive association with rs1800625 in logistic regression analysis, these results must be verified in a larger cohort to check if the association is due to polymorphism or by chance. Also, HDL was found to be negatively associated with rs2070600 in logistic regression analysis. The association results for rs3134940, rs3131300, and rs9391855 are the same as the corresponding SNPs in complete linkage disequilibrium (Appendix 5 and Appendix 10). Although we have found a weak association of SNPs with insulin and CRP in this study, SNPs are generally not used as diagnostic markers to detect insulin resistance in clinical settings compared to measuring insulin or CRP. In fact, the measurement of blood glucose is sufficient to diagnose diabetes. However, SNPs or other markers such as insulin or CRP could be helpful for predicting type 2 diabetes risk, and both of these parameters are associated with SNP rs1800625.

3.5 Conclusion

In this study, we used the Oxford Nanopore Technology-based DNA sequencing for detecting *RAGE* SNPs, contributing to developing diabetes and its complications. The nanopore sequencing method detected 33 *RAGE* polymorphisms with high accuracy for SNP detection, as validated by PCR-RFLP. Therefore, the application of nanopore sequencing can be extended to identify disease-specific genetic variations in clinical settings. Five of the *RAGE* gene polymorphisms detected, i.e., rs1800625, rs3131300, rs3134940, rs2070600, and rs9391855, were associated with an increased type 2 diabetes risk. The usefulness of these five *RAGE* SNPs as type 2 diabetes risk prediction markers requires to be studied in a larger cohort, which would also facilitate the study of the less frequent *RAGE* SNPs for their association with type 2 diabetes and its complications.

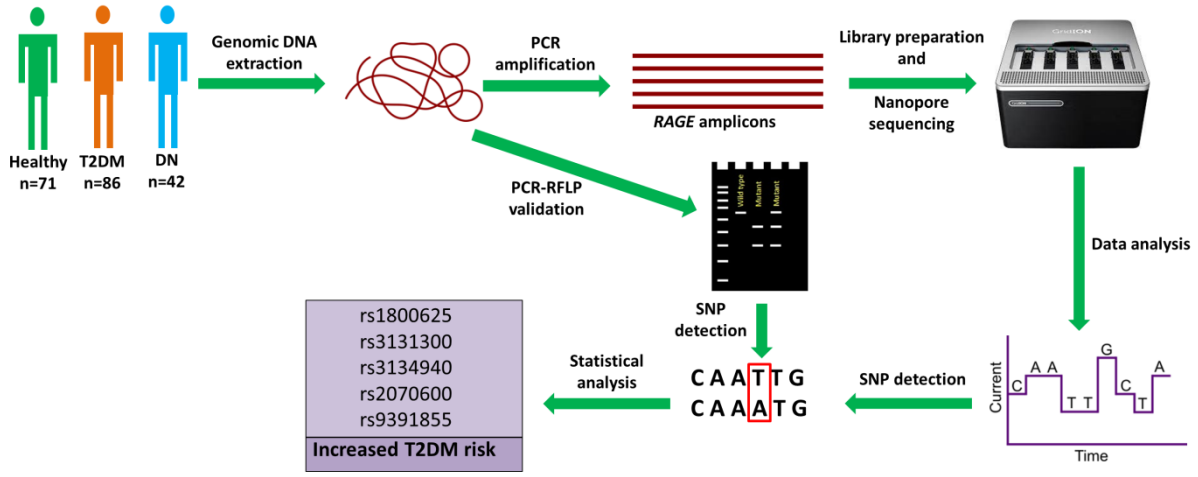

Figure 3.3 Summary figure

References

(1) International Diabetes Federation. IDF Diabetes Atlas, 10th edn. Brussels, Belgium: International Diabetes Federation, 2021.
(2) Kharroubi, A. T.; Darwish, H. M. Diabetes mellitus: The epidemic of the century. *World journal of diabetes* **2015**, *6* (6), 850-867. DOI: 10.4239/wjd.v6.i6.850
(3) Nethan, S.; Sinha, D.; Mehrotra, R. Non Communicable Disease Risk Factors and their Trends in India. *Asian Pacific journal of cancer prevention : APJCP* **2017**, *18* (7), 2005-2010. DOI: 10.22034/apjcp.2017.18.7.2005
(4) Diagnosis and classification of diabetes mellitus. *Diabetes care* **2010**, *33 Suppl 1* (Suppl 1), S62-69. DOI: 10.2337/dc10-S062
(5) Association, A. D. Diagnosis and Classification of Diabetes Mellitus. *Diabetes care* **2013**, *37* (Supplement_1), S81-S90. DOI: 10.2337/dc14-S081
(6) 2. Classification and Diagnosis of Diabetes: Standards of Medical Care in Diabetes-2021. *Diabetes care* **2021**, *44* (Suppl 1), S15-s33. DOI: 10.2337/dc21-S002
(7) Cohrs, C. M.; Panzer, J. K.; Drotar, D. M.; Enos, S. J.; Kipke, N.; Chen, C.; Bozsak, R.; Schöniger, E.; Ehehalt, F.; Distler, M.; Brennand, A.; Bornstein, S. R.; Weitz, J.; Solimena, M.; Speier, S. Dysfunction of Persisting β Cells Is a Key Feature of Early Type 2 Diabetes Pathogenesis. *Cell reports* **2020**, *31* (1), 107469. DOI: 10.1016/j.celrep.2020.03.033
(8) Deshpande, A. D.; Harris-Hayes, M.; Schootman, M. Epidemiology of diabetes and diabetes-related complications. *Physical therapy* **2008**, *88* (11), 1254-1264. DOI: 10.2522/ptj.20080020
(9) Kampmann, U.; Madsen, L. R.; Skajaa, G. O.; Iversen, D. S.; Moeller, N.; Ovesen, P. Gestational diabetes: A clinical update. *World journal of diabetes* **2015**, *6* (8), 1065-1072. DOI: 10.4239/wjd.v6.i8.1065
(10) Mitanchez, D. Foetal and neonatal complications in gestational diabetes: perinatal mortality, congenital malformations, macrosomia, shoulder dystocia, birth injuries, neonatal complications. *Diabetes & metabolism* **2010**, *36* (6 Pt 2), 617-627. DOI: 10.1016/j.diabet.2010.11.013
(11) Köck, K.; Köck, F.; Klein, K.; Bancher-Todesca, D.; Helmer, H. Diabetes mellitus and the risk of preterm birth with regard to the risk of spontaneous preterm birth. *The journal of maternal-fetal & neonatal medicine : the official journal of the European Association of Perinatal Medicine, the Federation of Asia and Oceania Perinatal Societies, the International Society of Perinatal Obstet* **2010**, *23* (9), 1004-1008. DOI: 10.3109/14767050903551392
(12) Dinh Le, T.; Minh Bui, T.; Hien Vu, T.; Phi Thi Nguyen, N.; Thanh Thi Tran, H.; Nguyen, S. T.; Ho Thi Nguyen, L.; Van Ngo, M.; Huy Duong, H.; Thanh Vu, B.; Dinh, H. T.; Nhu Do, B.; Le, D. C.; Thi Nguyen, H.; Trung Nguyen, K. Insulin Resistance in Gestational Diabetes Mellitus and Its Association With Anthropometric Fetal Indices. *Clinical medicine insights. Endocrinology and diabetes* **2022**, *15*, 11795514221098403. DOI: 10.1177/11795514221098403
(13) Sacks, D. B. A1C versus glucose testing: a comparison. *Diabetes care* **2011**, *34* (2), 518-523. DOI: 10.2337/dc10-1546
(14) Chehregosha, H.; Khamseh, M. E.; Malek, M.; Hosseinpanah, F.; Ismail-Beigi, F. A View Beyond HbA1c: Role of Continuous Glucose Monitoring. *Diabetes therapy : research, treatment and education of diabetes and related disorders* **2019**, *10* (3), 853-863. DOI: 10.1007/s13300-019-0619-1
(15) Shen, C. Y.; Lu, C. H.; Wu, C. H.; Li, K. J.; Kuo, Y. M.; Hsieh, S. C.; Yu, C. L. The Development of Maillard Reaction, and Advanced Glycation End Product (AGE)-Receptor for AGE (RAGE) Signaling Inhibitors as Novel Therapeutic Strategies for Patients with AGE-Related Diseases. *Molecules (Basel, Switzerland)* **2020**, *25* (23). DOI: 10.3390/molecules25235591
(16) Peng, X.; Ma, J.; Chen, F.; Wang, M. Naturally occurring inhibitors against the formation of advanced glycation end-products. *Food & function* **2011**, *2* (6), 289-301. DOI: 10.1039/c1fo10034c
(17) Jagadeeshaprasad, M. G.; Batkulwar, K. B.; Meshram, N. N.; Tiwari, S.; Korwar, A. M.; Unnikrishnan, A. G.; Kulkarni, M. J. Targeted quantification of N-1-(carboxymethyl) valine and N-1-(carboxyethyl) valine peptides of β-hemoglobin for better diagnostics in diabetes. *Clinical Proteomics* **2016**, *13* (1), 7. DOI: 10.1186/s12014-016-9108-y.

(18) Ott, C.; Jacobs, K.; Haucke, E.; Navarrete Santos, A.; Grune, T.; Simm, A. Role of advanced glycation end products in cellular signaling. *Redox biology* **2014**, *2*, 411-429. DOI: 10.1016/j.redox.2013.12.016
(19) Gkogkolou, P.; Böhm, M. Advanced glycation end products: Key players in skin aging? *Dermato-endocrinology* **2012**, *4* (3), 259-270. DOI: 10.4161/derm.22028
(20) Soboleva, A.; Mavropulo-Stolyarenko, G.; Karonova, T.; Thieme, D.; Hoehenwarter, W.; Ihling, C.; Stefanov, V.; Grishina, T.; Frolov, A. Multiple Glycation Sites in Blood Plasma Proteins as an Integrated Biomarker of Type 2 Diabetes Mellitus. *International journal of molecular sciences* **2019**, *20* (9). DOI: 10.3390/ijms20092329
(21) Qiu, H. Y.; Hou, N. N.; Shi, J. F.; Liu, Y. P.; Kan, C. X.; Han, F.; Sun, X. D. Comprehensive overview of human serum albumin glycation in diabetes mellitus. *World journal of diabetes* **2021**, *12* (7), 1057-1069. DOI: 10.4239/wjd.v12.i7.1057
(22) Schmidt, A. M.; Vianna, M.; Gerlach, M.; Brett, J.; Ryan, J.; Kao, J.; Esposito, C.; Hegarty, H.; Hurley, W.; Clauss, M.; et al. Isolation and characterization of two binding proteins for advanced glycosylation end products from bovine lung which are present on the endothelial cell surface. *The Journal of biological chemistry* **1992**, *267* (21), 14987-14997.
(23) Serveaux-Dancer, M.; Jabaudon, M.; Creveaux, I.; Belville, C.; Blondonnet, R.; Gross, C.; Constantin, J. M.; Blanchon, L.; Sapin, V. Pathological Implications of Receptor for Advanced Glycation End-Product (AGER) Gene Polymorphism. *Disease markers* **2019**, *2019*, 2067353. DOI: 10.1155/2019/2067353
(24) Yonchuk, J. G.; Silverman, E. K.; Bowler, R. P.; Agustí, A.; Lomas, D. A.; Miller, B. E.; Tal-Singer, R.; Mayer, R. J. Circulating soluble receptor for advanced glycation end products (sRAGE) as a biomarker of emphysema and the RAGE axis in the lung. *American journal of respiratory and critical care medicine* **2015**, *192* (7), 785-792. DOI: 10.1164/rccm.201501-0137PP
(25) Dong, H.; Zhang, Y.; Huang, Y.; Deng, H. Pathophysiology of RAGE in inflammatory diseases. *Frontiers in Immunology* **2022**, *13*, Review. DOI: 10.3389/fimmu.2022.931473.
(26) Rojas, A.; Morales, M. A.; Araya, P.; González, I. RAGE – The Receptor of Advanced Glycation End Products. In *Encyclopedia of Life Sciences*, pp 1-7.
(27) Chakraborty, A.; Sami, S. A.; Marma, K. K. S. A comprehensive review on RAGE-facilitated pathological pathways connecting Alzheimer's disease, diabetes mellitus, and cardiovascular diseases. *The Egyptian Journal of Internal Medicine* **2021**, *33* (1), 47. DOI: 10.1186/s43162-021-00081-w.
(28) Gilmore, T. D. Introduction to NF-kappaB: players, pathways, perspectives. *Oncogene* **2006**, *25* (51), 6680-6684. DOI: 10.1038/sj.onc.1209954
(29) Tanaka, N.; Yonekura, H.; Yamagishi, S.; Fujimori, H.; Yamamoto, Y.; Yamamoto, H. The receptor for advanced glycation end products is induced by the glycation products themselves and tumor necrosis factor-alpha through nuclear factor-kappa B, and by 17beta-estradiol through Sp-1 in human vascular endothelial cells. *The Journal of biological chemistry* **2000**, *275* (33), 25781-25790. DOI: 10.1074/jbc.M001235200
(30) Azegami, T.; Nakayama, T.; Hayashi, K.; Hishikawa, A.; Yoshimoto, N.; Nakamichi, R.; Itoh, H. Vaccination Against Receptor for Advanced Glycation End Products Attenuates the Progression of Diabetic Kidney Disease. *Diabetes* **2021**, *70* (9), 2147-2158. DOI: 10.2337/db20-1257
(31) Ramasamy, R.; Vannucci, S. J.; Yan, S. S. D.; Herold, K.; Yan, S. F.; Schmidt, A. M. Advanced glycation end products and RAGE: a common thread in aging, diabetes, neurodegeneration, and inflammation. *Glycobiology* **2005**, *15* (7), 16R-28R. DOI: 10.1093/glycob/cwi053
(32) Cheng, H. S.; Ton, S. H.; Kadir, K. b. A. Therapeutic Agents Targeting at AGE-RAGE Axis for the Treatment of Diabetes and Cardiovascular Disease: A Review of Clinical Evidence. 2017.
(33) Mengstie, M. A.; Chekol Abebe, E.; Behaile Teklemariam, A.; Tilahun Mulu, A.; Agidew, M. M.; Teshome Azezew, M.; Zewde, E. A.; Agegnehu Teshome, A. Endogenous advanced glycation end products in the pathogenesis of chronic diabetic complications. *Frontiers in molecular biosciences* **2022**, *9*, 1002710. DOI: 10.3389/fmolb.2022.1002710
(34) Nowotny, K.; Jung, T.; Höhn, A.; Weber, D.; Grune, T. Advanced glycation end products and oxidative stress in type 2 diabetes mellitus. *Biomolecules* **2015**, *5* (1), 194-222. DOI: 10.3390/biom5010194
(35) Cade, W. T. Diabetes-related microvascular and macrovascular diseases in the physical therapy setting. *Physical therapy* **2008**, *88* (11), 1322-1335. DOI: 10.2522/ptj.20080008

(36) Cheung, N.; Mitchell, P.; Wong, T. Y. Diabetic retinopathy. *Lancet (London, England)* **2010**, *376* (9735), 124-136. DOI: 10.1016/s0140-6736(09)62124-3
(37) Wong, T. Y.; Sabanayagam, C. The War on Diabetic Retinopathy: Where Are We Now? *Asia-Pacific journal of ophthalmology (Philadelphia, Pa.)* **2019**, *8* (6), 448-456. DOI: 10.1097/apo.0000000000000267
(38) Coyne, K. S.; Margolis, M. K.; Kennedy-Martin, T.; Baker, T. M.; Klein, R.; Paul, M. D.; Revicki, D. A. The impact of diabetic retinopathy: perspectives from patient focus groups. *Family practice* **2004**, *21* (4), 447-453. DOI: 10.1093/fampra/cmh417
(39) Lin, K.-Y.; Hsih, W.-H.; Lin, Y.-B.; Wen, C.-Y.; Chang, T.-J. Update in the epidemiology, risk factors, screening, and treatment of diabetic retinopathy. *Journal of Diabetes Investigation* **2021**, *12* (8), 1322-1325. DOI: https://doi.org/10.1111/jdi.13480.
(40) Kollias, A. N.; Ulbig, M. W. Diabetic retinopathy: Early diagnosis and effective treatment. *Deutsches Arzteblatt international* **2010**, *107* (5), 75-83; quiz 84. DOI: 10.3238/arztebl.2010.0075
(41) Association, A. D. 11. Microvascular Complications and Foot Care: Standards of Medical Care in Diabetes—2021. *Diabetes care* **2020**, *44* (Supplement_1), S151-S167. DOI: 10.2337/dc21-S011
(42) Feldman, E. L.; Callaghan, B. C.; Pop-Busui, R.; Zochodne, D. W.; Wright, D. E.; Bennett, D. L.; Bril, V.; Russell, J. W.; Viswanathan, V. Diabetic neuropathy. *Nature reviews. Disease primers* **2019**, *5* (1), 41. DOI: 10.1038/s41572-019-0092-1
(43) Forbes, J. M.; Cooper, M. E. Mechanisms of Diabetic Complications. *Physiological Reviews* **2013**, *93* (1), 137-188. DOI: 10.1152/physrev.00045.2011.
(44) Vinik, A. I.; Nevoret, M. L.; Casellini, C.; Parson, H. Diabetic neuropathy. *Endocrinology and metabolism clinics of North America* **2013**, *42* (4), 747-787. DOI: 10.1016/j.ecl.2013.06.001
(45) Zakin, E.; Abrams, R.; Simpson, D. M. Diabetic Neuropathy. *Seminars in neurology* **2019**, *39* (5), 560-569. DOI: 10.1055/s-0039-1688978
(46) Dewanjee, S.; Das, S.; Das, A. K.; Bhattacharjee, N.; Dihingia, A.; Dua, T. K.; Kalita, J.; Manna, P. Molecular mechanism of diabetic neuropathy and its pharmacotherapeutic targets. *European journal of pharmacology* **2018**, *833*, 472-523. DOI: 10.1016/j.ejphar.2018.06.034
(47) Neelofar, K.; Ahmad, J. Amadori albumin in diabetic nephropathy. *Indian journal of endocrinology and metabolism* **2015**, *19* (1), 39-46. DOI: 10.4103/2230-8210.146863
(48) Arif, E.; Nihalani, D. Glomerular Filtration Barrier Assembly: An insight. *Postdoc journal : a journal of postdoctoral research and postdoctoral affairs* **2013**, *1* (4), 33-45.
(49) Thomas, S.; Karalliedde, J. Diabetic nephropathy. *Medicine* **2015**, *43* (1), 20-25. DOI: https://doi.org/10.1016/j.mpmed.2014.10.007.
(50) Association, A. D. Nephropathy in Diabetes. *Diabetes care* **2004**, *27* (suppl_1), s79-s83. DOI: 10.2337/diacare.27.2007.S79
(51) Sampaio, E.; Delfino, V. D. Assessing albuminuria in spot morning samples from diabetic patients. *Arquivos brasileiros de endocrinologia e metabologia* **2008**, *52* (9), 1482-1488. DOI: 10.1590/s0004-27302008000900012
(52) Hemmati, R.; Gharipour, M.; Khosravi, A.; Jozan, M. A Cost-Benefit and Accurate Method for Assessing Microalbuminuria: Single versus Frequent Urine Analysis. *International journal of hypertension* **2013**, *2013*, 752903. DOI: 10.1155/2013/752903
(53) Mogensen, C. E. Microalbuminuria, blood pressure and diabetic renal disease: origin and development of ideas. *Diabetologia* **1999**, *42* (3), 263-285. DOI: 10.1007/s001250051151
(54) Zou, Y.; Zhao, L.; Zhang, J.; Wang, Y.; Wu, Y.; Ren, H.; Wang, T.; Zhang, R.; Wang, J.; Zhao, Y.; Qin, C.; Xu, H.; Li, L.; Chai, Z.; Cooper, M. E.; Tong, N.; Liu, F. Development and internal validation of machine learning algorithms for end-stage renal disease risk prediction model of people with type 2 diabetes mellitus and diabetic kidney disease. *Renal failure* **2022**, *44* (1), 562-570. DOI: 10.1080/0886022x.2022.2056053
(55) Kanwar, Y. S.; Sun, L.; Xie, P.; Liu, F. Y.; Chen, S. A glimpse of various pathogenetic mechanisms of diabetic nephropathy. *Annual review of pathology* **2011**, *6*, 395-423. DOI: 10.1146/annurev.pathol.4.110807.092150
(56) Thomas, M. C.; Brownlee, M.; Susztak, K.; Sharma, K.; Jandeleit-Dahm, K. A.; Zoungas, S.; Rossing, P.; Groop, P. H.; Cooper, M. E. Diabetic kidney disease. *Nature reviews. Disease primers* **2015**, *1*, 15018. DOI: 10.1038/nrdp.2015.18

(57) Jefferson, J. A.; Shankland, S. J.; Pichler, R. H. Proteinuria in diabetic kidney disease: a mechanistic viewpoint. *Kidney international* **2008**, *74* (1), 22-36. DOI: 10.1038/ki.2008.128
(58) Samsu, N. Diabetic Nephropathy: Challenges in Pathogenesis, Diagnosis, and Treatment. *BioMed Research International* **2021**, *2021*, 1497449. DOI: 10.1155/2021/1497449.
(59) Gross, J. L.; de Azevedo, M. J.; Silveiro, S. P.; Canani, L. s. H.; Caramori, M. L.; Zelmanovitz, T. Diabetic Nephropathy: Diagnosis, Prevention, and Treatment. *Diabetes care* **2005**, *28* (1), 164-176. DOI: 10.2337/diacare.28.1.164
(60) Frostegård, J. Immunity, atherosclerosis and cardiovascular disease. *BMC Medicine* **2013**, *11* (1), 117. DOI: 10.1186/1741-7015-11-117.
(61) Papatheodorou, K.; Papanas, N.; Banach, M.; Papazoglou, D.; Edmonds, M. Complications of Diabetes 2016. *Journal of diabetes research* **2016**, *2016*, 6989453. DOI: 10.1155/2016/6989453
(62) Donaghue, K. C.; Chiarelli, F.; Trotta, D.; Allgrove, J.; Dahl-Jorgensen, K. Microvascular and macrovascular complications associated with diabetes in children and adolescents. *Pediatric diabetes* **2009**, *10 Suppl 12*, 195-203. DOI: 10.1111/j.1399-5448.2009.00576.x
(63) Jun, J. E.; Hur, K. Y.; Lee, Y. B.; Lee, S. E.; Jin, S. M.; Lee, M. K.; Kim, J. H. Glycated albumin predicts the development of early diabetic nephropathy in patients with type 2 diabetes. *Diabetes & metabolism* **2018**, *44* (2), 178-180. DOI: 10.1016/j.diabet.2017.08.003
(64) Yoon, H. J.; Lee, Y. H.; Kim, S. R.; Rim, T. H.; Lee, E. Y.; Kang, E. S.; Cha, B. S.; Lee, H. C.; Lee, B. W. Glycated albumin and the risk of micro- and macrovascular complications in subjects with type 1 diabetes. *Cardiovascular diabetology* **2015**, *14*, 53. DOI: 10.1186/s12933-015-0219-y
(65) Raoufinia, R.; Mota, A.; Keyhanvar, N.; Safari, F.; Shamekhi, S.; Abdolalizadeh, J. Overview of Albumin and Its Purification Methods. *Advanced pharmaceutical bulletin* **2016**, *6* (4), 495-507. DOI: 10.15171/apb.2016.063
(66) Freedman, B. I.; Bostrom, M.; Daeihagh, P.; Bowden, D. W. Genetic factors in diabetic nephropathy. *Clinical journal of the American Society of Nephrology : CJASN* **2007**, *2* (6), 1306-1316. DOI: 10.2215/cjn.02560607
(67) Ali, O. Genetics of type 2 diabetes. *World journal of diabetes* **2013**, *4* (4), 114-123. DOI: 10.4239/wjd.v4.i4.114
(68) Kundu, A.; Bag, S.; Ramaiah, S.; Anbarasu, A. Leucine to proline substitution by SNP at position 197 in Caspase-9 gene expression leads to neuroblastoma: a bioinformatics analysis. *3 Biotech* **2013**, *3* (3), 225-234. DOI: 10.1007/s13205-012-0088-y
(69) Ramírez-Bello, J.; Jiménez-Morales, M. [Functional implications of single nucleotide polymorphisms (SNPs) in protein-coding and non-coding RNA genes in multifactorial diseases]. *Gaceta medica de Mexico* **2017**, *153* (2), 238-250.
(70) Nair, H. Chapter 2 - Application specific implementation of mass spectrometry platform in clinical laboratories. In *Mass Spectrometry for the Clinical Laboratory*, Nair, H., Clarke, W. Eds.; Academic Press, 2017; pp 17-35.
(71) Deribe, Y. L.; Pawson, T.; Dikic, I. Post-translational modifications in signal integration. *Nature Structural & Molecular Biology* **2010**, *17* (6), 666-672. DOI: 10.1038/nsmb.1842.
(72) Duan, G.; Walther, D. The roles of post-translational modifications in the context of protein interaction networks. *PLoS computational biology* **2015**, *11* (2), e1004049. DOI: 10.1371/journal.pcbi.1004049
(73) Santos, A. L.; Lindner, A. B. Protein Posttranslational Modifications: Roles in Aging and Age-Related Disease. *Oxid. Med. Cell. Longev.* **2017**, *2017*, 5716409. DOI: 10.1155/2017/5716409.
(74) Hyun, K.; Jeon, J.; Park, K.; Kim, J. Writing, erasing and reading histone lysine methylations. *Exp. Mol. Med.* **2017**, *49* (4), e324-e324. DOI: 10.1038/emm.2017.11.
(75) Ramazi, S.; Allahverdi, A.; Zahiri, J. Evaluation of post-translational modifications in histone proteins: A review on histone modification defects in developmental and neurological disorders. *Journal of biosciences* **2020**, *45*.
(76) Kim, K. H.; Park, G. W.; Jeong, J. E.; Ji, E. S.; An, H. J.; Kim, J. Y.; Yoo, J. S. Parallel reaction monitoring with multiplex immunoprecipitation of N-glycoproteins in human serum for detection of hepatocellular carcinoma. *Analytical and bioanalytical chemistry* **2019**, *411* (14), 3009-3019. DOI: 10.1007/s00216-019-01775-5

(77) Ahmad, S.; Khan, M. S.; Akhter, F.; Khan, M. S.; Khan, A.; Ashraf, J. M.; Pandey, R. P.; Shahab, U. Glycoxidation of biological macromolecules: a critical approach to halt the menace of glycation. *Glycobiology* **2014**, *24* (11), 979-990. DOI: 10.1093/glycob/cwu057
(78) Mnatsakanyan, R.; Shema, G.; Basik, M.; Batist, G.; Borchers, C. H.; Sickmann, A.; Zahedi, R. P. Detecting post-translational modification signatures as potential biomarkers in clinical mass spectrometry. *Expert review of proteomics* **2018**, *15* (6), 515-535. DOI: 10.1080/14789450.2018.1483340.
(79) Rhee, S. Y.; Kim, Y. S. The Role of Advanced Glycation End Products in Diabetic Vascular Complications. *Diabetes Metab. J.* **2018**, *42* (3), 188-195. DOI: 10.4093/dmj.2017.0105 PubMed.
(80) Tourzani, D. A.; Paudel, B.; Miranda, P. V.; Visconti, P. E.; Gervasi, M. G. Changes in Protein O-GlcNAcylation During Mouse Epididymal Sperm Maturation. *Frontiers in cell and developmental biology* **2018**, *6*, 60. DOI: 10.3389/fcell.2018.00060
(81) Bass, J. J.; Wilkinson, D. J.; Rankin, D.; Phillips, B. E.; Szewczyk, N. J.; Smith, K.; Atherton, P. J. An overview of technical considerations for Western blotting applications to physiological research. *Scandinavian journal of medicine & science in sports* **2017**, *27* (1), 4-25. DOI: 10.1111/sms.12702
(82) Freudenberg, J. A.; Bembas, K.; Greene, M. I.; Zhang, H. Non-invasive, ultra-sensitive, high-throughput assays to quantify rare biomarkers in the blood. *Methods (San Diego, Calif.)* **2008**, *46* (1), 33-38. DOI: 10.1016/j.ymeth.2008.05.005
(83) Solier, C.; Langen, H. Antibody-based proteomics and biomarker research - current status and limitations. *Proteomics* **2014**, *14* (6), 774-783. DOI: 10.1002/pmic.201300334
(84) Pagel, O.; Loroch, S.; Sickmann, A.; Zahedi, R. P. Current strategies and findings in clinically relevant post-translational modification-specific proteomics. *Expert review of proteomics* **2015**, *12* (3), 235-253. DOI: 10.1586/14789450.2015.1042867
(85) Niwa, T. Mass spectrometry for the study of protein glycation in disease. *Mass spectrometry reviews* **2006**, *25* (5), 713-723. DOI: 10.1002/mas.20089
(86) Doll, S.; Burlingame, A. L. Mass Spectrometry-Based Detection and Assignment of Protein Posttranslational Modifications. *ACS Chemical Biology* **2015**, *10* (1), 63-71. DOI: 10.1021/cb500904b.
(87) Cohen Freue, G. V.; Borchers, C. H. Multiple reaction monitoring (MRM): principles and application to coronary artery disease. *Circulation. Cardiovascular genetics* **2012**, *5* (3), 378. DOI: 10.1161/circgenetics.111.959528
(88) Rauniyar, N. Parallel Reaction Monitoring: A Targeted Experiment Performed Using High Resolution and High Mass Accuracy Mass Spectrometry. *International journal of molecular sciences* **2015**, *16* (12), 28566-28581. DOI: 10.3390/ijms161226120
(89) Huang, L.; Drouin, N.; Causon, J.; Wegrzyn, A.; Castro-Perez, J.; Fleming, R.; Harms, A.; Hankemeier, T. Reconstruction of Glutathione Metabolism in the Neuronal Model of Rotenone-Induced Neurodegeneration Using Mass Isotopologue Analysis with Hydrophilic Interaction Liquid Chromatography-Zeno High-Resolution Multiple Reaction Monitoring. *Analytical Chemistry* **2023**, *95* (6), 3255-3266. DOI: 10.1021/acs.analchem.2c04231.
(90) Korwar, A. M.; Vannuruswamy, G.; Jagadeeshaprasad, M. G.; Jayaramaiah, R. H.; Bhat, S.; Regin, B. S.; Ramaswamy, S.; Giri, A. P.; Mohan, V.; Balasubramanyam, M.; Kulkarni, M. J. Development of Diagnostic Fragment Ion Library for Glycated Peptides of Human Serum Albumin: Targeted Quantification in Prediabetic, Diabetic, and Microalbuminuria Plasma by Parallel Reaction Monitoring, SWATH, and MSE. *Molecular & cellular proteomics : MCP* **2015**, *14* (8), 2150-2159. DOI: 10.1074/mcp.M115.050518
(91) Kratochwil, C. F.; Kautt, A. F.; Rometsch, S. J.; Meyer, A. Benefits and limitations of a new genome-based PCR-RFLP genotyping assay (GB-RFLP): A SNP-based detection method for identification of species in extremely young adaptive radiations. *Ecology and evolution* **2022**, *12* (3), e8751. DOI: 10.1002/ece3.8751
(92) Weber, J. L.; David, D.; Heil, J.; Fan, Y.; Zhao, C.; Marth, G. Human diallelic insertion/deletion polymorphisms. *American journal of human genetics* **2002**, *71* (4), 854-862. DOI: 10.1086/342727
(93) Wright, A. F. Genetic Variation: Polymorphisms and Mutations. In *Encyclopedia of Life Sciences*.
(94) Gupta, A. Chapter 8 - Etiopathogenesis of insulin resistance. In *Understanding Insulin and Insulin Resistance*, Gupta, A. Ed.; Elsevier, 2022; pp 231-273.

(95) Deng, N.; Zhou, H.; Fan, H.; Yuan, Y. Single nucleotide polymorphisms and cancer susceptibility. *Oncotarget* **2017**, *8* (66), 110635-110649. DOI: 10.18632/oncotarget.22372
(96) Sitinjak, B. D. P.; Murdaya, N.; Rachman, T. A.; Zakiyah, N.; Barliana, M. I. The Potential of Single Nucleotide Polymorphisms (SNPs) as Biomarkers and Their Association with the Increased Risk of Coronary Heart Disease: A Systematic Review. *Vascular health and risk management* **2023**, *19*, 289-301. DOI: 10.2147/vhrm.s405039
(97) Blujus, J. K.; Korthauer, L. E.; Awe, E.; Frahmand, M.; Driscoll, I. Single Nucleotide Polymorphisms in Alzheimer's Disease Risk Genes Are Associated with Intrinsic Connectivity in Middle Age. *Journal of Alzheimer's disease : JAD* **2020**, *78* (1), 309-320. DOI: 10.3233/jad-200444
(98) Däbritz, J.; Friedrichs, F.; Weinhage, T.; Hampe, J.; Kucharzik, T.; Lügering, A.; Broeckel, U.; Schreiber, S.; Spieker, T.; Stoll, M.; Foell, D. The functional -374T/A polymorphism of the receptor for advanced glycation end products may modulate Crohn's disease. *American journal of physiology. Gastrointestinal and liver physiology* **2011**, *300* (5), G823-832. DOI: 10.1152/ajpgi.00115.2010
(99) Zeng, L.; Zhang, A. Q.; Gu, W.; Zhou, J.; Zhang, L. Y.; Du, D. Y.; Zhang, M.; Wang, H. Y.; Yan, J.; Yang, C.; Jiang, J. X. Identification of haplotype tag single nucleotide polymorphisms within the receptor for advanced glycation end products gene and their clinical relevance in patients with major trauma. *Critical care (London, England)* **2012**, *16* (4), R131. DOI: 10.1186/cc11436
(100) Miyashita, M.; Watanabe, T.; Ichikawa, T.; Toriumi, K.; Horiuchi, Y.; Kobori, A.; Kushima, I.; Hashimoto, R.; Fukumoto, M.; Koike, S.; Ujike, H.; Arinami, T.; Tatebayashi, Y.; Kasai, K.; Takeda, M.; Ozaki, N.; Okazaki, Y.; Yoshikawa, T.; Amano, N.; Washizuka, S.; Yamamoto, H.; Miyata, T.; Itokawa, M.; Yamamoto, Y.; Arai, M. The regulation of soluble receptor for AGEs contributes to carbonyl stress in schizophrenia. *Biochemical and biophysical research communications* **2016**, *479* (3), 447-452. DOI: 10.1016/j.bbrc.2016.09.074
(101) Hashim, H. O.; Al-Shuhaib, M. B. S. Exploring the Potential and Limitations of PCR-RFLP and PCR-SSCP for SNP Detection: A Review. *Journal of Applied Biotechnology Reports* **2019**, *6* (4), 137-144. DOI: 10.29252/jabr.06.04.02.
(102) Yang, W.; Kang, X.; Yang, Q.; Lin, Y.; Fang, M. Review on the development of genotyping methods for assessing farm animal diversity. *Journal of animal science and biotechnology* **2013**, *4* (1), 2. DOI: 10.1186/2049-1891-4-2
(103) Wang, S.; Ding, M.; Duan, X.; Wang, T.; Feng, X.; Wang, P.; Yao, W.; Wu, Y.; Yan, Z.; Feng, F.; Yu, S. Detection of the Single Nucleotide Polymorphism at Position rs2735940 in the Human Telomerase Reverse Transcriptase Gene by the Introduction of a New Restriction Enzyme Site for the PCR-RFLP Assay. *Annals of Clinical and Laboratory Science* **2017**, *47*, 546-550.
(104) Kumar, S.; Banks, T.; Cloutier, S. SNP Discovery Through Next Generation Sequencing and its Applications. *International Journal of Plant Genomics* **2012**, *2012*. DOI: 10.1155/2012/831460.
(105) Heather, J. M.; Chain, B. The sequence of sequencers: The history of sequencing DNA. *Genomics* **2016**, *107* (1), 1-8. DOI: 10.1016/j.ygeno.2015.11.003
(106) Gaastra, W. Chemical cleavage (maxam and gilbert) method for DNA sequence determination. *Methods in molecular biology (Clifton, N.J.)* **1985**, *2*, 333-341. DOI: 10.1385/0-89603-064-4:333
(107) Chen, P.; Sun, Z.; Wang, J.; Liu, X.; Bai, Y.; Chen, J.; Liu, A.; Qiao, F.; Chen, Y.; Yuan, C.; Sha, J.; Zhang, J.; Xu, L. Q.; Li, J. Portable nanopore-sequencing technology: Trends in development and applications. *Frontiers in microbiology* **2023**, *14*, 1043967. DOI: 10.3389/fmicb.2023.1043967
(108) Cai, G.; Buxbaum, J. Next-Generation Sequencing For Gene and Pathway Discovery and Analysis in Autism Spectrum Disorders. *The Neuroscience of Autism Spectrum Disorders* **2013**, 169-177. DOI: 10.1016/B978-0-12-391924-3.00011-9.
(109) Zhou, Y.; Ren, M.; Zhang, P.; Jiang, D.; Yao, X.; Luo, Y.; Yang, Z.; Wang, Y. Application of Nanopore Sequencing in the Detection of Foodborne Microorganisms. *Nanomaterials (Basel, Switzerland)* **2022**, *12* (9). DOI: 10.3390/nano12091534
(110) MacKenzie, M.; Argyropoulos, C. An Introduction to Nanopore Sequencing: Past, Present, and Future Considerations. *Micromachines* **2023**, *14* (2). DOI: 10.3390/mi14020459
(111) Payne, A.; Holmes, N.; Rakyan, V.; Loose, M. BulkVis: a graphical viewer for Oxford nanopore bulk FAST5 files. *Bioinformatics (Oxford, England)* **2019**, *35* (13), 2193-2198. DOI: 10.1093/bioinformatics/bty841
(112) van Dijk, E. L.; Jaszczyszyn, Y.; Naquin, D.; Thermes, C. The Third Revolution in Sequencing Technology. *Trends in genetics : TIG* **2018**, *34* (9), 666-681. DOI: 10.1016/j.tig.2018.05.008

(113) Campion, C. G.; Sanchez-Ferras, O.; Batchu, S. N. Potential Role of Serum and Urinary Biomarkers in Diagnosis and Prognosis of Diabetic Nephropathy. *Canadian journal of kidney health and disease* **2017**, *4*, 2054358117705371. DOI: 10.1177/2054358117705371
(114) Gheith, O.; Farouk, N.; Nampoory, N.; Halim, M. A.; Al-Otaibi, T. Diabetic kidney disease: world wide difference of prevalence and risk factors. *Journal of nephropharmacology* **2016**, *5* (1), 49-56.
(115) Gross, J. L.; de Azevedo, M. J.; Silveiro, S. P.; Canani, L. H.; Caramori, M. L.; Zelmanovitz, T. Diabetic nephropathy: diagnosis, prevention, and treatment. *Diabetes care* **2005**, *28* (1), 164-176. DOI: 10.2337/diacare.28.1.164
(116) Umayahara, Y.; Fujita, Y.; Watanabe, H.; Kasai, N.; Fujiki, N.; Hatazaki, M.; Koga, M. Association of glycated albumin to HbA1c ratio with diabetic retinopathy but not diabetic nephropathy in patients with type 2 diabetes. *Clinical biochemistry* **2017**, *50* (6), 270-273. DOI: 10.1016/j.clinbiochem.2016.11.032
(117) Wang, N.; Xu, Z.; Han, P.; Li, T. Glycated albumin and ratio of glycated albumin to glycated hemoglobin are good indicators of diabetic nephropathy in type 2 diabetes mellitus. *Diabetes/metabolism research and reviews* **2017**, *33* (2). DOI: 10.1002/dmrr.2843
(118) Kondaveeti, S. B.; D, K.; Mishra, S.; Kumar, R. A.; Shaker, I. A. Evaluation of glycated albumin and microalbuminuria as early risk markers of nephropathy in type 2 diabetes mellitus. *Journal of clinical and diagnostic research : JCDR* **2013**, *7* (7), 1280-1283. DOI: 10.7860/jcdr/2013/5145.3117
(119) Vetter, S. W. Glycated Serum Albumin and AGE Receptors. *Advances in clinical chemistry* **2015**, *72*, 205-275. DOI: 10.1016/bs.acc.2015.07.005
(120) Nathan, D. M.; McGee, P.; Steffes, M. W.; Lachin, J. M. Relationship of glycated albumin to blood glucose and HbA1c values and to retinopathy, nephropathy, and cardiovascular outcomes in the DCCT/EDIC study. *Diabetes* **2014**, *63* (1), 282-290. DOI: 10.2337/db13-0782
(121) Parrinello, C. M.; Selvin, E. Beyond HbA1c and glucose: the role of nontraditional glycemic markers in diabetes diagnosis, prognosis, and management. *Current diabetes reports* **2014**, *14* (11), 548. DOI: 10.1007/s11892-014-0548-3
(122) Frolov, A.; Blüher, M.; Hoffmann, R. Glycation sites of human plasma proteins are affected to different extents by hyperglycemic conditions in type 2 diabetes mellitus. *Analytical and bioanalytical chemistry* **2014**, *406* (24), 5755-5763. DOI: 10.1007/s00216-014-8018-y
(123) Rathore, R.; Sonwane, B. P.; Jagadeeshaprasad, M. G.; Kahar, S.; Santhakumari, B.; Unnikrishnan, A. G.; Kulkarni, M. J. Glycation of glucose sensitive lysine residues K36, K438 and K549 of albumin is associated with prediabetes. *Journal of proteomics* **2019**, *208*, 103481. DOI: 10.1016/j.jprot.2019.103481
(124) Crutchfield, C. A.; Thomas, S. N.; Sokoll, L. J.; Chan, D. W. Advances in mass spectrometry-based clinical biomarker discovery. *Clinical Proteomics* **2016**, *13* (1), 1. DOI: 10.1186/s12014-015-9102-9.
(125) Frolov, A.; Hoffmann, R. Identification and relative quantification of specific glycation sites in human serum albumin. *Analytical and bioanalytical chemistry* **2010**, *397* (6), 2349-2356. DOI: 10.1007/s00216-010-3810-9
(126) Brede, C.; Hop, B.; Jørgensen, K.; Skadberg, Ø. Measurement of glycated albumin in serum and plasma by LC-MS/MS. *Scandinavian journal of clinical and laboratory investigation* **2016**, *76* (3), 195-201. DOI: 10.3109/00365513.2015.1129671
(127) Natesan, V.; Kim, S. J. Diabetic Nephropathy - a Review of Risk Factors, Progression, Mechanism, and Dietary Management. *Biomolecules & therapeutics* **2021**, *29* (4), 365-372. DOI: 10.4062/biomolther.2020.204
(128) Barnaby, O. S.; Cerny, R. L.; Clarke, W.; Hage, D. S. Comparison of modification sites formed on human serum albumin at various stages of glycation. *Clinica chimica acta; international journal of clinical chemistry* **2011**, *412* (3-4), 277-285. DOI: 10.1016/j.cca.2010.10.018
(129) Takahashi, S.; Uchino, H.; Shimizu, T.; Kanazawa, A.; Tamura, Y.; Sakai, K.; Watada, H.; Hirose, T.; Kawamori, R.; Tanaka, Y. Comparison of glycated albumin (GA) and glycated hemoglobin (HbA1c) in type 2 diabetic patients: usefulness of GA for evaluation of short-term changes in glycemic control. *Endocrine journal* **2007**, *54* (1), 139-144. DOI: 10.1507/endocrj.k06-103

(130) Day, J. F.; Ingebretsen, C. G.; Ingebretsen, W. R., Jr; Baynes, J. W.; Thorpe, S. R. Nonenzymatic Glucosylation of Serum Proteins and Hemoglobin: Response to Changes in Blood Glucose Levels in Diabetic Rats. *Diabetes* **1980**, *29* (7), 524-527. DOI: 10.2337/diab.29.7.524
(131) Singh, V. P.; Bali, A.; Singh, N.; Jaggi, A. S. Advanced glycation end products and diabetic complications. *The Korean journal of physiology & pharmacology : official journal of the Korean Physiological Society and the Korean Society of Pharmacology* **2014**, *18* (1), 1-14. DOI: 10.4196/kjpp.2014.18.1.1
(132) Aldukhayel, A. Prevalence of diabetic nephropathy among Type 2 diabetic patients in some of the Arab countries. *International journal of health sciences* **2017**, *11* (1), 1-4.
(133) Yuan, C. M.; Nee, R.; Ceckowski, K. A.; Knight, K. R.; Abbott, K. C. Diabetic nephropathy as the cause of end-stage kidney disease reported on the medical evidence form CMS2728 at a single center. *Clinical kidney journal* **2017**, *10* (2), 257-262. DOI: 10.1093/ckj/sfw112
(134) Satirapoj, B.; Adler, S. G. Comprehensive approach to diabetic nephropathy. *Kidney research and clinical practice* **2014**, *33* (3), 121-131. DOI: 10.1016/j.krcp.2014.08.001
(135) Adeghate, E.; Schattner, P.; Dunn, E. An update on the etiology and epidemiology of diabetes mellitus. *Annals of the New York Academy of Sciences* **2006**, *1084*, 1-29. DOI: 10.1196/annals.1372.029
(136) Murea, M.; Ma, L.; Freedman, B. I. Genetic and environmental factors associated with type 2 diabetes and diabetic vascular complications. *The review of diabetic studies : RDS* **2012**, *9* (1), 6-22. DOI: 10.1900/rds.2012.9.6
(137) Mambiya, M.; Shang, M.; Wang, Y.; Li, Q.; Liu, S.; Yang, L.; Zhang, Q.; Zhang, K.; Liu, M.; Nie, F.; Zeng, F.; Liu, W. The Play of Genes and Non-genetic Factors on Type 2 Diabetes. *Frontiers in public health* **2019**, *7*, 349. DOI: 10.3389/fpubh.2019.00349
(138) Singh, S. The genetics of Type 2 diabetes mellitus: a review. *J Sci Res* **2011**, *55*.
(139) Doria, A. Genetics of diabetes complications. *Current diabetes reports* **2010**, *10* (6), 467-475. DOI: 10.1007/s11892-010-0147-x
(140) Perez-Alcantara, M.; Honoré, C.; Wesolowska-Andersen, A.; Gloyn, A. L.; McCarthy, M. I.; Hansson, M.; Beer, N. L.; van de Bunt, M. Patterns of differential gene expression in a cellular model of human islet development, and relationship to type 2 diabetes predisposition. *Diabetologia* **2018**, *61* (7), 1614-1622. DOI: 10.1007/s00125-018-4612-4
(141) Xue, J.; Rai, V.; Singer, D.; Chabierski, S.; Xie, J.; Reverdatto, S.; Burz, D. S.; Schmidt, A. M.; Hoffmann, R.; Shekhtman, A. Advanced glycation end product recognition by the receptor for AGEs. *Structure (London, England : 1993)* **2011**, *19* (5), 722-732. DOI: 10.1016/j.str.2011.02.013
(142) Vlassara, H.; Uribarri, J. Advanced glycation end products (AGE) and diabetes: cause, effect, or both? *Current diabetes reports* **2014**, *14* (1), 453. DOI: 10.1007/s11892-013-0453-1
(143) Xie, J.; Reverdatto, S.; Frolov, A.; Hoffmann, R.; Burz, D. S.; Shekhtman, A. Structural basis for pattern recognition by the receptor for advanced glycation end products (RAGE). *The Journal of biological chemistry* **2008**, *283* (40), 27255-27269. DOI: 10.1074/jbc.M801622200
(144) Hudson, B. I.; Stickland, M. H.; Futers, T. S.; Grant, P. J. Effects of novel polymorphisms in the RAGE gene on transcriptional regulation and their association with diabetic retinopathy. *Diabetes* **2001**, *50* (6), 1505-1511. DOI: 10.2337/diabetes.50.6.1505
(145) Athanasopoulou, K.; Boti, M. A.; Adamopoulos, P. G.; Skourou, P. C.; Scorilas, A. Third-Generation Sequencing: The Spearhead towards the Radical Transformation of Modern Genomics. *Life (Basel, Switzerland)* **2021**, *12* (1). DOI: 10.3390/life12010030
(146) Kumar, S.; Banks, T. W.; Cloutier, S. SNP Discovery through Next-Generation Sequencing and Its Applications. *Int J Plant Genomics* **2012**, *2012*, 831460. DOI: 10.1155/2012/831460
(147) Ramachandran, A. Know the signs and symptoms of diabetes. *The Indian journal of medical research* **2014**, *140* (5), 579-581.
(148) Report of the expert committee on the diagnosis and classification of diabetes mellitus. *Diabetes care* **2003**, *26 Suppl 1*, S5-20. DOI: 10.2337/diacare.26.2007.s5
(149) Horáková, D.; Štěpánek, L.; Janout, V.; Janoutová, J.; Pastucha, D.; Kollárová, H.; Petráková, A.; Štěpánek, L.; Husár, R.; Martiník, K. Optimal Homeostasis Model Assessment of Insulin Resistance (HOMA-IR) Cut-Offs: A Cross-Sectional Study in the Czech Population. *Medicina (Kaunas, Lithuania)* **2019**, *55* (5). DOI: 10.3390/medicina55050158

(150) De Coster, W.; D'Hert, S.; Schultz, D. T.; Cruts, M.; Van Broeckhoven, C. NanoPack: visualizing and processing long-read sequencing data. *Bioinformatics (Oxford, England)* **2018**, *34* (15), 2666-2669. DOI: 10.1093/bioinformatics/bty149
(151) Li, H. Minimap2: pairwise alignment for nucleotide sequences. *Bioinformatics (Oxford, England)* **2018**, *34* (18), 3094-3100. DOI: 10.1093/bioinformatics/bty191 (acccessed 7/27/2023).
(152) Li, H.; Handsaker, B.; Wysoker, A.; Fennell, T.; Ruan, J.; Homer, N.; Marth, G.; Abecasis, G.; Durbin, R. The Sequence Alignment/Map format and SAMtools. *Bioinformatics (Oxford, England)* **2009**, *25* (16), 2078-2079. DOI: 10.1093/bioinformatics/btp352
(153) Loman, N. J.; Quick, J.; Simpson, J. T. A complete bacterial genome assembled de novo using only nanopore sequencing data. *Nature methods* **2015**, *12* (8), 733-735. DOI: 10.1038/nmeth.3444
(154) Koren, S.; Walenz, B. P.; Berlin, K.; Miller, J. R.; Bergman, N. H.; Phillippy, A. M. Canu: scalable and accurate long-read assembly via adaptive k-mer weighting and repeat separation. *Genome research* **2017**, *27* (5), 722-736. DOI: 10.1101/gr.215087.116
(155) Vaser, R.; Sović, I.; Nagarajan, N.; Šikić, M. Fast and accurate de novo genome assembly from long uncorrected reads. *Genome research* **2017**, *27* (5), 737-746. DOI: 10.1101/gr.214270.116
(156) Lee, J. Y.; Kong, M.; Oh, J.; Lim, J.; Chung, S. H.; Kim, J.-M.; Kim, J.-S.; Kim, K.-H.; Yoo, J.-C.; Kwak, W. Comparative evaluation of Nanopore polishing tools for microbial genome assembly and polishing strategies for downstream analysis. *Scientific Reports* **2021**, *11* (1), 20740. DOI: 10.1038/s41598-021-00178-w.
(157) Cingolani, P.; Platts, A.; Wang le, L.; Coon, M.; Nguyen, T.; Wang, L.; Land, S. J.; Lu, X.; Ruden, D. M. A program for annotating and predicting the effects of single nucleotide polymorphisms, SnpEff: SNPs in the genome of Drosophila melanogaster strain w1118; iso-2; iso-3. *Fly* **2012**, *6* (2), 80-92. DOI: 10.4161/fly.19695
(158) Afgan, E.; Baker, D.; Batut, B.; van den Beek, M.; Bouvier, D.; Cech, M.; Chilton, J.; Clements, D.; Coraor, N.; Grüning, B. A.; Guerler, A.; Hillman-Jackson, J.; Hiltemann, S.; Jalili, V.; Rasche, H.; Soranzo, N.; Goecks, J.; Taylor, J.; Nekrutenko, A.; Blankenberg, D. The Galaxy platform for accessible, reproducible and collaborative biomedical analyses: 2018 update. *Nucleic acids research* **2018**, *46* (W1), W537-w544. DOI: 10.1093/nar/gky379
(159) Solé, X.; Guinó, E.; Valls, J.; Iniesta, R.; Moreno, V. SNPStats: a web tool for the analysis of association studies. *Bioinformatics (Oxford, England)* **2006**, *22* (15), 1928-1929. DOI: 10.1093/bioinformatics/btl268
(160) Cai, W.; Li, J.; Xu, J. X.; Liu, Y.; Zhang, W.; Xiao, J. R.; Zhu, L. Y.; Liu, J. Y. Association of 2184AG Polymorphism in the RAGE Gene with Diabetic Nephropathy in Chinese Patients with Type 2 Diabetes. *Journal of diabetes research* **2015**, *2015*, 310237. DOI: 10.1155/2015/310237
(161) Yang, H. Y.; Chuang, S. Y.; Fang, W. H.; Huang, G. S.; Wang, C. C.; Huang, Y. Y.; Chu, M. Y.; Lin, C.; Su, W.; Chen, C. Y.; Yang, Y. T.; Su, S. L. Effect of RAGE polymorphisms on susceptibility to and severity of osteoarthritis in a Han Chinese population: a case-control study. *Genetics and molecular research : GMR* **2015**, *14* (3), 11362-11370. DOI: 10.4238/2015.September.25.3
(162) Kalousová, M.; Jáchymová, M.; Mestek, O.; Hodková, M.; Kazderová, M.; Tesar, V.; Zima, T. Receptor for advanced glycation end products--soluble form and gene polymorphisms in chronic haemodialysis patients. *Nephrology, dialysis, transplantation : official publication of the European Dialysis and Transplant Association - European Renal Association* **2007**, *22* (7), 2020-2026. DOI: 10.1093/ndt/gfm050
(163) Serveaux-Dancer, M.; Jabaudon, M.; Creveaux, I.; Belville, C.; Blondonnet, R.; Gross, C.; Constantin, J. M.; Blanchon, L.; Sapin, V. Pathological Implications of Receptor for Advanced Glycation End-Product (AGER) Gene Polymorphism. **2019**, *2019*, 2067353. DOI: 10.1155/2019/2067353
(164) Goulart, A. C.; Germer, S.; Rexrode, K. M.; Martin, M.; Zee, R. Y. Polymorphisms in advanced glycosylation end product-specific receptor (AGER) gene, insulin resistance, and type 2 diabetes mellitus. *Clinica chimica acta; international journal of clinical chemistry* **2008**, *398* (1-2), 95-98. DOI: 10.1016/j.cca.2008.08.020
(165) Kang, P.; Tian, C.; Jia, C. Association of RAGE gene polymorphisms with type 2 diabetes mellitus, diabetic retinopathy and diabetic nephropathy. *Gene* **2012**, *500* (1), 1-9. DOI: 10.1016/j.gene.2012.03.056

(166) Niu, W.; Qi, Y.; Wu, Z.; Liu, Y.; Zhu, D.; Jin, W. A meta-analysis of receptor for advanced glycation end products gene: four well-evaluated polymorphisms with diabetes mellitus. *Molecular and cellular endocrinology* **2012**, *358* (1), 9-17. DOI: 10.1016/j.mce.2012.02.010
(167) Cheng, H.; Zhu, W.; Zhu, M.; Sun, Y.; Sun, X.; Jia, D.; Yang, C.; Yu, H.; Zhang, C. Susceptibility of six polymorphisms in the receptor for advanced glycation end products to type 2 diabetes: a systematic review and meta-analysis. *Endocrine journal* **2021**, *68* (8), 993-1010. DOI: 10.1507/endocrj.EJ21-0130
(168) Shi, Z.; Lu, W.; Xie, G. Association between the RAGE gene -374T/A, -429T/C polymorphisms and diabetic nephropathy: a meta-analysis. *Renal failure* **2015**, *37* (5), 751-756. DOI: 10.3109/0886022x.2015.1014754
(169) Yang, L.; Wu, Q.; Li, Y.; Fan, X.; Hao, Y.; Sun, H.; Cui, Y.; Han, L. Association of the receptor for advanced glycation end products gene polymorphisms and circulating RAGE levels with diabetic retinopathy in the Chinese population. *Journal of diabetes research* **2013**, *2013*, 264579. DOI: 10.1155/2013/264579
(170) Ramprasad, S.; Radha, V.; Mathias, R. A.; Majumder, P. P.; Rao, M. R.; Rema, M. Rage gene promoter polymorphisms and diabetic retinopathy in a clinic-based population from South India. *Eye (London, England)* **2007**, *21* (3), 395-401. DOI: 10.1038/sj.eye.6702239
(171) Balasubbu, S.; Sundaresan, P.; Rajendran, A.; Ramasamy, K.; Govindarajan, G.; Perumalsamy, N.; Hejtmancik, J. F. Association analysis of nine candidate gene polymorphisms in Indian patients with type 2 diabetic retinopathy. *BMC medical genetics* **2010**, *11*, 158. DOI: 10.1186/1471-2350-11-158
(172) Picheth, G.; Heidemann, M.; Pedrosa, F. O.; Chautard-Freire-Maia, E. A.; Costantini, C. O.; da Rocha Martinez, T. L.; de Souza, E. M. The -429 T>C polymorphism of the receptor for advanced glycation end products (RAGE) is associated with type 1 diabetes in a Brazilian population. *Clinica chimica acta; international journal of clinical chemistry* **2007**, *383* (1-2), 163-164. DOI: 10.1016/j.cca.2007.03.026
(173) Zhang, Y.; Jia, N.; Hu, F.; Fan, N.; Guo, X.; Du, H.; Mei, C.; Gao, C. Association of single-nucleotide polymorphisms in the RAGE gene and its gene- environment interactions with diabetic nephropathy in Chinese patients with type 2 diabetes. *Oncotarget* **2017**, *8* (57), 96885-96892. DOI: 10.18632/oncotarget.18785
(174) Kanková, K.; Márová, I.; Záhejský, J.; Muzík, J.; Stejskalová, A.; Znojil, V.; Vácha, J. Polymorphisms 1704G/T and 2184A/G in the RAGE gene are associated with antioxidant status. *Metabolism: clinical and experimental* **2001**, *50* (10), 1152-1160. DOI: 10.1053/meta.2001.26757
(175) Blech, I.; Katzenellenbogen, M.; Katzenellenbogen, A.; Wainstein, J.; Rubinstein, A.; Harman-Boehm, I.; Cohen, J.; Pollin, T. I.; Glaser, B. Predicting Diabetic Nephropathy Using a Multifactorial Genetic Model. *PLOS ONE* **2011**, *6* (4), e18743. DOI: 10.1371/journal.pone.0018743.
(176) Forbes, J. M.; Söderlund, J.; Yap, F. Y.; Knip, M.; Andrikopoulos, S.; Ilonen, J.; Simell, O.; Veijola, R.; Sourris, K. C.; Coughlan, M. T.; Forsblom, C.; Slattery, R.; Grey, S. T.; Wessman, M.; Yamamoto, H.; Bierhaus, A.; Cooper, M. E.; Groop, P. H. Receptor for advanced glycation end-products (RAGE) provides a link between genetic susceptibility and environmental factors in type 1 diabetes. *Diabetologia* **2011**, *54* (5), 1032-1042. DOI: 10.1007/s00125-011-2058-z
(177) Poirier, O.; Nicaud, V.; Vionnet, N.; Raoux, S.; Tarnow, L.; Vlassara, H.; Parving, H. H.; Cambien, F. Polymorphism screening of four genes encoding advanced glycation end-product putative receptors. Association study with nephropathy in type 1 diabetic patients. *Diabetes* **2001**, *50* (5), 1214-1218. DOI: 10.2337/diabetes.50.5.1214
(178) Yoshioka, K.; Yoshida, T.; Takakura, Y.; Umekawa, T.; Kogure, A.; Toda, H.; Yoshikawa, T. Association study of G1704T and G82S polymorphisms of RAGE gene for microalbuminuria in Japanese type 2 diabetic patients. *Metabolism: clinical and experimental* **2005**, *54* (4), 488-491. DOI: 10.1016/j.metabol.2004.11.001
(179) Lim, S. C.; Dorajoo, R.; Zhang, X.; Wang, L.; Ang, S. F.; Tan, C. S. H.; Yeoh, L. Y.; Ng, X. W.; Li, N.; Su, C.; Liu, S.; Wong, M. D. S.; Low, K. M. S.; Yao, A. O.; Babitha, J.; Fun, S.; Zhou, S.; Lee, S. B. M.; Tang, W. E.; Tavintharan, S.; Sum, C. F.; Liu, J. J. Genetic variants in the receptor for advanced glycation end products (RAGE) gene were associated with circulating soluble RAGE level but not with renal function among Asians with type 2 diabetes: a genome-wide association study.

Nephrology, dialysis, transplantation : official publication of the European Dialysis and Transplant Association - European Renal Association **2017**, *32* (10), 1697-1704. DOI: 10.1093/ndt/gfw263
(180) Wong, F. N.; Chua, K. H.; Kuppusamy, U. R.; Wong, C. M.; Lim, S. K.; Tan, J. A. Association of the receptor for advanced glycation end-products (RAGE) gene polymorphisms in Malaysian patients with chronic kidney disease. *PeerJ* **2016**, *4*, e1908. DOI: 10.7717/peerj.1908
(181) Li, J.; Cai, W.; Zhang, W.; Zhu, W. F.; Liu, Y.; Yue, L. X.; Zhu, L. Y.; Xiao, J. R.; Liu, J. Y.; Xu, J. X. Polymorphism 2184A/G in the AGER gene is not associated with diabetic retinopathy in Han Chinese patients with type 2 diabetes. *The Journal of international medical research* **2016**, *44* (3), 520-528. DOI: 10.1177/0300060516638990
(182) Ng, Z. X.; Kuppusamy, U. R.; Poh, R.; Tajunisah, I.; Koay, A. C.; Fong, K. C.; Chua, K. H. Lack of association between Gly82Ser, 1704G/T and 2184A/G of RAGE gene polymorphisms and retinopathy susceptibility in Malaysian diabetic patients. *Genetics and molecular research : GMR* **2012**, *11* (1), 455-461. DOI: 10.4238/2012.March.1.2
(183) Kanková, K.; Stejskalová, A.; Hertlová, M.; Znojil, V. Haplotype analysis of the RAGE gene: identification of a haplotype marker for diabetic nephropathy in type 2 diabetes mellitus. *Nephrology Dialysis Transplantation* **2005**, *20* (6), 1093-1102. DOI: 10.1093/ndt/gfh711
(184) Chocholatý, M.; Jáchymová, M.; Schmidt, M.; Havlová, K.; Křepelová, A.; Zima, T.; Babjuk, M.; Kalousová, M. Polymorphisms of the receptor for advanced glycation end-products and glyoxalase I in patients with renal cancer. *Tumour biology : the journal of the International Society for Oncodevelopmental Biology and Medicine* **2015**, *36* (3), 2121-2126. DOI: 10.1007/s13277-014-2821-0
(185) C, R. C.; Lukose, B.; Rani, P. G82S RAGE polymorphism influences amyloid-RAGE interactions relevant in Alzheimer's disease pathology. *PLOS ONE* **2020**, *15* (10), e0225487. DOI: 10.1371/journal.pone.0225487.
(186) Hofmann, M. A.; Drury, S.; Hudson, B. I.; Gleason, M. R.; Qu, W.; Lu, Y.; Lalla, E.; Chitnis, S.; Monteiro, J.; Stickland, M. H.; Bucciarelli, L. G.; Moser, B.; Moxley, G.; Itescu, S.; Grant, P. J.; Gregersen, P. K.; Stern, D. M.; Schmidt, A. M. RAGE and arthritis: the G82S polymorphism amplifies the inflammatory response. *Genes and immunity* **2002**, *3* (3), 123-135. DOI: 10.1038/sj.gene.6363861
(187) Park, S. J.; Kleffmann, T.; Hessian, P. A. The G82S polymorphism promotes glycosylation of the receptor for advanced glycation end products (RAGE) at asparagine 81: comparison of wild-type rage with the G82S polymorphic variant. *The Journal of biological chemistry* **2011**, *286* (24), 21384-21392. DOI: 10.1074/jbc.M111.241281
(188) Peng, W. H.; Lu, L.; Wang, L. J.; Yan, X. X.; Chen, Q. J.; Zhang, Q.; Zhang, R. Y.; Shen, W. F. RAGE gene polymorphisms are associated with circulating levels of endogenous secretory RAGE but not with coronary artery disease in Chinese patients with type 2 diabetes mellitus. *Archives of medical research* **2009**, *40* (5), 393-398. DOI: 10.1016/j.arcmed.2009.06.008
(189) Maruthur, N. M.; Li, M.; Halushka, M. K.; Astor, B. C.; Pankow, J. S.; Boerwinkle, E.; Coresh, J.; Selvin, E.; Kao, W. H. L. Genetics of Plasma Soluble Receptor for Advanced Glycation End-Products and Cardiovascular Outcomes in a Community-based Population: Results from the Atherosclerosis Risk in Communities Study. *PLOS ONE* **2015**, *10* (6), e0128452. DOI: 10.1371/journal.pone.0128452.
(190) Miller, S.; Henry, A. P.; Hodge, E.; Kheirallah, A. K.; Billington, C. K.; Rimington, T. L.; Bhaker, S. K.; Obeidat, M. e.; Melén, E.; Merid, S. K.; Swan, C.; Gowland, C.; Nelson, C. P.; Stewart, C. E.; Bolton, C. E.; Kilty, I.; Malarstig, A.; Parker, S. G.; Moffatt, M. F.; Wardlaw, A. J.; Hall, I. P.; Sayers, I. The Ser82 RAGE Variant Affects Lung Function and Serum RAGE in Smokers and sRAGE Production In Vitro. *PLOS ONE* **2016**, *11* (10), e0164041. DOI: 10.1371/journal.pone.0164041.
(191) Schmidt, J.; Berghaus, S.; Blessing, F.; Herbeck, H.; Blessing, J.; Schierack, P.; Rödiger, S.; Roggenbuck, D.; Wenzel, F. Genotyping of familial Mediterranean fever gene (MEFV)-Single nucleotide polymorphism-Comparison of Nanopore with conventional Sanger sequencing. *PLoS One* **2022**, *17* (3), e0265622. DOI: 10.1371/journal.pone.0265622
(192) Matern, B. M.; Olieslagers, T. I.; Groeneweg, M.; Duygu, B.; Wieten, L.; Tilanus, M. G. J.; Voorter, C. E. M. Long-Read Nanopore Sequencing Validated for Human Leukocyte Antigen Class I

Typing in Routine Diagnostics. *The Journal of molecular diagnostics : JMD* **2020**, *22* (7), 912-919. DOI: 10.1016/j.jmoldx.2020.04.001
(193) Crossley, B. M.; Rejmanek, D.; Baroch, J.; Stanton, J. B.; Young, K. T.; Killian, M. L.; Torchetti, M. K.; Hietala, S. K. Nanopore sequencing as a rapid tool for identification and pathotyping of avian influenza A viruses. *Journal of veterinary diagnostic investigation : official publication of the American Association of Veterinary Laboratory Diagnosticians, Inc* **2021**, *33* (2), 253-260. DOI: 10.1177/1040638720984114
(194) Watson, C. M.; Crinnion, L. A.; Lindsay, H.; Mitchell, R.; Camm, N.; Robinson, R.; Joyce, C.; Tanteles, G. A.; Halloran, D. J. O.; Pena, S. D. J.; Carr, I. M.; Bonthron, D. T. Assessing the utility of long-read nanopore sequencing for rapid and efficient characterization of mobile element insertions. *Laboratory investigation; a journal of technical methods and pathology* **2021**, *101* (4), 442-449. DOI: 10.1038/s41374-020-00489-y
(195) Gaens, K. H.; Ferreira, I.; van der Kallen, C. J.; van Greevenbroek, M. M.; Blaak, E. E.; Feskens, E. J.; Dekker, J. M.; Nijpels, G.; Heine, R. J.; t Hart, L. M.; de Groot, P. G.; Stehouwer, C. D.; Schalkwijk, C. G. Association of polymorphism in the receptor for advanced glycation end products (RAGE) gene with circulating RAGE levels. *The Journal of clinical endocrinology and metabolism* **2009**, *94* (12), 5174-5180. DOI: 10.1210/jc.2009-1067
(196) Lampropoulou, I. T.; Stangou, M.; Papagianni, A.; Didangelos, T.; Iliadis, F.; Efstratiadis, G. TNF-α and microalbuminuria in patients with type 2 diabetes mellitus. *Journal of diabetes research* **2014**, *2014*, 394206. DOI: 10.1155/2014/394206
(197) Navarro, J. F.; Mora-Fernández, C. The role of TNF-alpha in diabetic nephropathy: pathogenic and therapeutic implications. *Cytokine & growth factor reviews* **2006**, *17* (6), 441-450. DOI: 10.1016/j.cytogfr.2006.09.011
(198) Chen, Y. L.; Qiao, Y. C.; Xu, Y.; Ling, W.; Pan, Y. H.; Huang, Y. C.; Geng, L. J.; Zhao, H. L.; Zhang, X. X. Serum TNF-α concentrations in type 2 diabetes mellitus patients and diabetic nephropathy patients: A systematic review and meta-analysis. *Immunology letters* **2017**, *186*, 52-58. DOI: 10.1016/j.imlet.2017.04.003
(199) Donate-Correa, J.; Martín-Núñez, E.; Muros-de-Fuentes, M.; Mora-Fernández, C.; Navarro-González, J. F. Inflammatory cytokines in diabetic nephropathy. *Journal of diabetes research* **2015**, *2015*, 948417. DOI: 10.1155/2015/948417
(200) Janssen, J. Hyperinsulinemia and Its Pivotal Role in Aging, Obesity, Type 2 Diabetes, Cardiovascular Disease and Cancer. *International journal of molecular sciences* **2021**, *22* (15). DOI: 10.3390/ijms22157797
(201) Stanimirovic, J.; Radovanovic, J.; Banjac, K.; Obradovic, M.; Essack, M.; Zafirovic, S.; Gluvic, Z.; Gojobori, T.; Isenovic, E. R. Role of C-Reactive Protein in Diabetic Inflammation. *Mediators of inflammation* **2022**, *2022*, 3706508. DOI: 10.1155/2022/3706508
(202) Kanmani, S.; Kwon, M.; Shin, M. K.; Kim, M. K. Association of C-Reactive Protein with Risk of Developing Type 2 Diabetes Mellitus, and Role of Obesity and Hypertension: A Large Population-Based Korean Cohort Study. *Sci Rep* **2019**, *9* (1), 4573. DOI: 10.1038/s41598-019-40987-8
(203) Cheng, L.; Zhuang, H.; Yang, S.; Jiang, H.; Wang, S.; Zhang, J. Exposing the Causal Effect of C-Reactive Protein on the Risk of Type 2 Diabetes Mellitus: A Mendelian Randomization Study. *Frontiers in genetics* **2018**, *9*, 657. DOI: 10.3389/fgene.2018.00657

Plasma membrane and DNA images used in Figure 1.3, Figure 1.4 and Figure 1.6 are taken from https:// smart.servier.com/

Appendix

Appendix 1. Precursor masses and corresponding collision energies specified in the MRM-HR acquisition method

Peptide	m/z of precursor	Collision energy (eV)
FKDLGEENFK	613.8062	31.1
F***K(DFL)***DLGEENFK	694.8326	34.6
KQTALVELVK	564.853	28.9
K(DFL)QTALVELVK	645.8794	32.5
KVPQVSTPTLVEVSR	547.3174	30.4
K(DFL)VPQVSTPTLVEVSR	601.335	33.1

Appendix 2. Comparison of potential markers for diabetic nephropathy risk prediction based on ROC curve

Sr. No.	Comparison	*p*-value (DM vs DN)
1	F***K(DFL)***DLGEENFK vs. ***K(DFL)***QTALVELVK	0.3021
2	F***K(DFL)***DLGEENFK vs. ***K(DFL)***VPQVSTPTLVEVSR	0.0044*
3	***K(DFL)***QTALVELVK vs. ***K(DFL)***VPQVSTPTLVEVSR	0.0034*
4	F***K(DFL)***DLGEENFK vs. HbA_{1c}	0.3911
5	K***(DFL)***QTALVELVK vs. HbA_{1c}	0.0932
6	***K(DFL)***VPQVSTPTLVEVSR vs. HbA_{1c}	0.084

* $p<0.01$

Appendix 3. PCR amplification of *RAGE* gene

Agarose gel image showing a DNA band of PCR-amplified product containing the *RAGE* gene in the expected size of 4184bp. (Lane 1- 1kb plus DNA ladder, Lane 2- PCR-amplified *RAGE* gene)

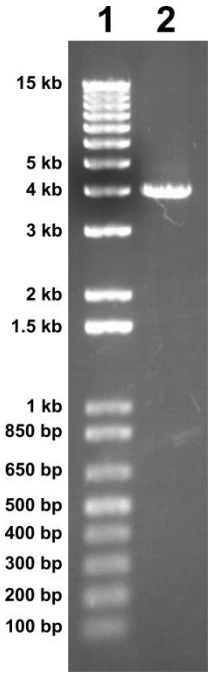

Appendix 4. Result of the nanopore, PCR-RFLP, and Sanger sequencing for verification of the discrepant results between nanopore and PCR-RFLP for two samples

Sample	Nanopore	PCR-RFLP	Sanger
Healthy_1	A/G	G/G	G/G
Diabetic_1	A/A	A/G	A/G

Appendix 5. *RAGE* SNPs in perfect linkage disequilibrium as determined by SNPStats

Linked SNPs	D'	r	*p*
rs1800625-rs3131300-rs3134940	0.9995	0.99*	0
rs2070600-rs9391855	0.9995	0.9995	0
rs204996-rs2853807	0.9993	0.9993	0
rs1554139845-rs2071288	0.9968	0.9968	0
rs118122061-Novel 2	0.995	0.995	0

*r=0.9995 for linkage disequilibrium between rs3131300 and rs3134940

Appendix 6. Linkage disequilibrium map of *RAGE* SNPs generated by SNPStats

The SNPs are numbered as shown in Appendix 5. Darker red color shades indicate stronger linkage disequilibrium between two SNPs.

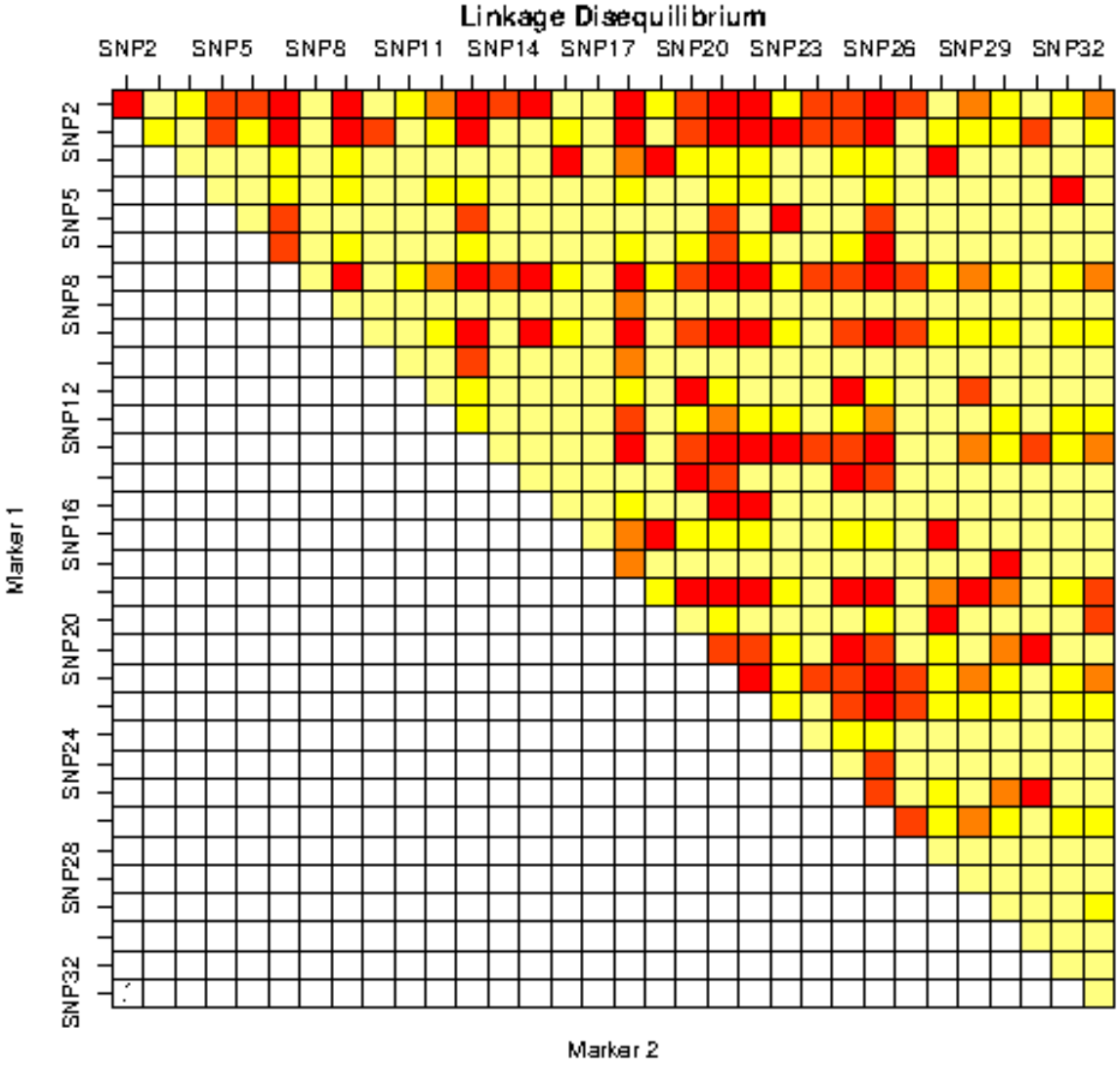

Appendix 7. Allele frequency of *RAGE* polymorphisms in healthy, DM and DN, and DM+DN groups

Sr. No.	Polymorphism	Genomic position	Location	Wild-type allele/mutated allele	Healthy		DM		DN		DM + DN	
					Wild-type	Mutant	Wild-type	Mutant	Wild-type	Mutant	Wild-type	Mutant
1	rs1800625	32184665	Upstream	T/C	0.87	0.13	0.81	0.19	0.87	0.13	0.83	0.17
2	rs1800624	32184610	Upstream	T/A	0.85	0.15	0.86	0.14	0.85	0.15	0.86	0.14
3	rs1554139845	32184580	Upstream	63bp deletion[#]	0.96	0.04	0.99	0.01	0.96	0.04	0.98	0.02
4	rs118122061	32184479	Upstream	G/A	0.99	0.01	0.98	0.02	0.99	0.01	0.98	0.02
5	rs143118560	32184478	Upstream	A/T	1	0	0.99	0.01	1	0	1	0
6	rs1800684	32184217	Exon 1	T/A	0.98	0.02	0.98	0.02	0.96	0.04	0.98	0.02
7	rs3131300	32184157	Intron 1	T/C	0.87	0.13	0.81	0.19	0.87	0.13	0.83	0.17
8	rs80096349	32183681	Exon 3	C/T	0.99	0.01	1	0	1	0	1	0
9	rs2070600	32183666	Exon 3	G/A	0.91	0.09	0.85	0.15	0.83	0.17	0.84	0.16
10	rs774609967	32183650	Exon 3	C/T	0.99	0.01	1	0	1	0	1	0
11	rs35795092	32183643	Exon 3	C/G	0.98	0.02	1	0	1	0	1	0
12	rs2269422	32183517	Intron 3	A/G	0.95	0.05	0.95	0.05	0.94	0.06	0.95	0.05
13	rs1035798	32183445	Intron 3	C/T	0.84	0.16	0.87	0.13	0.86	0.14	0.86	0.14
14	rs750111750	32182808	Intron 6	G/A	1	0	1	0	0.99	0.01	1	0
15	rs372248959	32182728	Intron 6	T/C	1	0	0.99	0.01	1	0	0.99	0.01
16	rs17846798	32182721	Intron 6	C/T	0.96	0.04	0.99	0.01	0.96	0.04	0.98	0.02
17	rs539453209	32182697	Exon 7	G/C	0.99	0.01	1	0	1	0	1	0
18	rs184003	32182519	Intron 7	G/T	0.75	0.25	0.77	0.23	0.77	0.23	0.77	0.23
19	rs186754929	32182494	Intron 7	G/A	0.99	0.01	1	0	0.98	0.02	0.99	0.01
20	rs204996	32182106	Intron 8	G/A	0.89	0.11	0.94	0.06	0.93	0.07	0.93	0.07
21	rs3134940	32182039	Intron 8	A/G	0.87	0.13	0.81	0.19	0.87	0.13	0.83	0.17
22	rs9391855	32182024	Intron 8	G/A	0.91	0.09	0.85	0.15	0.83	0.17	0.84	0.16
23	rs55640627	32181979	Intron 8	G/A	0.97	0.03	0.97	0.03	0.99	0.01	0.98	0.02
24	Novel 1	32181834	Intron 8	G/A	0.99	0.01	1	0	1	0	1	0

Sr. No.	Polymorphism	Genomic position	Location	Wild-type allele/mutated allele	Healthy		DM		DN		DM + DN	
					Wild-type	Mutant	Wild-type	Mutant	Wild-type	Mutant	Wild-type	Mutant
25	rs2853807	32181795	Intron 8	C/T	0.89	0.11	0.94	0.06	0.93	0.07	0.93	0.07
26	rs3134941	32181760	Intron 8	G/C	0.87	0.13	0.83	0.17	0.87	0.13	0.84	0.16
27	rs748427282	32181673	Intron 8	C/T	1	0	0.99	0.01	1	0	1	0
28	rs2071288	32181483	Intron 9	G/A	0.96	0.04	0.99	0.01	0.96	0.04	0.98	0.02
29	rs143357175	32181442	Exon 10	C/T	0.96	0.04	0.97	0.03	0.93	0.07	0.96	0.04
30	rs3176931	32181363	Exon 10	G/A	0.96	0.04	0.98	0.02	0.99	0.01	0.98	0.02
31	rs560762988	32181266	Intron 10	C/T	1	0	1	0	0.99	0.01	1	0
32	Novel 2	32181132	3' UTR	CAG/G	0.99	0.01	0.98	0.02	0.99	0.01	0.98	0.02
33	rs41270464	32180947	Downstream	G/A	0.96	0.04	0.96	0.04	0.95	0.05	0.96	0.04

[#]63bp deletion: TTCCCCAGCCTTGCCTTCATGATGCAGGCCCAATTGCACCCTTGCAGACAACAGTCTGGCCTGA/A

Appendix 8. Association of mutated alleles of *RAGE* polymorphisms with type 2 diabetes and diabetic nephropathy

Polymorphism	Healthy vs. DM			Healthy vs. DN			DM vs. DN			Healthy vs. DM + DN		
	χ^2	*p*	OR (95% CI)	χ^2	*p*	OR (95% CI)	χ^2	*p*	OR (95% CI)	χ^2	*p*	OR (95% CI)
rs1800625	1.897	0.168	1.537 (0.833-2.809)	0.004	0.951	0.976 (0.449-2.146)	1.471	0.225	0.635 (0.296-1.281)	0.994	0.319	1.344 (0.755-2.423)
rs1800624	0.129	0.72	0.888 (0.459-1.658)	0.002	0.964	1.018 (0.462-2.167)	0.125	0.723	1.146 (0.538-2.478)	0.059	0.808	0.929 (0.523-1.694)
rs1554139845	-	0.251	0.322 (0.064-1.532)	-	> 0.999	1.015 (0.263-3.964)	-	0.335	3.148 (0.63-17.93)	0.917	0.338	0.546 (0.176-1.699)
rs118122061	-	0.63	2.503 (0.369-32.72)	-	> 0.999	1.699 (0.088-32.48)	-	> 0.999	0.679 (0.052-4.614)	-	0.659	2.238 (0.367-27.57)
rs143118560	-	-	-	-	-	-	-	-	-	-	-	-
rs1800684	-	> 0.999	0.823 (0.19-3.569)	-	0.673	1.716 (0.392-7.467)	-	0.397	2.086 (0.477-9.062)	-	> 0.999	1.112 (0.285-4.109)
rs3131300	1.561	0.212	1.48 (0.796-2.694)	0.004	0.951	0.976 (0.449-2.146)	1.226	0.268	0.659 (0.306-1.338)	0.811	0.368	1.307 (0.732-2.363)
rs80096349	-	-	-	-	-	-	-	-	-	-	-	-
rs2070600	2.541	0.111	1.767 (0.898-3.565)	2.831	0.093	1.985 (0.903-4.442)	0.103	0.748	1.123 (0.54-2.227)	3.312	0.069	1.838 (0.949-3.621)
rs774609967	-	-	-	-	-	-	-	-	-	-	-	-
rs35795092	-	-	-	-	-	-	-	-	-	-	-	-
rs2269422	0.013	0.908	0.941 (0.331-2.484)	0.11	0.74	1.221 (0.427-3.640)	0.198	0.656	1.297 (0.465-4.263)	0.004	0.948	1.032 (0.42-2.666)
rs1035798	0.497	0.481	0.799 (0.427-1.494)	0.147	0.701	0.862 (0.405-1.867)	0.04	0.842	1.08 (0.51-2.316)	0.468	0.494	0.819 (0.459-1.479)
rs750111750	-	-	-	-	-	-	-	-	-	-	-	-
rs372248959	-	-	-	-	-	-	-	-	-	-	-	-
rs17846798	-	0.251	0.322 (0.064-1.532)	-	> 0.999	1.015 (0.263-3.964)	-	0.335	3.148 (0.63-17.93)	0.917	0.338	0.546 (0.176-1.699)
rs539453209	-	-	-	-	-	-	-	-	-	-	-	-

Polymorphism	Healthy vs. DM			Healthy vs. DN			DM vs. DN			Healthy vs. DM + DN		
	χ^2	*p*	OR (95% CI)	χ^2	*p*	OR (95% CI)	χ^2	*p*	OR (95% CI)	χ^2	*p*	OR (95% CI)
rs184003	0.186	0.666	0.892 (0.528-1.520)	0.214	0.644	0.861 (0.463-1.606)	0.013	0.91	0.965 (0.532-1.797)	0.267	0.605	0.882 (0.555-1.406)
rs186754929	-	-	-	-	0.557	3.439 (0.393-50.14)	-	-	-	-	> 0.999	1.11 (0.128-16.19)
rs204996	1.779	0.182	0.579 (0.266-1.242)	0.733	0.392	0.651 (0.248-1.785)	0.051	0.822	1.126 (0.404-3.194)	1.901	0.168	0.602 (0.3-1.25)
rs3134940	1.561	0.212	1.48 (0.796-2.694)	0.004	0.951	0.976 (0.449-2.146)	1.226	0.268	0.659 (0.306-1.338)	0.811	0.368	1.307 (0.732-2.363)
rs9391855	2.541	0.111	1.767 (0.898-3.565)	2.831	0.093	1.985 (0.903-4.442)	0.103	0.749	1.123 (0.54-2.227)	3.312	0.069	1.838 (0.949-3.621)
rs55640627	-	> 0.999	1.033 (0.304-3.421)	-	0.653	0.416 (0.034-2.578)	-	0.667	0.402 (0.034-3.004)	-	0.749	0.828 (0.219-2.639)
Novel 1	-	-	-	-	-	-	-	-	-	-	-	-
rs2853807	1.779	0.182	0.579 (0.266-1.242)	0.733	0.392	0.651 (0.248-1.785)	0.051	0.822	1.126 (0.404-3.194)	1.901	0.168	0.602 (0.3-1.25)
rs3134941	1.07	0.301	1.397 (0.76-2.606)	0.008	0.927	1.038 (0.479-2.331)	0.607	0.436	0.743 (0.34-1.539)	0.638	0.424	1.276 (0.694-2.304)
rs748427282	-	-	-	-	-	-	-	-	-	-	-	-
rs2071288	-	0.251	0.322 (0.064-1.532)	-	> 0.999	1.015 (0.263-3.964)	-	0.335	3.148 (0.63-17.93)	0.917	0.338	0.546 (0.176-1.699)
rs143357175	0.095	0.758	0.82 (0.263-2.564)	1.495	0.221	2.108 (0.594-6.285)	2.463	0.117	2.569 (0.726-7.632)	0.143	0.706	1.23 (0.414-3.245)
rs3176931	-	0.309	0.402 (0.109-1.563)	-	0.263	0.273 (0.024-1.716)	-	> 0.999	0.679 (0.052-4.614)	-	0.177	0.36 (0.113-1.363)
rs560762988	-	-	-	-	-	-	-	-	-	-	-	-
Novel 2	-	0.63	2.503 (0.369-32.72)	-	> 0.999	1.699 (0.088-32.48)	-	> 0.999	0.679 (0.052-4.614)	-	0.659	2.238 (0.367-27.57)
rs41270464	0.064	0.801	1.162 (0.397-3.288)	-	0.73	1.37 (0.41-4.722)	-	0.754	1.179 (0.377-3.833)	0.143	0.706	1.23 (0.414-3.245)

χ^2: Chi-square value; OR: Odds ratio; CI: Confidence interval.

Appendix 9. Association of type 2 diabetes-associated *RAGE* SNPs with AGEs, TNF-α, diabetes diagnosis markers, MDA, insulin, HOMA IR and CRP

SNP	Biochemical parameters	Healthy			DM			DN			Healthy + DM + DN		
		Plasma concentration		*p* value	Plasma concentration		*p* value	Plasma concentration		*p* value	Plasma concentration		*p* value
		Wild-type	Carrier	Wild-type vs carrier	Wild-type	Carrier	Wild-type vs carrier	Wild-type	Carrier	Wild-type vs carrier	Wild-type	Carrier	Wild-type vs carrier
rs1800625	FMN (µM/g)	25.19 ± 8.54 (36)	27.46 ± 13.24 (15)	0.468	38.32 ± 14.5 (41)	38.16 ± 12.15 (23)	0.964	43.11 ± 15.9 (30)	33.31 ± 8.95 (10)	0.073	35.25 ± 15.11 (107)	33.81 ± 12.6 (48)	0.565
	GA (µM/g)	0.81 ± 0.33 (36)	0.68 ± 0.24 (15)	0.175	1.06 ± 0.38 (41)	0.94 ± 0.4 (23)	0.265	1.19 ± 0.46 (30)	1.12 ± 0.39 (10)	0.667	1.01 ± 0.42 (107)	0.9 ± 0.39 (48)	0.11
	TNF-α (µM/g)	12.72 ± 6.97 (16)	23.78 ± 34.36 (10)	0.219	12.97 ± 14.39 (13)	27.64 ± 24.04 (9)	0.088	47.68 ± 65.76 (18)	19.91 ± 10.9 (10)	0.2	26.18 ± 44.29 (47)	23.65 ± 24.35 (29)	0.779
	FBG (mg/dl)	99.39 ± 8.34 (56)	101 ± 8.24 (15)	0.509	226 ± 89.35 (55)	206.4 ± 57.21 (31)	0.276	258.5 ± 83.79 (31)	231.8 ± 57.81 (11)	0.337	183.2 ± 96.58 (142)	183.6 ± 70.28 (57)	0.976
	HbA_{1c} (%)	5.5 ± 0.58 (56)	5.69 ± 0.59 (15)	0.271	9.32 ± 2.13 (55)	8.84 ± 2.23 (31)	0.321	8.67 ± 2.11 (31)	8.1 ± 1.16 (11)	0.405	7.67 ± 2.44 (142)	7.87 ± 2.19 (57)	0.6
	MDA (nM/ml)	37.19 ± 25.18 (19)	42.94 ± 34.43 (10)	0.611	51.33 ± 40.19 (15)	52.62 ± 21.38 (9)	0.93	51.41 ± 31.17 (21	35.19 ± 31.58 (10)	0.188	46.48 ± 32.19 (55)	43.27 ± 29.73 (29)	0.657
	Insulin (µM/ml)	16.67 ± 15.57 (46)	19.87 ± 20.61 (13)	0.546	15.47 ± 16.88 (46)	22.32 ± 17.64 (22)	0.128	21.23 ± 54.73 (27)	17.07 ± 18.61 (9)	0.826	17.6 ± 35.6 (73)	20.79 ± 17.78 (31)	0.636
	HOMA-IR	4.08 ± 3.97 (46)	4.76 ± 4.76 (13)	0.602	7.93 ± 7.08 (46)	11.11 ± 8.59 (22)	0.111	15.71 ± 43.96 (27)	8.91 ± 9.48 (9)	0.6511	10.81 ± 27.26 (73)	10.47 ± 8.76 (31)	0.947
	CRP (mg/L)	18.89 ± 44.91 (41)	7.58 ± 10.6 (12)	0.394	34.16 ± 63.62 (45)	37.96 ± 53.9 (21)	0.814	51.24 ± 82.04 (27)	58.89 ± 70.3 (9)	0.804	40.57 ± 71.01 (72)	44.24 ± 58.84 (30)	0.803
rs2070600	FMN (µM/g)	25.77 ± 10.71 (40)	26.16 ± 7.66 (11)	0.912	38.92 ± 15.37 (42)	37.01 ± 9.57 (22)	0.597	40.7 ± 15.12 (29)	40.57 ± 15.42 (11)	0.982	34.65 ± 15.24 (111)	35.19 ± 11.98 (44)	0.834
	GA (µM/g)	0.77 ± 0.33 (40)	0.75 ± 0.26 (11)	0.821	1 ± 0.41 (42)	1.05 ± 0.35 (22)	0.581	1.21 ± 0.45 (29)	1.09 ± 0.44 (11)	0.475	0.97 ± 0.42 (111)	0.99 ± 0.38 (44)	0.828

SNP	Biochemical parameters	Healthy			DM			DN			Healthy + DM + DN		
		Plasma concentration		*p* value	Plasma concentration		*p* value	Plasma concentration		*p* value	Plasma concentration		*p* value
		Wild-type	Carrier	Wild-type vs carrier	Wild-type	Carrier	Wild-type vs carrier	Wild-type	Carrier	Wild-type vs carrier	Wild-type	Carrier	Wild-type vs carrier
	TNF-α (μM/g)	11.76 ± 11.29 (16)	25.31 ± 31.74 (10)	0.129	22.3 ± 22.67 (12)	14.98 ± 16.02 (10)	0.401	35.9 ± 50.76 (18)	41.12 ± 62.85 (10)	0.813	23.96 ± 35.39 (46)	27.13 ± 41.69 (30)	0.723
	FBG (mg/dl)	99.47 ± 8.55 (60)	101.2 ± 6.79 (11)	0.532	221.6 ± 77.09 (61)	212.4 ± 86.32 (25)	0.631	255 ± 76.51 (31)	241.7 ± 85.3 (11)	0.635	180.2 ± 89.35 (152)	193.3 ± 90.93 (47)	0.384
	HbA_{1c} (%)	5.57 ± 0.54 (60)	5.36 ± 0.8 (11)	0.286	9.23 ± 2.29 (61)	8.94 ± 1.85 (25)	0.577	8.63 ± 2.13 (31)	8.2 ± 1.09 (11)	0.528	7.66 ± 2.45 (152)	7.93 ± 2.08 (47)	0.499
	MDA (nM/ml)	40.4 ± 26.68 (18)	37.17 ± 31.83 (11)	0.771	50.49 ± 40.14 (14)	53.66 ± 24.22 (10)	0.827	49.18 ± 36.59 (20)	40.72 ± 20.6 (11)	0.487	46.5 ± 34.16 (52)	43.55 ± 26.16 (32)	0.677
	Insulin (μM/ml)	17.26 ± 16.97 (55)	18.95 ± 13.46 (4)	0.847	16.95 ± 13.06 (48)	19.46 ± 25.06 (20)	0.59	14.13 ± 14.17 (26)	35.92 ± 89.64 (10)	0.228	15.96 ± 13.44 (74)	24.94 ± 54.48 (30)	0.186
	HOMA-IR	4.21 ± 4.21 (55)	4.54 ± 3.14 (4)	0.878	9.08 ± 7.36 (48)	8.67 ± 8.6 (20)	0.842	9.24 ± 11.02 (26)	26.4 ± 71.58 (10)	0.234	9.14 ± 8.75 (74)	14.58 ± 41.36 (30)	0.282
	CRP (mg/L)	16.12 ± 41.34 (47)	18 ± 29.85 (6)	0.915	39.49 ± 67.99 (46)	25.9 ± 36.86 (20)	0.404	57.76 ± 80.52 (26)	41.18 ± 75.2 (10)	0.5772	46.09 ± 72.74 (72)	30.99 ± 51.95 (30)	0.305

Data are presented as mean±SD. Data in parentheses represent the number of subjects. Note that rs3134940 and rs3131300 were in perfect disequilibrium with rs1800625, and rs9391855 was in perfect disequilibrium with rs2070600. Hence the association result for the SNPs in perfect linkage disequilibrium will be the same.

Appendix 10. Logistic regression analysis results for clinical parameters and genetic variants (SNPs)

Variable	rs1800625				rs2070600			
	Coefficient	**Std. Error**	***p*-value**	**Odds ratio**	**Coefficient**	**Std. Error**	***p*-value**	**Odds ratio**
Fasting blood glucose	0.006	0.011	0.566	1.006	0.008	0.009	0.352	1.008
HbA_{1c}	0.222	0.259	0.393	1.248	0.145	0.195	0.456	1.156
Blood urea	0.053	0.025	0.038*	1.054	-0.035	0.025	0.174	0.966
Serum creatinine	-0.851	0.442	0.054	0.427	0.544	0.373	0.144	1.724
Cholesterol	-0.001	0.011	0.940	0.999	0.012	0.010	0.251	1.012
Triglyceride	-0.005	0.010	0.647	0.995	-0.009	0.009	0.328	0.991
HDL	-0.033	0.055	0.544	0.967	-0.128	0.055	0.019*	0.880
Normalized fructosamine	0.021	0.042	0.621	1.021	-0.013	0.030	0.661	0.987
Normalized glycated albumin	-1.002	1.766	0.570	0.367	-0.513	1.420	0.718	0.598
TNF-α	-0.027	0.015	0.076	0.973	-0.025	0.021	0.231	0.975
MDA	-0.057	0.021	0.006*	0.944	-0.001	0.013	0.922	0.999
Insulin	0.197	0.095	0.038*	1.218	0.060	0.067	0.372	1.062
HOMA-IR	-0.270	0.120	0.024*	0.763	-0.043	0.082	0.596	0.958
CRP	0.033	0.013	0.012*	1.034	-0.023	0.014	0.101	0.978

CRP: C-reactive protein. The groups were comparable with respect to age and gender, so not adjusted for these demographic parameters.

Abstract

Name of the Student: Arvindkumar Chaurasiya **Registration No:** 10BB16A26042
Faculty of Study: Biological Sciences **Year of Submission:** 2023
AcSIR academic centre/CSIR Lab: CSIR-National Chemical Laboratory, Pune **Name of the Supervisor:** Dr. Mahesh J. Kulkarni

Title of the thesis: Evaluation of *RAGE* polymorphisms and glycated albumin peptides for the risk prediction of type 2 diabetes and diabetic nephropathy

---

Over 10% of the global population is afflicted with diabetes, and its prevalence is projected to increase rapidly. Diabetes-related morbidity and mortality are one of the highest in non-communicable diseases. Chronic hyperglycemic condition in diabetes promotes the formation of advanced glycation end products (AGEs), which are responsible for several deleterious physiological effects. AGEs interact with their cell surface receptors, RAGE, to induce several downstream signaling cascades that activate pro-inflammatory pathways and oxidative stress, accelerating the development of various diabetic vascular complications. Diabetic nephropathy is a major diabetic complication that affects 20-40 % of the diabetic population. It causes a gradual reduction in renal filtration, and regular renal dialysis or renal transplantation is a must at the end stage. Therefore, it's crucial to detect diabetes and diabetic nephropathy early and predict the risk of their development, giving a scope of early preventive and therapeutic intervention.

In the present thesis, the first chapter provides an introduction to diabetes and its complications, AGE formation, AGE-RAGE interaction leading to diabetic complications' development, the importance of early detection and prediction of diabetes and its complications, and tools for detecting *RAGE* polymorphisms. The second chapter describes the evaluation of glycated human serum albumin (HSA) peptides for predicting the risk of diabetic nephropathy, as glycated albumin represents the largest share of glycated plasma proteins. By measuring the glycation modification at three glycation-sensitive sites, it was observed that the glycation at K36 and K549 residues of HSA detected diabetic nephropathy more sensitively than HbA_{1c}. Early detection of diabetic nephropathy is crucial as early stages of diabetic nephropathy are asymptomatic. The third chapter describes the detection of all *RAGE* gene polymorphisms in healthy, type 2 diabetes, and diabetic nephropathy subjects using nanopore sequencing. 33 *RAGE* polymorphisms, including two novel polymorphisms, were detected by nanopore sequencing, and it showed 99.75% accuracy for detecting *RAGE* single nucleotide polymorphisms (SNPs), as cross-validated by PCR-RFLP. Genotype distribution analysis revealed that five RAGE SNPs, namely, rs1800625, rs3131300, rs3134940, rs2070600, and rs 9391855were associated with an increased type 2 diabetes risk. The utility of the glycated albumin peptides and type 2 diabetes risk-associated *RAGE* SNPs as early detection and risk prediction markers, respectively, should be validated in a larger cohort.

Details of the publications emanating from the thesis work

1) List of publications in SCI Journals (published & accepted) emanating from the thesis work, with complete bibliographic details

i) **Chaurasiya AH**, Jaiswal MR, Bayatigeri S, Kahar S, Tiwari S, Unnikrishnan AG, Kulkarni MJ: Elevated level of glycated KQTALVELVK peptide of albumin is associated with the risk of diabetic nephropathy. ACS Omega **2023**;8(23):20654-20660, doi:10.1021/acsomega.3c01219.

ii) **Chaurasiya AH**, Khilari AA, Kazi R, Jaiswal MR, Bhoite GM, Padwal MK, Momin AA, Shanmugam D, Kulkarni MJ: Nanopore sequencing of *RAGE* gene polymorphisms and their association with type 2 diabetes. ACS Omega **2023,** doi:10.1021/acsomega.3c00297.

2) List of papers with abstract presented (oral/poster) at national/international conferences/seminars with complete details

i) Poster presentation at Joint 11th AOHUPO and 7th AOAPO Congress, Singapore, from 8th-10th May 2023

Title: Elevated level of glycated KQTALVELVK peptide of albumin is associated with the risk of diabetic nephropathy

Abstract: Diabetic nephropathy is a leading cause of end-stage renal disease. Hence, early detection of diabetic nephropathy is essential to mitigate the disease burden. Microalbuminuria, the currently used diagnostic marker of diabetic nephropathy, is not efficient in detecting it at an early stage. Therefore, we explored the utility of glycated human serum albumin (HSA) peptides for risk prediction of diabetic nephropathy. Three glycation-sensitive HSA peptides, namely, FKDLGEENFK, KQTALVELVK, and KVPQVSTPTLVEVSR, with deoxyfructosyllysine (DFL) modification were quantified by targeted mass spectrometry in a study population comprising of healthy, and type II diabetes with and without nephropathy. Mass spectrometry, ROC curve, and correlation analysis revealed that the DFL-modified KQTALVELVK peptide was better than other glycated HSA peptides and HbA_{1c} for identifying diabetic nephropathy. DFL-modified KQTALVELVK could be a potential marker for risk prediction of diabetic nephropathy.

ii) Oral presentation at 7th International Diabetes Summit organized by Chellaram Diabetes Institute, Pune, from 10th-12th March 2023

Title: Elevated level of glycated KQTALVELVK peptide of albumin is associated with the risk of diabetic nephropathy

Abstract:

Objective: Diabetic nephropathy is a leading cause of end-stage renal disease. Hence, early detection of diabetic nephropathy is essential to mitigate the disease burden. Microalbuminuria, the currently used diagnostic marker of diabetic nephropathy, is not efficient in detecting it at an early stage. Therefore, there is a need of marker for predicting the risk of diabetic nephropathy.

Materials and methods: We explored the utility of glycated human serum albumin (HSA) peptides for risk prediction of diabetic nephropathy. Three glycation-sensitive HSA peptides, namely, FKDLGEENFK, KQTALVELVK, and KVPQVSTPTLVEVSR, with

deoxyfructosyllysine (DFL) modification were quantified by targeted mass spectrometry (high-resolution multiple reaction monitoring approach) in a study population comprising of 25 subjects each from healthy, type II diabetes without nephropathy and type II diabetes with nephropathy group. ROC curve analysis was used to compare the diabetic nephropathy risk prediction by glycated HSA peptides. Correlation analysis of glycated HSA peptides with clinical parameters was performed.

Result: Mass spectrometry, ROC curve, and correlation analysis revealed that the DFL-modified KQTALVELVK peptide was better than other glycated HSA peptides and HbA_{1c} for identifying diabetic nephropathy.

Conclusion: DFL-modified KQTALVELVK peptide could be a potential marker for risk prediction of diabetic nephropathy.

iii) Oral presentation at 5th International Diabetes Summit (virtual) organized by Chellaram Diabetes Institute, Pune, from 12th-14th March 2021

Title: Investigation of association of *RAGE* polymorphism, AGE-RAGE singnaling and diabetic nephropathy.

Abstract:

Introduction: Prolonged hyperglycemic condition leads to increased formation and accumulation of advanced glycation end products (AGEs), which interact with their receptor called receptor for advanced glycation end product (RAGE). AGE-RAGE interaction leads to activation of transcription factor NF-κB, which in turn leads to increased expression of pro-inflammatory cytokines and oxidative stress. AGE-RAGE axis is implicated in development and exacerbation of diabetic nephropathy. Genetic make-up of an individual may also plays an important role in the development of diabetic nephropathy. In this work, we are identifying the presence of different single nucleotide polymorphisms (SNP) in RAGE gene and their association with diabetic nephropathy.

Objective: The objective of this study is to identify any association of single nucleotide polymorphisms (SNP) present in RAGE gene and AGE-RAGE signaling with diabetic nephropathy.

Materials and methods: Blood sample of 32 healthy, 32 diabetic and 26 diabetic nephropathy subjects were collected from Bharati Hospital, Pune. DNA was extracted from leucocytes and PCR-RFLP technique was used to identify the presence of three SNPs, i.e. 429T/C, 2184A/G and Gly82Ser. Concentration of fructosamine, and glycated albumin in plasma was estimated

by respective commercially available kits. IL-6 concentration in plasma will be estimated by using ELISA kit. Further SNP identification will be done by nanopore DNA sequencing of RAGE gene, which can identify all SNPs present in it.

Result: Presence or absence of three SNPs in 18 healthy, 24 diabetic and 15 diabetic nephropathy subjects were determined by PCR-RFLP technique. Glycated albumin and fructosamine were found to be significantly elevated ($p<0.05$) in diabetic nephropathy subjects.

Conclusion: Odds ratio will be calculated to assess the association between any SNP and diabetic nephropathy after SNP identification in all samples. Any positive association can serve as a marker for identification of individuals at higher risk of developing diabetic nephropathy.

iv) Oral presentation at 4th International Diabetes Summit organized by Chellaram Diabetes Institute, Pune, from 6th-8th March 2020

Title: Investigation of association of *RAGE* polymorphism, AGE-RAGE singnaling and diabetic nephropathy.

Abstract: Prolonged hyperglycemic condition leads to increased formation and accumulation of advanced glycation end products (AGEs). These AGEs interact with their receptor called receptor for advanced glycation end product (RAGE). RAGE is a multiligand receptor of immunoglobulin superfamily, which can interact with its ligands including AGEs. AGE-RAGE interaction leads to activation of transcription factor NF-κB which in turn leads to increased expression of pro-inflammatory cytokines and oxidative stress. AGE-RAGE axis is implicated in development and exacerbation of diabetic nephropathy. Apart from hyperglycemia and hypertension, genetic constitution of an individual also plays a role in the development of diabetic nephropathy. Single nucleotide polymorphisms (SNP) in RAGE gene have been studied for their association with diabetic complications. In this study we are investigating association of three RAGE polymorphisms- 429T/C, 2184A/G and Gly82Ser as well as level of AGEs, fructosamine and pro-inflammatory cytokine with diabetic nephropathy. We have identified presence or absence of these three SNPs in 18 healthy, 24 diabetic and 15 diabetic nephropathy subjects by PCR-RFLP technique. Plasma fructosamine levels were significantly elevated in diabetic nephropathy subjects. Glycated albumin was also elevated in diabetic nephropathy subjects but it was non-significant difference. Quantification of sRAGE and IL-6 levels as well as AGEs and SNP information collected so

far will be used for studying their association with diabetic nephropathy.

v) Oral presentation at 12th virtual annual meeting of Proteomics Society, India, organized by CSIR-National Chemical Laboratory, Pune, from 22nd-24th November 2020

Title: Investigation of association of *RAGE* polymorphism, AGE-RAGE singnaling and diabetic nephropathy.

Abstract: Prolonged hyperglycemic condition leads to increased formation and accumulation of advanced glycation end products (AGEs). These AGEs interact with their receptor called receptor for advanced glycation end product (RAGE). RAGE is a multiligand receptor of immunoglobulin superfamily, which can interact with its ligands including AGEs. AGE-RAGE interaction leads to activation of transcription factor NF-κB which in turn leads to increased expression of pro-inflammatory cytokines and oxidative stress. AGE-RAGE axis is implicated in development and exacerbation of diabetic nephropathy. Apart from hyperglycemia and hypertension, genetic constitution of an individual also plays a role in the development of diabetic nephropathy. Single nucleotide polymorphisms (SNP) in RAGE gene have been studied for their association with diabetic complications. In this study we are investigating association of three RAGE polymorphisms- 429T/C, 2184A/G and Gly82Ser as well as level of AGEs, fructosamine and pro-inflammatory cytokine with diabetic nephropathy. We have identified presence or absence of these three SNPs in 18 healthy, 24 diabetic and 15 diabetic nephropathy subjects by PCR-RFLP technique. Plasma fructosamine levels were significantly elevated in diabetic nephropathy subjects. Glycated albumin was also elevated in diabetic nephropathy subjects although it was non-significant difference. Quantification of sRAGE and IL-6 levels as well as AGEs and SNP information collected so far will be used for studying their association with diabetic nephropathy.

ACS OMEGA

http://pubs.acs.org/journal/acsodf

Article

Elevated Level of Glycated KQTALVELVK Peptide of Albumin Is Associated with the Risk of Diabetic Nephropathy

Arvindkumar H. Chaurasiya, Meera R. Jaiswal, Santhakumari Bayatigeri, Shweta Kahar, Shalbha Tiwari, Ambika G. Unnikrishnan, and Mahesh J. Kulkarni*

Cite This: https://doi.org/10.1021/acsomega.3c01219

Read Online

ACCESS | Metrics & More | Article Recommendations | Supporting Information

ABSTRACT: Diabetic nephropathy is a leading cause of end-stage renal disease. Hence, early detection of diabetic nephropathy is essential to mitigate the disease burden. Microalbuminuria, the currently used diagnostic marker of diabetic nephropathy, is not efficient in detecting it at an early stage. Therefore, we explored the utility of glycated human serum albumin (HSA) peptides for risk prediction of diabetic nephropathy. Three glycation-sensitive HSA peptides, namely, FKDLGEENFK, KQTALVELVK, and KVPQVSTPTLVEVSR, with deoxyfructosyllysine (DFL) modification were quantified by targeted mass spectrometry (MS) in a study population comprising healthy and type II diabetes subjects with and without nephropathy. Mass spectrometry, receiver operating characteristic (ROC) curve, and correlation analysis revealed that the DFL-modified KQTALVELVK peptide was better than other glycated HSA peptides and HbA_{1c} for identifying diabetic nephropathy. DFL-modified KQTALVELVK could be a potential marker for risk prediction of diabetic nephropathy.

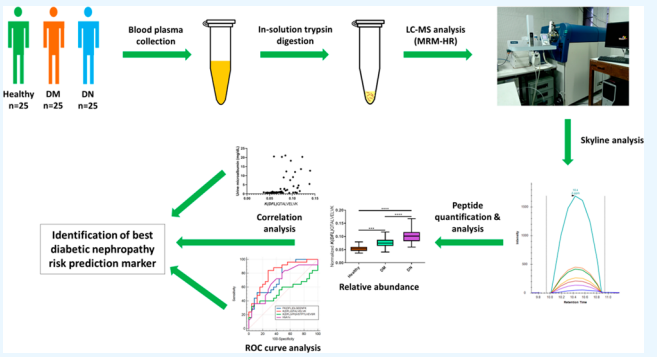

INTRODUCTION

Diabetic nephropathy is one of the major complications that affects about 20−40% of patients with diabetes. Due to glomerular damage, diabetic nephropathy patients have a progressive decrease in the glomerular filtration rate.[1] In diabetic nephropathy, there is an accumulation of nitrogenous waste in the blood, such as urea nitrogen and creatinine,[1,2] and increased excretion of blood proteins in the urine.[3] The diagnosis of diabetic nephropathy is typically based on the measurement of albumin concentration in the urine. The first clinical sign of diabetic nephropathy is microalbuminuria, which is detected by urinary albumin excretion of 30−299 mg in 24 h urine collection or 30−299 μg of albumin/mg creatinine in a spot urine sample.[4] The development and progression of diabetic nephropathy involve different stages.[5,6] Since the initial stages of diabetic nephropathy, before the development of microalbuminuria, are subclinical, there is a risk of developing diabetic nephropathy even when the urinary albumin concentration is within the normal range. Thus, it is crucial to detect diabetic nephropathy early to take timely preventive measures, but the currently used diagnostic markers may not be sensitive enough to detect diabetic nephropathy at an early stage. Therefore, there is an urgent need of a marker to predict the risk of diabetic nephropathy development.

Increased glycation is known to promote the development of several complications in patients with diabetes, including diabetic nephropathy. Several studies have evaluated the ability of well-established glycemic markers like glycated hemoglobin (HbA_{1c}) and other markers, such as glycated albumin, to predict diabetic nephropathy.[1,7−10] Due to the causal link of glycation with diabetic complications,[1] glycated proteins could be useful markers for risk prediction of diabetic nephropathy. HbA_{1c} and glycated albumin have been evaluated for their association with the progression of diabetic nephropathy.[7,11] In a longitudinal study involving 449 patients with type II diabetes, glycated albumin levels were found to be better predictors of diabetic nephropathy development than HbA_{1c} levels.[8] In another longitudinal study conducted on 154 participants, glycated albumin could predict the progression of diabetic nephropathy, but HbA_{1c} could not.[12] Similarly, another study reported superior performance of glycated albumin over HbA_{1c} for the prediction of diabetic nephropathy.[9] Therefore, it is worth evaluating the diabetic nephropathy risk prediction performance of glycated albumin.

Human serum albumin (HSA) has a half-life of 19 days;[13] hence, it represents a short-term glycemic status. HSA is directly exposed to reducing sugars in plasma, and it is the

Received: February 23, 2023
Accepted: March 31, 2023

most abundant plasma protein containing 59 lysine and 24 arginine residues, many of which can be glycated.[14] Therefore, glycated albumin represents a large share of glycated plasma proteins, and measuring glycated albumin could be more sensitive than other glycated plasma proteins.

Glycated albumin has been increasingly investigated in recent years for its role in the pathogenesis of diabetic complications, as well as for its prediction.[1,11,15] Several reports have found an association between glycated albumin and diabetic nephropathy.[1,9,11,12] However, most of the reports on the association of albumin glycation and diabetic nephropathy have focused on the quantification of total glycated albumin, but it has been reported previously that the lysine residues of albumin vary in their glycation sensitivity.[16−18] Therefore, quantifying glycation-sensitive peptides rather than overall glycated HSA can make the analysis more sensitive. Mass spectrometry is being increasingly used for the discovery and quantification of disease biomarkers.[19] Mass spectrometry is the best tool to characterize and quantify glycated peptides by bottom-up proteomics. It offers great sensitivity and resolution to measure the level of peptides and proteins accurately. In this context, targeted mass spectrometry-based approaches, such as high-resolution multiple reaction monitoring (MRM-HR), offer accurate and sensitive quantification of target peptides with the ease of the mass spectrometry acquisition method setup. Herein, we selected three glycation-sensitive HSA peptides, namely FKDLGEENFK, KQTALVELVK, and KVPQVSTPTLVEVSR, corresponding to sites K36, K549, and K438, respectively, based on previous literatures;[16,18,20−23] quantified these peptides in unmodified and DFL-modified form by MRM-HR approach in a study group comprising healthy and type II diabetes subjects with and without nephropathy; and evaluated if these glycated peptides can be good predictors for diabetic nephropathy.

MATERIALS AND METHODS

Materials. All chemicals, including ammonium bicarbonate, dithiothreitol, iodoacetamide, formic acid, and proteomics grade trypsin, were purchased from Sigma-Aldrich (St. Louis, MO, USA). Bradford reagent was purchased from Bio-Rad Laboratories Inc. (Hercules, CA, USA). LC-MS grade water and acetonitrile (ACN) were purchased from JT Baker (PA, USA). Sep-Pak C18 cartridges were purchased from Waters (Waters Corporation, MA, USA). Eksigent micro-LC column (ChromXP C18, 100 × 0.3 mm, 3 μM, 120 Å) was procured from Sciex (Framingham, MA, USA).

Study Design. This cross-sectional study was designed to assess three glycated HSA peptides as a marker for the risk prediction of diabetic nephropathy. Peripheral blood samples from healthy, type II diabetes subjects without nephropathy (DM) and type II diabetes subjects with nephropathy (DN) were collected, and the plasma was separated. Plasma samples were digested by trypsin, and the tryptic peptides were analyzed by targeted mass spectrometry for the quantification of deoxyfructosyllysine (DFL)-modified HSA peptides, namely, FKDLGEENFK, KQTALVELVK, and KVPQVSTPTLVEVSR. Statistical analysis was performed to check if these glycated peptides were significantly elevated in DM and DN groups. Also, ROC curve analysis was performed to compare the accuracy of these glycated peptides in differentiating between healthy, DM, and DN groups.

Subjects. Five mL blood samples were collected from 25 healthy, 25 DM, and 25 DN subjects in EDTA-coated vacutainers. Subjects without a history of known diabetes having HbA_{1c} < 5.7% were categorized as healthy, while those having $HbA_{1c} \geq 6.5\%$ and spot urine microalbumin <2 mg/dl were categorized as type II diabetes subjects without nephropathy. Subjects with $HbA_{1c} \geq 6.5\%$ and spot urine microalbumin ≥2 mg/dl were grouped as subjects with diabetic nephropathy. Subjects with chronic disease, inflammation, thyroid disorder, cardiovascular disease, and pregnancy were excluded from the study. Written informed consent was obtained from all the study participants before blood sample collection, and the study was performed in accordance with the principles of the Declaration of Helsinki. The study was approved by the institute ethics committee of Chellaram Diabetes Institute, Pune. Clinical characteristics of the subjects, such as fasting blood glucose (FBG) level, 2 h postprandial blood glucose (PPBG) level, HbA_{1c}, total cholesterol, triglycerides, HDL, LDL, VLDL, serum creatinine, serum albumin, and urine microalbumin were measured. Blood samples were centrifuged at 1000 rpm at 4 °C for 15 min to separate plasma from erythrocytes. Plasma in the supernatant was collected in a fresh collection tube and centrifuged again at 14000 rpm at 4 °C for 20 min to separate out cellular contaminants and debris. The clear plasma was collected and stored at minus 80 °C until further analysis.

Sample Preparation for MS Analysis. Plasma protein concentration was estimated by Bradford's method. 50 μg of the protein from each sample was diluted with 50 mM ammonium bicarbonate buffer (pH 8.0) to get the final protein concentration of 1 mg/mL in 50 μL reaction volume and was heated at 80 °C for 15 min to denature proteins. 2.5 μL of 100 mM dithiothreitol was added to the solution and heated at 60 °C for 15 min for disulfide bond reduction. Alkylation of the sulfhydryl group was performed by adding 2.5 μL of 200 mM iodoacetamide and incubating the solution in the dark at room temperature for 30 min. Trypsin was added at a 1:25 (w/w) trypsin to protein ratio, and the digestion was performed for 16 h at 37 °C. Trypsin action was stopped by adding 1 μL of formic acid and incubating at 37 °C for 20 min. The tryptic peptides were desalted using Sep-Pak C18 cartridges. The desalted tryptic peptide solution was dried by vacuum concentrator and stored at minus 80 °C until reconstitution for MS analysis.

Liquid Chromatography−Mass Spectrometry (LC-MS) Analysis. HSA peptides were reconstituted in 2% ACN with 0.1% formic acid. The peptide concentration was estimated by NanoDrop 2000 spectrophotometer (Thermo Scientific) at 205 nm, and 0.6 μg of peptides were loaded onto Eksigent C18-RP HPLC column (length 100 mm, ID 0.3 mm, particle size 3 μm, pore size 120 Å) using an Eksigent Ekspert MicroLC 200 system (Sciex, Framingham, MA, USA) which was connected to Triple TOF 5600 mass spectrometer (Sciex). The column temperature was maintained at 40 °C. Peptides were separated using a mixture of mobile phase A (water with 0.1% formic acid) and mobile phase B (ACN with 0.1% formic acid) at a flow rate of 7 μL/min and two linear LC gradient segments, i.e., 2 to 20% mobile phase B for 20 min followed by 20 to 40% mobile phase B for 14 min, were used. MRM-HR approach was used for the data acquisition. The m/z values of the unmodified and DFL-modified HSA peptides FKDLGEENFK, KQTALVELVK, and KVPQVSTPTLVEVSR and their corresponding collision energies were specified in the acquisition method (Table S1) with a collision energy spread as 10 eV. The ESI source was maintained at a temperature of

https://doi.org/10.1021/acsomega.3c01219
ACS Omega XXXX, XXX, XXX−XXX

Table 1. Details of Precursor Ions and Their Corresponding Fragment Ions Used for Quantification

Modification site	Peptide	Precursor m/z	Precursor charge state	Fragment ions used for precursor quantification (m/z)
K36	FKDLGEENFK	613.8062	2	$y6^+$ (723.3308), $y7^+$ (836.4149), $y8^+$ (951.4418), $y9^{+2}$ (540.272), $b2^+$ (276.1707), $b3^+$ (391.1976), $b8^+$ (933.4312)
K36	F***K(DFL)***DLGEENFK	694.8326	2	$y2^+$ (294.1812), $y6^+$ (723.3308), $y7^+$ (836.4149), $y8^+$ (951.4418), $b3^+$ (553.2504), $b4^+$ (666.3345), $b5^+$ (723.3559)
K549	KQTALVELVK	564.853	2	$y4^+$ (488.3079), $y7^+$ (771.4975), $y8^+$ (872.5451), $y9^+$ (1000.6037), $b7^+$ (770.4407), $b8^+$ (883.5247), $b9^+$ (982.5932)
K549	***K(DFL)***QTALVELVK	645.8794	2	$y2^+$ (246.1812), $y7^+$ (771.4975), $y8^+$ (872.5451), $y9^+$ (1000.6037), $b6^+$ (803.4509), $b7^+$ (932.4935), $b8^{+2}$ (523.2924)
K438	KVPQVSTPTLVEVSR	547.3174	3	$y4^+$ (490.262), $y5^+$ (589.3304), $y6^+$ (702.4145), $y8^+$ (900.5149), $b7^+$ (740.4301), $b9^+$ (938.5306), $b10^+$ (1051.6146)
K438	***K(DFL)***VPQVSTPTLVEVSR	601.335	3	$y5^+$ (589.3304), $y6^+$ (702.4145), $y7^+$ (803.4621), $y8^+$ (900.5149), $b4^+$ (615.3348), $b5^+$ (714.4032), $b7^+$ (902.4829)

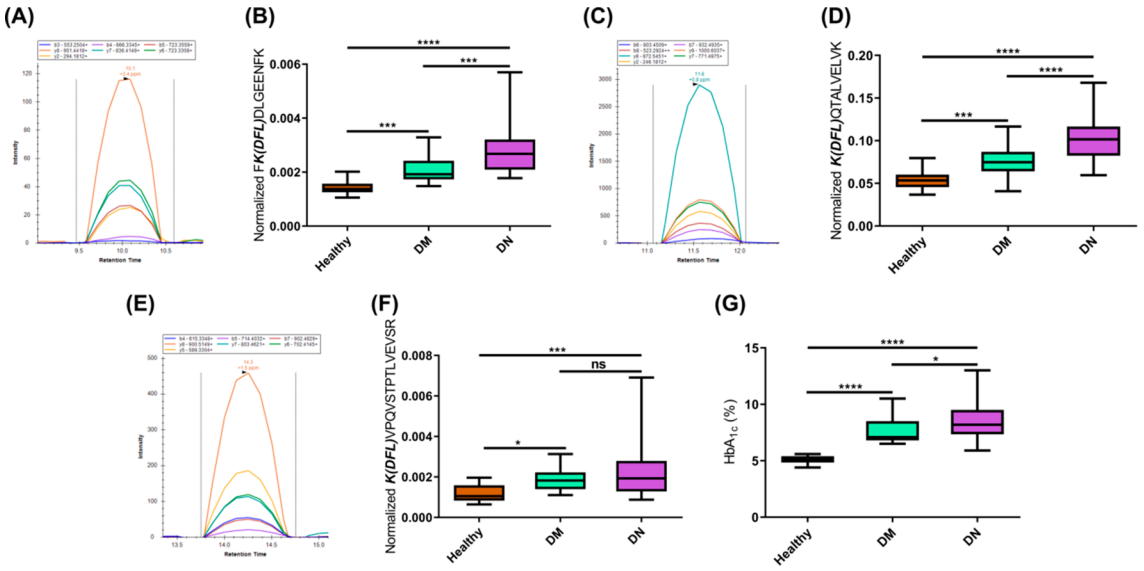

Figure 1. Representative DFL-modified peptide chromatograms and their quantification in healthy, type II diabetes without nephropathy (DM) and diabetic nephropathy (DN) groups. Chromatogram showing coeluting fragment ion peaks of F***K(DFL)***DLGEENFK (A); DM group showed an increased normalized AUC of F***K(DFL)***DLGEENFK than the healthy group. DN group had significantly elevated normalized AUC of F***K(DFL)*** DLGEENFK compared to the healthy and DM group (B); Chromatogram showing coeluting fragment ion peaks of ***K(DFL)***QTALVELVK (C); DM group had an increased normalized AUC of ***K(DFL)***QTALVELVK than the healthy group. DN group had significantly elevated normalized AUC of ***K(DFL)***QTALVELVK compared to the healthy and DM group (D); Chromatogram showing coeluting fragment ion peaks of ***K(DFL)*** VPQVSTPTLVEVSR (E); DM and DN groups had significantly elevated normalized ***K(DFL)***VPQVSTPTLVEVSR compared to the healthy group, but there was no difference in its level between DM and DN group (F); DM group had significantly elevated HbA_{1c} compared to the healthy group, whereas the DN group had elevated HbA_{1c} compared to both healthy and DM groups (G). ns: nonsignificant, * $p < 0.05$, ** $p < 0.01$, *** $p < 0.001$, **** $p < 0.0001$.

200 °C and a voltage of 5500 V. Nebulizer gas, heater gas, and curtain gas were set at 25 psi each. Declustering potential was set to 80 V. Accumulation time was set to 0.25 s for the TOF MS scan over the mass range of 350−1250 Da and 0.6 s for the fragment ion scan over the mass range of 100−1200 Da.

Data Analysis. The MS data generated were analyzed using Skyline version 22.2.0.255 (MacCoss Lab, University of Washington, WA, USA). The proteolytic enzyme was specified as trypsin, with one missed cleavage. Carbamidomethylation at cysteine (57.021464 Da) was specified as fixed modification, whereas DFL modification at lysine (162.052795 Da) was specified as variable modification. Target HSA peptides for quantification were specified as FKDLGEENFK, KQTALVELVK, and KVPQVSTPTVEVSR. The resolution was specified as 30000. Skyline-generated theoretical precursor and fragment ion masses based on the specified parameters served as the spectral library for precursor quantification. The retention times of the peptides were manually corrected wherever necessary. High-intensity b and y fragment ions of each precursor detected in all samples were selected, and their areas under curve (AUC) were integrated to calculate the AUC of the respective precursor. The AUC of DFL-modified peptides was normalized with the AUC of corresponding unmodified peptides to quantify the respective glycated peptides in each sample.

Statistical Analysis. One-way analysis of variance (ANOVA) followed by a *post hoc* Tukey's test was performed to compare the glycated HSA peptide level among different subject groups. Correlation analysis of DFL-modified peptides with all the recorded clinical parameters was performed using Pearson's correlation method. The ROC curve analysis was performed using MedCalc version 20.0.1 (MedCalc Software Ltd., Ostend, Belgium) to assess and compare the accuracy of glycated HSA peptides as a marker to detect diabetic nephropathy. *p*-values less than 0.05 were considered statistically significant.

https://doi.org/10.1021/acsomega.3c01219
ACS Omega XXXX, XXX, XXX−XXX

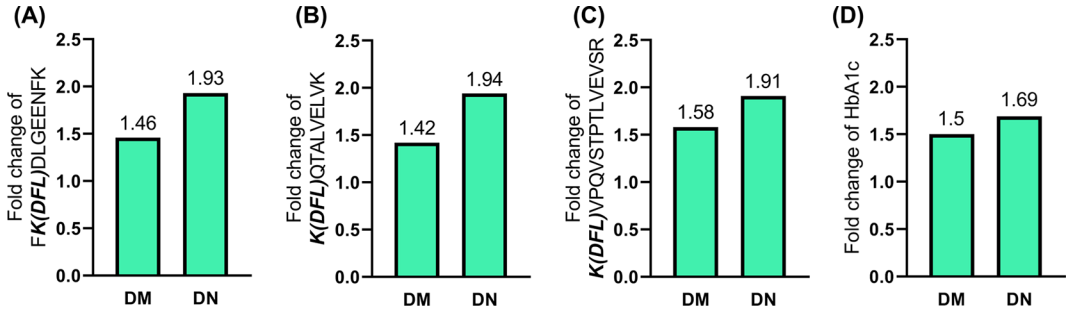

Figure 2. Fold-change in DFL-modified HSA peptide levels and HbA_{1c} in different subject groups. Compared to the healthy group, an increase in the level of F***K(DFL)***DLGEENFK (A), ***K(DFL)***QTALVELVK (B), ***K(DFL)***VPQVSTPTLVEVSR (C), and HbA_{1c} (D) was observed in both DM and DN groups.

RESULT AND DISCUSSION

Diabetic nephropathy is a major complication of diabetes. With the increasing prevalence of diabetes, the burden of diabetic nephropathy will also increase in parallel. At the last stage of diabetic nephropathy, known as end-stage renal disease, patients must undergo dialysis or renal transplant.[24] Therefore, it is vital to predict and detect diabetic nephropathy early to resort to early preventive and therapeutic measures to delay or stop the progression to end-stage renal disease. However, it has been reported that the currently used markers, based on urinary albumin concentration measurement, are not efficient in detecting diabetic nephropathy at early stages; and it can be detected only when there is increased albumin excretion in urine, a condition called microalbuminuria. At this stage, the kidneys are already damaged.[5] Hence, there is an urgent need of a marker for predicting diabetic nephropathy.

Plasma proteins with different half-lives can reflect the glycemic status of varying periods.[16] Among these, there has been a growing interest in glycated albumin as a marker for monitoring glycemic status and predicting diabetic complications.[1,11,15] Glycated albumin has several advantages as a marker. Being the most abundant plasma protein with many glycation-sensitive lysine and arginine residues directly exposed to plasma, HSA is prone to extensive glycation.[14] It has a half-life of 19 days, which is sufficient for glycation reactions. Therefore, glycated albumin could be a potential candidate marker for the risk prediction of diabetic nephropathy. Also, since different lysine and arginine residues of albumin have different propensities for glycation,[18,25] measuring the glycation on glycation-sensitive residues can be more sensitive for diabetic nephropathy prediction instead of measuring total glycation on albumin. In this context, we evaluated the level of glycation of the three glycation-sensitive HSA peptides, namely, FKDLGEENFK, KQTALVELVK, and KVPQVSTPTLVEVSR, in healthy, type II diabetes and diabetic nephropathy subjects using a targeted mass spectrometry approach, MRM-HR, to assess the utility of glycated HSA peptides as marker for risk prediction of diabetic nephropathy.

The site of glycation-sensitive lysine residues in HSA focused in this study, m/z values of glycated HSA peptides, and their corresponding unmodified peptides are shown in Table 1. The DFL-modified peptides are characterized by a mass increase of 162 Da. The MS output data were analyzed using Skyline. Representative chromatograms depicting coeluting fragment ions of DFL-modified HSA peptides are shown in Figure 1. Fragment ions present in all samples with good intensity were used for precursor quantification (Table 1). The b ions bearing DFL modification were considered as qualifier ions for glycation. The precursor AUC was derived by integrating the AUC of selected fragment ions, and the DFL-modified precursor AUC was normalized with the respective unglycated precursor AUC. The normalized AUC of DFL-modified HSA peptides and HbA_{1c} were compared between healthy, DM, and DN groups (Figure 1).

An increase in DFL modification of HSA peptides was observed from healthy to type II diabetes and further to diabetic nephropathy condition. DM group had significantly elevated levels of F***K(DFL)***DLGEENFK, ***K(DFL)***QTALVELVK, and ***K(DFL)***VPQVSTPTLVEVSR compared to the healthy group. Similarly, the level of F***K(DFL)***DLGEENFK, and ***K(DFL)***QTALVELVK was elevated in the DN group compared to the healthy and DM group. However, the DN group showed a significantly elevated level of ***K(DFL)***VPQVSTPTLVEVSR compared to the healthy group but not when compared to the DM group. Thus, all three DFL-modified HSA peptides, namely, F***K(DFL)***DLGEENFK, ***K(DFL)***QTALVELVK, and ***K(DFL)***VPQVSTPTLVEVSR, were able to differentiate between healthy and type II diabetes subjects. However, for diabetic nephropathy detection, only F***K(DFL)***DLGEENFK and ***K(DFL)***QTALVELVK were useful. ***K(DFL)***QTALVELVK levels showed a relatively higher statistically significant difference ($p < 0.0001$) between DM and DN groups than F***K(DFL)***DLGEENFK ($p = 0.0006$). Although HbA_{1c} also could differentiate between DM and DN groups, it had a lesser statistically significant difference ($p = 0.0163$) than that observed with F***K(DFL)***DLGEENFK and ***K(DFL)***QTALVELVK for detecting diabetic nephropathy. This was also evident when the increase in DFL modification of HSA peptides in DM and DN groups compared to the healthy group was represented in terms of fold change and compared to that of HbA_{1c} (Figure 2). While HbA_{1c} showed only a 1.69 fold increase in the DN group, F***K(DFL)***DLGEENFK and ***K(DFL)***QTALVELVK were increased by 1.93 and 1.94 fold, respectively, in the DN group compared to healthy subjects. This finding indicates that F***K(DFL)***DLGEENFK and ***K(DFL)***QTALVELVK are more sensitive than HbA_{1c} and may better predict diabetic nephropathy risk. The higher DFL modification of HSA peptides in the DN group could be attributed to the faster DFL modification of albumin than hemoglobin.[1] Also, since albumin has a short half-life than hemoglobin, glycated albumin can reflect glycemic changes faster than HbA_{1c}.[9] Therefore, DFL-modified HSA peptides may detect diabetic nephropathy sensitively and earlier than HbA_{1c}. Thus, the faster increase in DFL modification of albumin compared to hemoglobin translates into higher

https://doi.org/10.1021/acsomega.3c01219
ACS Omega XXXX, XXX, XXX−XXX

glycated albumin to HbA_{1c} ratio observed in diabetic nephropathy.[9]

Glycated albumin has previously been assessed for the risk prediction of diabetic nephropathy and has been compared with HbA_{1c}.[1,11,15] Our results are in agreement with the earlier reports that glycated albumin predicts early diabetic nephropathy development than HbA_{1c}.[8,9] This can be explained by the fact that the glycation of albumin changes faster than glycated hemoglobin in response to the serum glycemic index, i.e., albumin is more sensitive to glycation than hemoglobin.[26,27] Different plasma proteins get glycated to different extents,[16,17] and the degree of glycation increases with the increase in glycemia.[28] Glycated albumin level also increases with the severity of diabetes.[10] Thus, being the most abundant plasma protein with a large number of lysine and arginine residues, the DFL-albumin accumulates in patients with diabetes and later promotes the development of diabetic complications, such as diabetic nephropathy.[1] While previous studies mostly quantified total albumin glycation using an enzymatic assay, quantification of glycation-sensitive HSA peptides by mass spectrometry could be more sensitive.

ROC curve analysis was performed to assess the diabetic nephropathy detection accuracy of glycated HSA peptides F*K(DFL)*DLGEENFK, *K(DFL)*QTALVELVK, and *K(DFL)*VPQVSTPTLVEVSR, and compared to that of HbA_{1c} (Figure 3). The sensitivity, specificity, and AUC of these peptides and HbA_{1c} are summarized in Table 2. The ROC plot for *K(DFL)*VPQVSTPTLVEVSR indicated that it was not useful as a marker for diabetic nephropathy detection (p = 0.6256). Among the other two DFL-modified peptides, the area under the ROC curve of *K(DFL)*QTALVELVK was more (AUC: 0.81, 95%CI: 0.674−0.907) than that of F*K(DFL)*DLGEENFK (AUC: 0.752, 95%CI: 0.610−0.863) for diabetic nephropathy detection. However, the difference between the AUCs of *K(DFL)*QTALVELVK and F*K(DFL)*DLGEENFK was insignificant (Table S2). Similarly, the AUC of the ROC curve for both F*K(DFL)*DLGEENFK and *K(DFL)*QTALVELVK was more than that of HbA_{1c}, though not statistically significant. Thus, among the three DFL-modified HSA peptides, *K(DFL)*QTALVELVK and F*K(DFL)*DLGEENFK could be useful markers for predicting diabetic nephropathy.

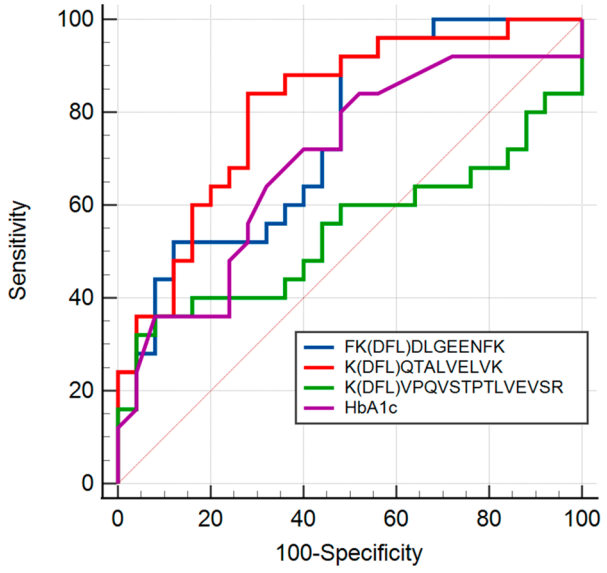

Figure 3. ROC curve analysis for DFL-modified HSA peptides and HbA_{1c} in the detection of diabetic nephropathy.

Pearson's correlation analysis was performed to check for the association of DFL-modified HSA peptides and HbA_{1c} with clinical parameters, especially with diabetic nephropathy-associated parameters, i.e., urine microalbumin and serum creatinine (Table 3). F*K(DFL)*DLGEENFK, *K(DFL)*QTALVELVK, and *K(DFL)*VPQVSTPTLVEVSR showed a strong positive correlation with fasting and postprandial blood glucose level and HbA_{1c}. Urine microalbumin represents the extent of urinary albumin excretion, a parameter used in diabetic nephropathy diagnosis. *K(DFL)*QTALVELVK showed a stronger positive correlation with urine microalbumin (r = 0.429***) than F*K(DFL)*DLGEENFK (r = 0.333**) and HbA_{1c} (r = 0.351**), while all these three markers showed a negative correlation with serum albumin. Only *K(DFL)*QTALVELVK showed a significant positive correlation with serum creatinine (r = 0.326**), a nitrogenous waste elevated in diabetic nephropathy. *K(DFL)*VPQVSTPTLVEVSR was not associated with urine microalbumin or serum creatinine levels. Therefore, *K(DFL)*QTALVELVK showed the best association with diabetic nephropathy-associated markers.

Thus, based on mass spectrometry, ROC curve, and correlation analysis, it can be concluded that *K(DFL)*QTALVELVK could be a better risk prediction marker for diabetic nephropathy, followed by F*K(DFL)*DLGEENFK and HbA_{1c}.

CONCLUSION

Currently, there are no markers in clinical practice that can detect diabetic nephropathy at very early stages. Therefore, in the search for a potential marker, we evaluated the glycated HSA peptides for the risk prediction of diabetic nephropathy. *K(DFL)*QTALVELVK and F*K(DFL)*DLGEENFK could detect diabetic nephropathy better than HbA_{1c}. *K(DFL)*QTALVELVK was better correlated with diabetic nephrop-

Table 2. Summary of ROC Curve Analysis for Assessing the Accuracy of DFL-Modified HSA Peptides and HbA_{1c} for Detecting Diabetic Nephropathy

	DM vs DN			
Peptide	Sensitivity	Specificity	p-value	AUC (95% CI)
F*K(DFL)*DLGEENFK	92	52	0.0002**	0.752 (0.610−0.863)
*K(DFL)*QTALVELVK	84	72	<0.0001***	0.81 (0.674−0.907)
*K(DFL)*VPQVSTPTLVEVSR	36	92	0.6256	0.542 (0.396−0.684)
HbA_{1c}	82	52	0.0101*	0.696 (0.550−0.818)

*p < 0.05. **p < 0.001. ***p < 0.0001

https://doi.org/10.1021/acsomega.3c01219
ACS Omega XXXX, XXX, XXX−XXX

Table 3. Correlation of DFL-Modified HSA Peptides and HbA_{1c} with Clinical Parameters

Clinical parameters	Correlation coefficient (r)			
	F*K(DFL)*DLGEENFK	*K(DFL)*QTALVELVK	*K(DFL)*VPQVSTPTLVEVSR	HbA_{1c}
FBG (n = 75)	0.606****	0.635****	0.574***	0.788****
PPBG (n = 74)	0.7****	0.656****	0.578***	0.783****
HbA_{1c} (n = 75)	0.727****	0.787****	0.558***	1****
Total cholesterol (n = 75)	−0.107	−0.127	−0.098	−0.026
Triglycerides (n = 75)	0.06	0.088	0.046	0.189
HDL (n = 75)	−0.116	−0.09	−0.027	−0.157
LDL (n = 75)	−0.158	−0.193	−0.111	−0.105
VLDL (n = 75)	0.061	0.098	0.043	0.194
Serum creatinine (n = 74)	0.161	0.326**	−0.091	0.221
Serum albumin (n = 74)	−0.28*	−0.356**	−0.107	−0.449****
Urine microalbumin (n = 63)	0.333**	0.429***	0.152	0.351**

*p < 0.05. **p < 0.01. ***p < 0.001. ****p < 0.0001.

athy-associated clinical parameters, i.e., serum creatinine and urine microalbumin, than F***K(DFL)***DLGEENFK. Absolute quantification and determining the range and cutoff value in a large cohort would help in developing ***K(DFL)***QTALVELVK peptide as a risk prediction marker for diabetic nephropathy.

■ ASSOCIATED CONTENT

Data Availability Statement

The mass spectrometry proteomics data have been deposited to the ProteomeXchange Consortium via the PRIDE partner repository (https://www.ebi.ac.uk/pride) with the data set identifier PXD040028.

Supporting Information

The Supporting Information is available free of charge at https://pubs.acs.org/doi/10.1021/acsomega.3c01219.

Precursor masses and collision energies specified in the MRM-HR acquisition method (Table S1); Comparison of potential markers for diabetic nephropathy risk prediction based on ROC curve (Table S2) (PDF)

■ AUTHOR INFORMATION

Corresponding Author

Mahesh J. Kulkarni − *Biochemical Sciences Division, CSIR-National Chemical Laboratory, Pune 411008, India; Academy of Scientific and Innovative Research (AcSIR), Ghaziabad 201002, India;* orcid.org/0000-0003-3932-9092; Email: mj.kulkarni@ncl.res.in

Authors

Arvindkumar H. Chaurasiya − *Biochemical Sciences Division, CSIR-National Chemical Laboratory, Pune 411008, India; Academy of Scientific and Innovative Research (AcSIR), Ghaziabad 201002, India*

Meera R. Jaiswal − *Biochemical Sciences Division, CSIR-National Chemical Laboratory, Pune 411008, India; Academy of Scientific and Innovative Research (AcSIR), Ghaziabad 201002, India*

Santhakumari Bayatigeri − *Academy of Scientific and Innovative Research (AcSIR), Ghaziabad 201002, India; Center for Materials Characterization, CSIR-National Chemical Laboratory, Pune 411008, India*

Shweta Kahar − *Department of Diabetes and Endocrine Research, Chellaram Diabetes Institute, Pune 411021, India*

Shalbha Tiwari − *Department of Diabetes and Endocrine Research, Chellaram Diabetes Institute, Pune 411021, India*

Ambika G. Unnikrishnan − *Department of Diabetes and Endocrine Research, Chellaram Diabetes Institute, Pune 411021, India*

Complete contact information is available at: https://pubs.acs.org/10.1021/acsomega.3c01219

Author Contributions

Conceptualization: M.J.K.; Formal analysis: A.H.C.; Investigation: A.H.C., M.R.J., S.K., and S.T.; Methodology: M.J.K., A.H.C., and S.T.; Resources: M.J.K., B.S.K., and A.G.U.; Data curation: A.H.C., S.K., and M.J.K.; Supervision: M.J.K. and S.T.; Writing - original draft: A.H.C. and M.J.K.; Writing - review and editing: M.J.K., S.T., A.G.U., S.K., B.S.K., and M.R.J.

Notes

The authors declare no competing financial interest.

■ ACKNOWLEDGMENTS

The authors thank all of the study participants. A.H.C. thanks the University Grants Commission for the fellowship.

■ REFERENCES

(1) Neelofar, K.; Ahmad, J. Amadori albumin in diabetic nephropathy. *Indian J. Endocrinol Metab* **2015**, *19* (1), 39−46.

(2) Campion, C. G.; Sanchez-Ferras, O.; Batchu, S. N. Potential Role of Serum and Urinary Biomarkers in Diagnosis and Prognosis of Diabetic Nephropathy. *Can. J. Kidney Health Dis* **2017**, *4*, 1−18.

(3) Gheith, O.; Farouk, N.; Nampoory, N.; Halim, M. A.; Al-Otaibi, T. Diabetic kidney disease: world wide difference of prevalence and risk factors. *J. Nephropharmacol* **2016**, *5* (1), 49−56.

(4) American Diabetes Association.. Nephropathy in Diabetes. *Diabetes Care* **2004**, *27* (suppl_1), s79−s83.

(5) Mogensen, C. E. Microalbuminuria, blood pressure and diabetic renal disease: origin and development of ideas. *Diabetologia* **1999**, *42* (3), 263−285.

(6) Gross, J. L.; de Azevedo, M. J.; Silveiro, S. P.; Canani, L. H.; Caramori, M. L.; Zelmanovitz, T. Diabetic nephropathy: diagnosis, prevention, and treatment. *Diabetes Care* **2005**, *28* (1), 164−176.

(7) Umayahara, Y.; Fujita, Y.; Watanabe, H.; Kasai, N.; Fujiki, N.; Hatazaki, M.; Koga, M. Association of glycated albumin to HbA1c ratio with diabetic retinopathy but not diabetic nephropathy in patients with type 2 diabetes. *Clin Biochem* **2017**, *50* (6), 270−273.

(8) Jun, J. E.; Hur, K. Y.; Lee, Y. B.; Lee, S. E.; Jin, S. M.; Lee, M. K.; Kim, J. H. Glycated albumin predicts the development of early diabetic nephropathy in patients with type 2 diabetes. *Diabetes Metab* **2018**, *44* (2), 178−180.

(9) Wang, N.; Xu, Z.; Han, P.; Li, T. Glycated albumin and ratio of glycated albumin to hemoglobin are good indicators of diabetic nephropathy in type 2 diabetes mellitus. *Diabetes/metabolism research and reviews* **2017**, *33*, e2843.
(10) Kondaveeti, S. B.; D, K.; Mishra, S.; Kumar, R. A.; Shaker, I. A. Evaluation of glycated albumin and microalbuminuria as early risk markers of nephropathy in type 2 diabetes mellitus. *J. Clin Diagn Res.* **2013**, *7* (7), 1280−1283.
(11) Nathan, D. M.; McGee, P.; Steffes, M. W.; Lachin, J. M. Relationship of glycated albumin to blood glucose and HbA1c values and to retinopathy, nephropathy, and cardiovascular outcomes in the DCCT/EDIC study. *Diabetes* **2014**, *63* (1), 282−290.
(12) Yoon, H. J.; Lee, Y. H.; Kim, S. R.; Rim, T. H.; Lee, E. Y.; Kang, E. S.; Cha, B. S.; Lee, H. C.; Lee, B. W. Glycated albumin and the risk of micro- and macrovascular complications in subjects with type 1 diabetes. *Cardiovasc Diabetol* **2015**, *14*, 53.
(13) Raoufinia, R.; Mota, A.; Keyhanvar, N.; Safari, F.; Shamekhi, S.; Abdolalizadeh, J. Overview of Albumin and Its Purification Methods. *Adv. Pharm. Bull.* **2016**, *6* (4), 495−507.
(14) Vetter, S. W. Glycated Serum Albumin and AGE Receptors. *Adv. Clin Chem.* **2015**, *72*, 205−275.
(15) Parrinello, C. M.; Selvin, E. Beyond HbA1c and glucose: the role of nontraditional glycemic markers in diabetes diagnosis, prognosis, and management. *Curr. Diab Rep* **2014**, *14* (11), 548.
(16) Soboleva, A.; Mavropulo-Stolyarenko, G.; Karonova, T.; Thieme, D.; Hoehenwarter, W.; Ihling, C.; Stefanov, V.; Grishina, T.; Frolov, A. Multiple Glycation Sites in Blood Plasma Proteins as an Integrated Biomarker of Type 2 Diabetes Mellitus. *International journal of molecular sciences* **2019**, *20*, 2329.
(17) Frolov, A.; Blüher, M.; Hoffmann, R. Glycation sites of human plasma proteins are affected to different extents by hyperglycemic conditions in type 2 diabetes mellitus. *Anal. Bioanal. Chem.* **2014**, *406* (24), 5755−5763.
(18) Rathore, R.; Sonwane, B. P.; Jagadeeshaprasad, M. G.; Kahar, S.; Santhakumari, B.; Unnikrishnan, A. G.; Kulkarni, M. J. Glycation of glucose sensitive lysine residues K36, K438 and K549 of albumin is associated with prediabetes. *Journal of proteomics* **2019**, *208*, 103481.
(19) Crutchfield, C. A.; Thomas, S. N.; Sokoll, L. J.; Chan, D. W. Advances in mass spectrometry-based clinical biomarker discovery. *Clinical Proteomics* **2016**, *13* (1), 1.
(20) Korwar, A. M.; Vannuruswamy, G.; Jagadeeshaprasad, M. G.; Jayaramaiah, R. H.; Bhat, S.; Regin, B. S.; Ramaswamy, S.; Giri, A. P.; Mohan, V.; Balasubramanyam, M.; Kulkarni, M. J. Development of Diagnostic Fragment Ion Library for Glycated Peptides of Human Serum Albumin: Targeted Quantification in Prediabetic, Diabetic, and Microalbuminuria Plasma by Parallel Reaction Monitoring, SWATH, and MSE. *Mol. Cell Proteomics* **2015**, *14* (8), 2150−2159.
(21) Frolov, A.; Hoffmann, R. Identification and relative quantification of specific glycation sites in human serum albumin. *Anal. Bioanal. Chem.* **2010**, *397* (6), 2349−2356.
(22) Qiu, H. Y.; Hou, N. N.; Shi, J. F.; Liu, Y. P.; Kan, C. X.; Han, F.; Sun, X. D. Comprehensive overview of human serum albumin glycation in diabetes mellitus. *World journal of diabetes* **2021**, *12* (7), 1057−1069.
(23) Brede, C.; Hop, B.; Jørgensen, K.; Skadberg, Ø. Measurement of glycated albumin in serum and plasma by LC-MS/MS. *Scandinavian journal of clinical and laboratory investigation* **2016**, *76* (3), 195−201.
(24) Natesan, V.; Kim, S. J. Diabetic Nephropathy - a Review of Risk Factors, Progression, Mechanism, and Dietary Management. *Biomol Ther (Seoul)* **2021**, *29* (4), 365−372.
(25) Barnaby, O. S.; Cerny, R. L.; Clarke, W.; Hage, D. S. Comparison of modification sites formed on human serum albumin at various stages of glycation. *Clin. Chim. Acta* **2011**, *412* (3−4), 277−285.
(26) Takahashi, S.; Uchino, H.; Shimizu, T.; Kanazawa, A.; Tamura, Y.; Sakai, K.; Watada, H.; Hirose, T.; Kawamori, R.; Tanaka, Y. Comparison of glycated albumin (GA) and glycated hemoglobin (HbA1c) in type 2 diabetic patients: usefulness of GA for evaluation of short-term changes in glycemic control. *Endocr J.* **2007**, *54* (1), 139−144.
(27) Day, J. F.; Ingebretsen, C. G.; Ingebretsen, W. R., Jr; Baynes, J. W.; Thorpe, S. R. Nonenzymatic Glucosylation of Serum Proteins and Hemoglobin: Response to Changes in Blood Glucose Levels in Diabetic Rats. *Diabetes* **1980**, *29* (7), 524−527.
(28) Jagadeeshaprasad, M. G.; Batkulwar, K. B.; Meshram, N. N.; Tiwari, S.; Korwar, A. M.; Unnikrishnan, A. G.; Kulkarni, M. J. Targeted quantification of N-1-(carboxymethyl) valine and N-1-(carboxyethyl) valine peptides of β-hemoglobin for better diagnostics in diabetes. *Clinical Proteomics* **2016**, *13* (1), 7.

https://doi.org/10.1021/acsomega.3c01219
ACS Omega XXXX, XXX, XXX−XXX

ACS OMEGA

http://pubs.acs.org/journal/acsodf

Article

Nanopore Sequencing of *RAGE* Gene Polymorphisms and Their Association with Type 2 Diabetes

Arvindkumar H. Chaurasiya, Ajinkya A. Khilari, Rubina Kazi, Meera R. Jaiswal, Gouri M. Bhoite, Meghana K. Padwal, Abdulrahaman A. Momin,* Dhanasekaran Shanmugam,* and Mahesh J. Kulkarni*

Cite This: https://doi.org/10.1021/acsomega.3c00297

Read Online

ACCESS | Metrics & More | Article Recommendations | Supporting Information

ABSTRACT: The receptor for advanced glycation end products (RAGE) is a transmembrane protein that interacts with its ligands, advanced glycation end products (AGEs). AGEs are elevated in diabetes and diabetic complications, leading to increased oxidative stress and activation of pro-inflammatory pathways facilitated by AGE−RAGE signaling. Polymorphisms in the *RAGE* gene can potentially affect AGE−RAGE interaction and its downstream signaling, which plays a crucial role in the progression of diabetes and its complications. In this study, we used nanopore sequencing for genotyping of *RAGE* polymorphism and identified a maximum number of 33 polymorphisms, including two previously unreported novel mutations in a cohort of healthy, type 2 diabetics without nephropathy and type 2 diabetics with nephropathy in order to identify associations. Two novel *RAGE* polymorphisms in the intron 8 and 3′UTR region at genomic locations 32181834 and 32181132, respectively, were detected with a low frequency. For four previously reported polymorphisms, cross-validation by PCR-RFLP showed 99.75% concordance with nanopore sequencing. Analysis of genotype distribution and allele frequencies revealed that five single nucleotide polymorphisms, i.e., rs1800625, rs3131300, rs3134940, rs2070600, and rs9391855, were associated with an increased risk for type 2 diabetes.

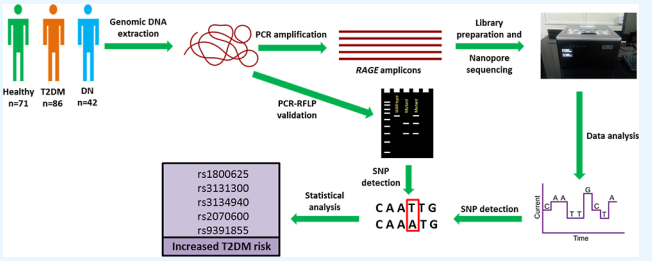

1. INTRODUCTION

Diabetes is a complex metabolic disorder caused by insufficient insulin secretion, as in type 1 diabetes mellitus, or insulin resistance, as in type 2 diabetes mellitus. According to the International Diabetes Federation, 537 million adults worldwide had diabetes in 2021, which is projected to increase to 783 million by 2045. Chronic hyperglycemic condition in diabetics promotes the development of several microvascular and macrovascular complications, such as diabetic retinopathy, diabetic nephropathy, diabetic neuropathy, and cardiovascular diseases.[1] Among these, diabetic nephropathy is a major complication of diabetes, and 20−40% of diabetic patients develop diabetic nephropathy in their lifetime.[2,3] It is a leading cause of end-stage renal disease.[4]

Several etiological factors, including lifestyle, genetics, environment, and ethnicity, are among the major factors responsible for the development of diabetes and its complications.[5−7] Among these, genetic factors are responsible for differential susceptibility to the progression of diabetes and its complications. Differential expression and polymorphism in several genes have been reported to be associated with diabetes and its complications, such as *PPARG*, *IRS*-1, *IRS*-2, *IL*-1*β*, *SLC2A2*, *PI3KR1*, *VEGF*, *ELMO1*, *ADIPOQ*, and *RAGE*.[8−12] The *RAGE* gene is highly polymorphic, and *RAGE* polymorphisms are among the most investigated for their association with numerous diseases.[11] The *RAGE* gene encodes for a protein called receptor for advanced glycation end products. It is a membrane-bound multiligand receptor belonging to the immunoglobulin superfamily. It consists of an extracellular variable domain, two extracellular constant domains, one transmembrane domain, and one cytosolic domain. RAGE binds to AGEs, and this AGE−RAGE interaction activates the nuclear transcription factor NF-*κ*B, which increases cytokine production, oxidative stress, and inflammation and contributes to the pathogenesis of diabetes and its complications.[1,13,14]

The involvement of RAGE in diabetes and diabetic nephropathy has been well established.[11] The single nucleotide polymorphisms (SNPs) present in the exonic regions of the *RAGE* gene can cause non-synonymous replacement of the amino acids that can alter the RAGE structure.[15] Alteration in the RAGE structure can potentially affect its binding with its ligands and downstream signaling. Also, SNPs present in the promoter region of *RAGE* can affect the transcriptional activity of *RAGE*, hence affecting its expression.[16] Although SNPs in

Received: January 15, 2023
Accepted: May 22, 2023

the intron region may not directly affect the RAGE structure, they might affect the splicing of RAGE mRNA, leading to the expression of different RAGE isoforms.[11] The sequences for 13 different splice variants of RAGE have been reported and are available in GenBank (ncbi.nlm.nih.gov/genbank, Oct 2022).

Polymerase chain reaction-restriction fragment length polymorphism (PCR-RFLP) is routinely used for SNP detection. However, it is not a high-throughput method as it detects only one SNP at a time and is time-consuming.[17] Moreover, by PCR-RFLP, one can interrogate only previously reported mutations. On the other hand, DNA sequencing facilitates the identification of all variations associated with the locus of interest. Oxford Nanopore Technology (ONT) (nanoporetech.com) based DNA sequencing is a third-generation nucleic acid sequencing technology that has recently gained attention for rapid and high-throughput sequencing of DNA and RNA. The ONT approach generates long-read sequences with high accuracy and is increasingly used for high-throughput *de novo* sequencing and SNP detection.[18−20]

Several studies have reported the association of *RAGE* polymorphisms with the risk of diabetes and its complications;[11] however, the reported findings are often contradictory and may have missed many mutations due to reliance on techniques such as PCR-RFLP. In this study, nanopore sequencing of the *RAGE* gene was performed to detect all *RAGE* polymorphisms (known and novel) in a cohort population from Pune, India, and to evaluate the possibility of establishing this technique as a robust and routine diagnostic method for SNP detection. To compare and cross-validate the findings from nanopore sequencing, we used the PCR-RFLP method to interrogate the four most commonly reported SNPs of the *RAGE* gene, i.e., rs3134940, rs1800624, rs1800625, and rs2070600 from the samples. Statistical analyses were performed to check for the association of detected *RAGE* SNPs with type 2 diabetes and diabetic nephropathy. Further, we quantified diabetes-associated biochemical markers, such as fasting blood glucose (FBG) and HbA_{1c} (glycated hemoglobin). We also measured plasma fructosamine, glycated albumin, an inflammatory cytokine, i.e., tumor necrosis factor-α (TNF-α), malondialdehyde (MDA), fasting insulin, homeostatic model assessment for insulin resistance (HOMA-IR), and C-reactive protein (CRP). Finally, we assessed these clinical and biochemical parameters for their association with type 2 diabetes-associated *RAGE* SNPs. Since diabetes and its complications remain asymptomatic until the appearance of the first symptoms or diagnosis,[2,21] it is crucial to detect them early to reverse, stop, or regress the progression of diabetes and its complications. Any association of SNPs with the risk of diabetes or diabetic nephropathy development can serve as a disease risk biomarker, enabling the screening of individuals vulnerable to disease development at a much earlier stage for early preventive measures.

2. MATERIALS AND METHODS

2.1. Study Design. We designed a case−control study to check for the association of *RAGE* SNPs with type 2 diabetes. A few of the diabetic subjects had diabetic nephropathy, and hence *RAGE* SNPs were also evaluated for their association with diabetic nephropathy. DNA was extracted from the blood samples of healthy, type 2 diabetics without nephropathy (DM) and type 2 diabetics with nephropathy (DN). The full-length *RAGE* gene was PCR amplified from each sample, and the amplicons were sequenced by ONT for the purpose of identifying all genetic variations associated with the gene (such as SNPs and in-dels). This approach enabled us to determine the genotype and allele frequencies of the detected *RAGE* SNPs in each subject group and the possibility of detecting any novel polymorphisms in the *RAGE* gene in our cohort group. Appropriate statistical analyses were performed to determine the association of specific genotypes and alleles with type 2 diabetes and diabetic nephropathy. Four previously reported SNPs (rs3134940, rs1800624, rs1800625, and rs2070600), which were also detected by nanopore sequencing in the samples used in this study, were cross-validated by the PCR-RFLP method in all of the samples. To assess the effect of type 2 diabetes-associated SNPs, the levels of diabetes-associated biochemical markers such as FBG, HbA_{1c}, fructosamine, glycated albumin, TNF-α, MDA, fasting insulin, HOMA-IR, and CRP were compared between the wild-type and carrier genotype subjects.

2.2. Subjects. A total of 128 subjects who were confirmed as type 2 diabetic, with or without diabetic nephropathy, and 71 unrelated healthy subjects were recruited in this cross-sectional study at Bharati Vidyapeeth (DTU) Medical College, Pune, India. Subjects having FBG ≥126 mg/dL were diagnosed as type 2 diabetic based on the 2003 American Diabetes Association diagnostic criteria for diabetes.[22] Type 2 diabetic subjects were further divided into two subgroups, i.e., without diabetic nephropathy (n = 86), having a urinary-albumin-to-creatinine ratio <30 mg/g, and with diabetic nephropathy (n = 42), having a urinary-albumin-to-creatinine ratio ≥30 mg/g. Type 2 diabetic subjects with diabetic complications other than diabetic nephropathy, type 1 diabetic subjects, pregnant women, subjects with angina or heart failure, and patients suffering from severe concurrent illness were excluded from the study. This study was approved by the ethics committee of Bharati Vidyapeeth (DTU) Medical College, Pune, and each participant gave written informed consent before participating.

2.3. Biochemical Analysis. Clinical and biochemical parameters such as age, sex, FBG, HbA_{1c}, blood urea, serum creatinine, cholesterol, triglyceride, high-density lipoprotein (HDL), fasting insulin, and CRP were measured for each participating subject at Bharati Vidyapeeth (DTU) Medical College, Pune. Besides these parameters, the plasma concentration of total protein (estimated by Bradford's method), fructosamine (using the fructosamine assay kit from Abbexa Ltd, Cambridge, UK), albumin (using bromocresol green albumin assay kit MAK124 from Sigma-Aldrich), glycated albumin (using the Human glycated albumin ELISA kit, CSB-E09599h, Cusabio, China), and MDA (using lipid peroxidation assay kit from Sigma-Aldrich), were determined. The plasma fructosamine concentration was normalized to total plasma protein concentration and was expressed as μM/g of plasma protein. To determine the plasma glycated albumin concentration, a four-parameter logistic regression curve was plotted using the web tool GainData ELISA data calculator (Arigo Biolaboratories, Hsinchu City 300, Taiwan). Glycated albumin concentration was normalized with respective plasma albumin concentrations and expressed in μM/g of albumin. HOMA-IR was calculated based on the following formula.[23]

$$\text{HOMA-IR} = [\text{fasting glucose (mmol/L)} \times \text{fasting insulin (mIU/L)}]/\ 22.5$$

https://doi.org/10.1021/acsomega.3c00297
ACS Omega XXXX, XXX, XXX−XXX

2.4. Nanopore DNA Sequencing of *RAGE* Gene. *2.4.1. DNA Isolation from Blood and PCR Amplification of RAGE Gene.* The genomic DNA was extracted from whole blood collected from subjects enrolled in the study using a DNA isolation kit (Qiagen, Hilden, Germany) and used as template DNA to amplify the *RAGE* gene. The nucleotide sequence of the *RAGE* gene was retrieved from NCBI with gene ID-177 (Oct 2022). Forward and reverse primers were designed such that the complete *RAGE* gene could be amplified along with the promoter region and 5′UTR and 3′UTR regions. The nucleotide sequence of the forward primer was 5′-GGGCAGTTCTCTCCTCACTT-3′ and that of the reverse primer was 5′-GCAAAGTTCCCTCT-GACTCTTCC-3′. All PCR amplifications were performed in 25 μL reaction volume using the LongAmp Taq 2X master mix PCR reactions (New England BioLabs Inc, Ipswich, MA, USA) with the addition of 25 ng of genomic DNA as a template and 0.2 μmol/L of each primer. The PCR reactions were run on a Veriti 96-well thermal cycler (Applied Biosystems, Foster City, California, USA) using the following protocol: initial heating of the reaction mixture at 95 °C for 10 min, followed by 35 cycles of denaturation at 95 °C for 30 s, primer annealing at 61 °C for 30 s, and extension at 65 °C for 5 min. The final extension was done at 65 °C for 10 min, after which the reaction mixture was cooled to 4 °C.

2.4.2. Oxford Nanopore DNA Sequencing Library Preparation. For sequencing the DNA amplicons, the sequencing library was prepared using the Oxford Nanopore Technologies Ligation Sequencing (SQK-LSK109) and Native Barcoding (EXP-NBD196) Kits. The *RAGE* amplicons were first purified using 1X AMPure XP beads (Beckman Coulter, USA), and the DNA concentration was measured using Qubit dsDNA BR Assay Kit (Invitrogen, USA) on a Qubit 2.0 fluorometer (Invitrogen, USA). A total of 200 fmol of each amplicon, i.e., 517 ng, was taken forward for the end-repair step, where the 3′ end was A-tailed using NEBNext Ultra II End Prep Enzyme Mix (New England BioLabs Inc, USA). The reaction mixture was incubated at 20 °C for 10 min, followed by heating at 65 °C for 10 min. Following the end-repair step, the amplicons were attached with barcodes available from the EXP-NBD196 kit (Oxford Nanopore Technologies, UK) using the 1X Blunt/TA ligase reaction (New England BioLabs Inc, USA). The reaction mixture was incubated at RT for 20 min, followed by heating at 65 °C for 10 min to denature the enzyme and stop the ligation reaction. The barcoded samples were kept in ice for 1 min and pooled, and the pooled barcoded library was purified by using the AMPure XP beads (0.4X of sample volume) from the SQK-LSK109 kit (Oxford Nanopore Technologies, UK). The washed library was eluted in 35 μL nuclease-free water and quantified by the Qubit 2.0 fluorometer. Next, the sequencing adapters were added to the ends of the barcoded DNA fragments by combining 200 fmol of the purified library with Adapter Mix II (Oxford Nanopore Technologies, UK) and Quick T4 ligase (New England BioLabs Inc, USA) and incubating this reaction mixture for 30 min at room temperature. The adapter-ligated library was purified using 1X AMPure XP beads according to the manufacturer's instructions and eluted in 15 μL elution buffer available from the SQK-LSK109 kit (Oxford Nanopore Technologies, UK). The final adapter-ligated purified library (50 fmol) was loaded onto the FLO-MIN106D flow cell, and sequencing was done on the GridION MK1 sequencer (Oxford Nanopore Technologies, UK) until at least 200 sequence reads were collected for each barcode.

2.4.3. Analysis of Oxford Nanopore Sequence Reads and Variant Calling. While sequencing the samples, real-time base calling and demultiplexing were carried out using the Guppy v.5.0.14 program, which is part of the MinKNOW v21.05.12 operating software (Oxford Nanopore Technologies, UK), which runs the GridION sequencer. The super-accurate base calling model was selected for base calling, and demultiplexing was performed using the "require barcodes at both ends" option. A bash script was written to perform all the steps required for further analysis, such as length filtering, variant calling, and generation of consensus assembly. The bash script can be accessed through the GitHub link https://github.com/ajinkyakhilari/ampvar. After the demultiplexing step, the read length and quality filtering was carried out using the NanoFilt software v2.5.0.[24] Minimap2 v2.24[25] was used to align the length and quality-filtered nanopore reads to the sequence of full-length human chromosome 6 (where the *RAGE* gene is located) downloaded from GenBank (ncbi.nlm.nih.gov/genome/gdv/browser/gene/?id=7124, Oct 2022). The individual aligned reads were sorted according to genomic coordinates using the SAMtools v1.14[26] sort command, and variant calling was performed on the aligned and sorted reads using the Nanopolish v0.13[27] variant caller with the ploidy set to 2. Thereafter, *de novo* assembly and read polish were carried out using Canu v2.2,[28] Racon v1.4.3,[29] and Medaka v1.5[30] programs using their default parameter settings. Variant calling and annotation were performed using the SnpEff v4.3[31] from the Galaxy ToolShed,[32] and all *RAGE* SNPs detected were analyzed for linkage disequilibrium using the web tool SNPStats.[33]

2.5. Genotyping of the *RAGE* Gene by PCR-RFLP. Four previously reported SNPs of the *RAGE* gene (rs3134940, rs1800624, rs1800625, and rs2070600) were detected by nanopore sequencing in the samples analyzed in this study, and these were verified using the PCR-RFLP method. Previously reported primers were used to amplify the regions of the *RAGE* gene containing these SNPs,[34−36] except the reverse primer for rs1800624. The primer sequences used for PCR amplification and the length of PCR products are summarized in Table 1.

Table 1. PCR-RFLP Primer Pair Used for the Amplification of a Region Spanning the Polymorphic Site of the *RAGE* Gene and the Size of PCR-Amplified Product

SNP	primer sequence	PCR product size (bp)
rs3134940	forward primer: 5′-TAATTTCCTGCCCCATTCTG-3′	396
	reverse primer: 5′-CATCGCAATCTATGCCTCCT-3′	
rs1800624	forward primer: 5′-GGGGCAGTTCTCTCCTCACT-3′	502
	reverse primer: 5′-CGTCTTGTCACAGGGAATGC-3′	
rs1800625	forward primer: 5′-GGGGCAGTTCTCTCCTCACT-3′	249
	reverse primer: 5′-GGTTCAGGCCAGACTGTTGT-3′	
rs2070600	forward primer: 5′-GTAAGCGGGGCTCCTGTTGCA-3′	397
	reverse primer: 5′-GGCCAAGGCTGGGGTTGAAGG-3′	

https://doi.org/10.1021/acsomega.3c00297
ACS Omega XXXX, XXX, XXX−XXX

Table 2. Restriction Enzymes Used for SNP Detection by PCR-RFLP, Restriction Sites, and the Size of Restriction Digestion Products

SNP	restriction enzyme	restriction site	sequence in wild-type allele	sequence in mutant allele	restriction digestion product size (bp)	
					wild-type	mutant
rs3134940	BsmF1	GGGAC (10/14)[a]	GG**A**AC	GG**G**AC	396	160 + 236 (RS creation)
rs1800624	Mfe1	C/AATTG	CAATTG	CAAATG	215 + 287	502 (RS deletion)
rs1800625	Alu1	AG/CT	AG**T**T	AG**C**T	249	89 + 160 (RS creation)
rs2070600	Alu1	AG/CT	**G**GCT	**A**GCT	248 + 149	181 + 67 + 149 (RS creation)

[a]BsmFI cuts 10 nucleotides away from the restriction site in the same DNA strand and 14 nucleotides away in the complementary DNA strand. The nucleotide at the polymorphic site is represented by bold font. RS: restriction site.

Table 3. Clinical Characteristics of Healthy Control, DM, DN, and DM + DN Subjects[a]

clinical characteristics	healthy	DM	DN	DM + DN
age (years)	55.77 ± 10.16	56.4 ± 9.58	58.71 ± 11.27	57.16 ± 10.18
sex (male/female)	37/34	43/43	27/15	70/58
FBG (mg/dL)	99.73 ± 8.28	218.9 ± 79.48†	251.5 ± 78.06†,‡	229.6 ± 80.19†
HbA_{1c} (%)	5.54 ± 0.59	9.15 ± 2.16†	8.52 ± 1.91†	8.94 ± 2.1†
blood urea (mg/dL)	22.93 ± 6.83	24.52 ± 7.85	87.71 ± 28.63†,‡	45.26 ± 34.54†
serum creatinine (mg/dL)	0.82 ± 0.14	0.88 ± 0.19	4.8 ± 1.99†,‡	2.17 ± 2.17†
cholesterol (mg/dL)	149.3 ± 35.28	159.7 ± 43.71	177.8 ± 44.24†	165.7 ± 44.54†
triglyceride (mg/dL)	106.3 ± 34.92	138.9 ± 75.99†	187.1 ± 85.05†,‡	154.7 ± 81.95†
HDL (mg/dL)	42.27 ± 9.18	38.81 ± 12.01	34.68 ± 11.18†	37.45 ± 11.86†
normalized fructosamine (μM/g)	25.86 ± 10.06 (n = 51)	38.26 ± 13.61† (n = 64)	40.66 ± 15.00† (n = 40)	39.19 ± 14.14† (n = 104)
normalized glycated albumin (μM/g)	0.77 ± 0.31 (n = 51)	1.02 ± 0.39† (n = 64)	1.18 ± 0.44† (n = 40)	1.08 ± 0.41† (n = 104)
TNF-α (pg/mL)	16.97 ± 22.00 (n = 26)	18.97 ± 19.83 (n = 22)	37.76 ± 54.28 (n = 28)	29.50 ± 43.36 (n = 50)
MDA (nM/mL)	39.18 ± 28.22 (n = 29)	51.81 ± 33.8 (n = 24)	46.18 ± 31.72 (n = 31)	48.64 ± 32.46 (n = 55)
insulin (μM/mL)	17.38 ± 16.66 (59)	17.69 ± 17.3 (68)	20.19 ± 48.04 (36)	18.55 ± 31.31 (104)
HOMA-IR	4.23 ± 4.12 (59)	8.96 ± 7.68 (68)	14.01 ± 38.27 (36)	10.71 ± 23.28 (104)
CRP (mg/L)	16.33 ± 39.97 (53)	35.37 ± 60.31 (66)	53.15 ± 78.37 (36)	41.65 ± 67.39 (102)

[a]Data are presented as mean ± SD or number of subjects. Number of subjects: healthy, n = 71; DM, n = 86; DN, n = 42; unless otherwise mentioned, $^{\dagger}p < 0.05$ vs healthy; $^{\ddagger}p < 0.05$ vs DM. HDL: high-density lipoprotein; TNF-α: tumor necrosis factor-α.

All PCR amplifications were performed in 15 μL reaction volume by adding 10 ng of genomic DNA as a template and 0.3 μmol/L of each primer of primer pair in the master mix for PCR reactions (New England BioLabs Inc, USA). The PCR amplification protocol was the same as that used for amplifying the *RAGE* gene, except that the primer annealing temperature was set at 62 °C. The restriction digestion of the PCR amplicons was carried out using specific restriction enzymes (New England BioLabs Inc, USA) for each SNP, the details of which are shown in Table 2. The digested PCR products were resolved on a 2.5% (w/v) agarose gel, and the DNA bands were visualized under UV light. The number and size of DNA bands enabled differentiation between homozygous wild-type, heterozygous, and homozygous mutant subjects for the particular SNP, as shown in Table 2.

2.6. Statistical Analysis. All statistical analyses were performed using GraphPad Prism for Windows version 8.0.2 (GraphPad Software Inc, California, USA) or SPSS version 17.0 (SPSS Inc. Chicago, IL, USA). The clinical characteristics of the subjects were expressed as mean ± standard deviation (SD). The clinical characteristics and biochemical parameters across the groups were compared by one-way analysis of variance (ANOVA) followed by a *post hoc* Tukey's test. An unpaired Student's *t*-test was used to compare the biochemical parameters between wild-type and carriers (heterozygous and homozygous mutants). Intergroup genotype and allele distributions were compared by the Chi-square test, but Fisher's exact test was used for comparing genotype and allele distribution in cases where the number of subjects in any of the groups being compared was less than five. Logistic regression analysis was performed to check the association of the *RAGE* SNPs with clinical parameters. A p-value <0.05 was considered statistically significant. The odds ratio (OR) and 95% confidence interval (CI) were calculated.

3. RESULTS

3.1. Clinical Characteristics of Healthy Control, DM, DN, and DM + DN Subjects. The clinical characteristics of all the participating subjects are summarized in Table 3. There was no significant difference in the age of the participants in the different groups. The DM, DN, and DM + DN groups had significantly higher FBG, HbA_{1c}, and triglyceride levels than the healthy control group. FBG and triglycerides in the DN group were higher than in the DM group. Cholesterol levels were higher in the DN and DM + DN groups than in the healthy group. Blood urea and serum creatinine, which reflect the nitrogenous waste content in the blood, were significantly higher in the DN group than in the DM and healthy control groups. Blood urea and serum creatinine were also higher in the DM + DN group than in the healthy control group. The DN and DM + DN groups had higher cholesterol and lower HDL levels than the healthy group.

Normalized fructosamine concentration, which reflects a measure of glycation of all plasma proteins, was significantly elevated in the DM, DN, and DM + DN groups compared to the healthy control group. Similarly, the normalized glycated

https://doi.org/10.1021/acsomega.3c00297
ACS Omega XXXX, XXX, XXX−XXX

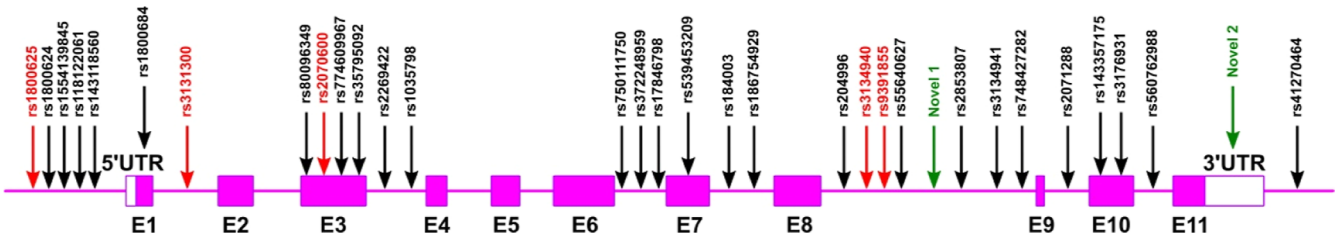

Figure 1. Schematic representation of the *RAGE* gene depicting the location of the polymorphisms detected. The locations of all the polymorphisms detected in this study are shown by arrows. Previously reported polymorphisms are shown by black arrows, whereas the two novel polymorphisms are indicated by green arrows. SNPs associated with type 2 diabetes are shown by red arrows.

Table 4. SNPs Detected in the *RAGE* Gene, Their Position on Chromosome 6, Location on the Gene, Nucleotide Change, and Genotype Distribution Among Healthy, DM, DN, and DM + DN Groups

				healthy		DM		DN		DM + DN	
polymorphism	genomic position	location	wild-type allele/mutated allele	wild-type	mutant	wild-type	mutant	wild-type	mutant	wild-type	mutant
rs1800625	32184665	upstream	T/C	56	15	55	31	31	11	86	42
rs1800624	32184610	upstream	T/A	50	16	64	20	28	11	92	31
rs1554139845	32184580	upstream	63 bp deletion[a]	66	5	84	2	39	3	123	5
rs118122061	32184479	upstream	G/A	70	1	83	3	41	1	124	4
rs143118560	32184478	upstream	A/T	71	0	85	1	42	0	127	1
rs1800684	32184217	exon 1	T/A	68	3	83	3	39	3	122	6
rs3131300	32184157	intron 1	T/C	56	15	55	31	31	11	86	42
rs80096349	32183681	exon 3	C/T	70	1	86	0	42	0	128	0
rs2070600	32183666	exon 3	G/A	60	11	61	25	31	11	92	36
rs774609967	32183650	exon 3	C/T	70	1	86	0	42	0	128	0
rs35795092	32183643	exon 3	C/G	68	3	86	0	42	0	128	0
rs2269422	32183517	intron 3	A/G	64	7	78	8	37	5	115	13
rs1035798	32183445	intron 3	C/T	52	19	66	20	31	11	97	31
rs750111750	32182808	intron 6	G/A	71	0	86	0	41	1	127	1
rs372248959	32182728	intron 6	T/C	71	0	84	2	42	0	126	2
rs17846798	32182721	intron 6	C/T	66	5	84	2	39	3	123	5
rs539453209	32182697	exon 7	G/C	70	1	86	0	42	0	128	0
rs184003	32182519	intron 7	G/T	43	28	51	35	25	17	76	52
rs186754929	32182494	intron 7	G/A	70	1	86	0	40	2	126	2
rs204996	32182106	intron 8	G/A	58	13	76	10	36	6	112	16
rs3134940	32182039	intron 8	A/G	56	15	55	31	31	11	86	42
rs9391855	32182024	intron 8	G/A	60	11	61	25	31	11	92	36
rs55640627	32181979	intron 8	G/A	67	4	81	5	41	1	122	6
novel 1	32181834	intron 8	G/A	70	1	86	0	42	0	128	0
rs2853807	32181795	intron 8	C/T	58	13	76	10	36	6	112	16
rs3134941	32181760	intron 8	G/C	56	15	58	28	31	11	89	39
rs748427282	32181673	intron 8	C/T	71	0	85	1	42	0	127	1
rs2071288	32181483	intron 9	G/A	66	5	84	2	39	3	123	5
rs143357175	32181442	exon 10	C/T	66	5	81	5	36	6	117	11
rs3176931	32181363	exon 10	G/A	66	5	84	2	41	1	125	3
rs560762988	32181266	intron 10	C/T	71	0	86	0	41	1	127	1
novel 2	32181132	3′ UTR	CAG/G	70	1	83	3	41	1	124	4
rs41270464	32180947	downstream	G/A	66	5	79	7	38	4	117	11

[a]63 bp deletion: TTCCCCAGCCTTGCCTTCATGATGCAGGCCCAATTGCACCCTTGCAGACAACAGTCTGGCCTGA/A.

albumin concentration was higher in the DM, DN, and DM + DN groups than in the healthy control group. However, there was no significant difference between the DM and DN groups in normalized fructosamine and normalized glycated albumin levels. The plasma levels of inflammatory cytokine TNF-α, MDA, insulin, HOMA-IR, and CRP were not significantly different between the subject groups.

3.2. PCR Amplification and SNP Detection by Nanopore Sequencing of the *RAGE* Gene. PCR amplification of the *RAGE* gene was verified by agarose gel electrophoresis and confirmed to be in the expected size of ∼4 kb (Figure S1). From nanopore sequencing of the *RAGE* gene amplicons, a total of 33 polymorphisms, including 8 exon variants, 18 intron variants, 5 upstream variants, 1 3′UTR variant, and 1 downstream variant of the *RAGE* gene, were detected. During validation by PCR-RFLP analysis, we observed that there was a discrepancy in the detection of rs3134940 by nanopore sequencing for one healthy and one diabetic sample. To resolve this discrepancy, Sanger sequencing of the amplicons spanning the mutation was carried out for these two samples

https://doi.org/10.1021/acsomega.3c00297
ACS Omega XXXX, XXX, XXX−XXX

Table 5. Association of Polymorphisms Detected in the *RAGE* Gene with Type 2 Diabetes and Diabetic Nephropathy[a]

	healthy vs DM			healthy vs DN			DM vs DN			healthy vs DM + DN		
polymorphism	χ^2	p	OR (95% CI)	χ^2	p	OR (95% CI)	χ^2	p	OR (95% CI)	χ^2	p	OR (95% CI)
rs1800625	**4.179**	**0.041**	**2.104 (1.039−4.396)**	0.382	0.537	1.325 (0.545−3.351)	1.243	0.265	0.63 (0.292−1.415)	3.051	0.081	1.823 (0.933−3.546)
rs1800624	0.004	0.951	0.977 (0.467−2.124)	0.202	0.654	1.228 (0.501−3.104)	0.273	0.601	1.257 (0.545−2.89)	0.021	0.884	1.053 (0.543−2.073)
rs1554139845		0.246	0.314 (0.061−1.547)		>0.999	1.015 (0.258−4.174)		0.33	3.231 (0.633−18.59)	0.941	0.332	0.537 (0.168−1.723)
rs118122061		0.627	2.53 (0.369−33.28)		>0.999	1.707 (0.088−32.84)		>0.999	0.675 (0.051−4.656)		0.657	2.258 (0.362−27.99)
rs143118560												
rs1800684		>0.999	0.819 (0.187−3.602)		0.669	1.744 (0.39−7.713)		0.393	2.128 (0.477−9.38)		>0.999	1.115 (0.294−4.17)
rs3131300	**4.179**	**0.041**	**2.104 (1.039−4.396)**	0.382	0.537	1.325 (0.545−3.351)	1.243	0.265	0.63 (0.292−1.415)	3.051	0.081	1.823 (0.933−3.546)
rs80096349												
rs2070600	**4.057**	**0.044**	**2.235 (1.042−4.773)**	1.926	0.165	1.935 (0.741−5.059)	0.116	0.734	0.866 (0.393−2.019)	**4.039**	**0.044**	**2.134 (1.035−4.667)**
rs774609967												
rs35795092												
rs2269422	0.014	0.906	0.938 (0.313−2.497)	0.116	0.733	1.236 (0.408−3.937)	0.209	0.647	1.318 (0.454−3.984)	0.004	0.947	1.034 (0.414−2.648)
rs1035798	0.256	0.613	0.829 (0.415−1.667)	0.004	0.947	0.971 (0.417−2.264)	0.132	0.716	1.171 (0.515−2.64)	0.157	0.692	0.875 (0.448−1.704)
rs750111750												
rs372248959												
rs17846798		0.246	0.314 (0.061−1.547)		>0.999	1.015 (0.258−4.174)		0.33	3.231 (0.633−18.59)	0.941	0.332	0.537 (0.168−1.723)
rs539453209												
rs184003	0.026	0.873	1.054 (0.555−2.025)	0.012	0.913	1.044 (0.48−2.282)	0.001	0.981	0.991 (0.46−2.043)	0.027	0.87	1.051 (0.585−1.938)
rs186754929					0.554	3.5 (0.393−51.33)					>0.999	1.111 (0.127−16.31)
rs204996	1.389	0.239	0.587 (0.236−1.409)	0.306	0.58	0.744 (0.256−2.142)	0.182	0.669	1.267 (0.416−3.55)	1.238	0.266	0.637 (0.295−1.411)
rs3134940	**4.179**	**0.041**	**2.104 (1.039−4.396)**	0.382	0.537	1.325 (0.545−3.351)	1.243	0.265	0.63 (0.292−1.415)	3.051	0.081	1.823 (0.933−3.546)
rs9391855	**4.057**	**0.044**	**2.235 (1.042−4.773)**	1.926	0.165	1.935 (0.741−5.059)	0.116	0.734	0.866 (0.393−2.019)	**4.039**	**0.044**	**2.134 (1.035−4.667)**
rs55640627		>0.999	1.034 (0.294−3.478)		0.649	0.409 (0.033−2.632)		0.663	0.395 (0.033−3.084)		0.747	0.824 (0.211−2.663)
Novel 1												
rs2853807	1.389	0.239	0.587 (0.236−1.409)	0.306	0.58	0.744 (0.256−2.142)	0.182	0.669	1.267 (0.416−3.55)	1.238	0.266	0.637 (0.295−1.411)
rs3134941	2.556	0.11	1.802 (0.874−3.805)	0.382	0.537	1.325 (0.545−3.351)	0.54	0.462	0.735 (0.338−1.677)	2.016	0.156	1.636 (0.829−3.203)
rs748427282												
rs2071288		0.246	0.314 (0.061−1.547)		>0.999	1.015 (0.258−4.174)		0.33	3.231 (0.633−18.59)	0.941	0.332	0.537 (0.168−1.723)
rs143357175	0.098	0.754	0.815 (0.252−2.639)	1.576	0.209	2.2 (0.579−6.928)	2.578	0.108	2.7 (0.715−8.434)	0.149	0.7	1.241 (0.435−3.328)
rs3176931		0.246	0.314 (0.061−1.547)		0.409	0.322 (0.027−2.533)		>0.999	1.024 (0.069−9.004)		0.137	0.317 (0.082−1.255)
rs560762988												
Novel 2		0.627	2.53 (0.369−33.28)		>0.999	1.707 (0.088−32.84)		>0.999	0.675 (0.051−4.656)		0.657	2.258 (0.362−27.99)
rs41270464	0.066	0.797	1.17 (0.383−3.405)		0.725	1.389 (0.405−5.045)		0.75	1.188 (0.37−4.1)	0.149	0.7	1.241 (0.435−3.328)

[a]χ^2: Chi-square value; OR: odds ratio; CI: confidence interval, the text in the bold indicates significant association.

(Table S1). In this case, the results from Sanger sequencing agreed with the PCR-RFLP results, and based on this, the result of the two discrepant cases was rectified in the SNP distribution detected by nanopore sequencing. The details of the *RAGE* polymorphisms and their distribution in healthy, DM, DN, and DM + DN groups are presented in Figure 1 and Table 4, respectively.

Out of the 33 *RAGE* polymorphisms detected, two SNPs are reported here for the first time, and these were not found in dbSNP (https://www.ncbi.nlm.nih.gov/snp, Oct 2022). One of these two novel variants is located on intron 8, causing a nucleotide change from G to A at position 32181834 of chromosome 6, and was detected in 0.5% of the subjects. The other novel variant is a deletion mutation, causing the nucleotide change from CAG to G in the 3′UTR of the

https://doi.org/10.1021/acsomega.3c00297
ACS Omega XXXX, XXX, XXX−XXX

RAGE gene at position 32181132 of chromosome 6 and was detected in 2.6% of the subjects.

3.3. Association of the Mutations with Cohort Groups. Due to the low frequency of homozygous mutant genotypes of the *RAGE* polymorphisms, we performed association analyses using the dominant inheritance model. For this, the subjects were grouped into homozygous wild-type and carrier populations (including both the heterozygous and homozygous mutant genotypes). The result of the association study is summarized in Table 5. The SNP rs1554139845 causes insertion/deletion of the 63 bp stretch in the upstream region of the *RAGE* gene. Since rs1800624 is located within this 63 bp stretch, deletion of this 63 bp also causes the absence of the location at which the SNP rs1800624 occurs. Hence, 10 subjects in the present study carrying rs1554139845 were not considered while analyzing the genotype distribution and allele frequency of rs1800624. Among the 33 *RAGE* polymorphisms detected, five SNPs were associated with an increased risk of type 2 diabetes. The SNP rs1800625 was found at a significantly higher frequency in the DM group (OR = 2.104, p = 0.041) as compared to the healthy group. However, this SNP was not associated with the DN group. Similarly, when DM and DN groups were merged as a diabetic group (DM + DN) and compared to the healthy group, the extent of the association of rs1800625 with the merged diabetic group was reduced (OR = 1.823, p = 0.081). The SNPs rs3134940 and rs3131300 were found to be in perfect linkage disequilibrium with rs1800625 (Table S2). Hence, their association with the DM and DN groups was the same as that of rs1800625.

The SNP rs2070600 was significantly associated with the DM group compared to the healthy group (OR = 2.235, p = 0.044). However, rs2070600 was not associated with the DN group compared to the healthy or DM group. When DM and DN groups were merged as a diabetic group, rs2070600 was associated with the merged diabetic group (DM + DN) compared to the healthy group (OR = 2.134, p = 0.044). Thus, this SNP is more strongly associated with type 2 diabetes than the other three SNPs discussed earlier. The SNP rs9391855 was found in perfect linkage disequilibrium with rs2070600 (Table S2), and hence this SNP, too, was associated with DM and DM + DN group as compared to the healthy group. The rest of the polymorphisms detected did not show any association with the DM or DM + DN group. When the DN group was compared with the DM group as a control, none of the 33 polymorphisms detected were associated with the DN group. Association analysis couldn't be performed for many low-frequency polymorphisms due to the absence of carrier genotypes in one or more subject groups. A few other SNPs were also found to be in perfect linkage disequilibrium with each other (Table S2 and Figure S2). Wild-type major allele and mutated minor allele frequencies for *RAGE* polymorphisms were calculated and are presented in Table S3. The result of allele association with type 2 diabetes or diabetic nephropathy is shown in Table S4. We conclude that there was no association of any alleles detected from the *RAGE* gene with type 2 diabetes or diabetic nephropathy.

3.4. Validation of Mutations Identified in Nanopore Sequencing of the *RAGE* Gene by PCR-RFLP. PCR-RFLP was used to detect the SNPs rs3134940, rs1800624, rs1800625, and rs2070600 to compare and validate the nanopore sequencing results. These four SNPs were chosen for the comparison as they have a relatively high frequency than most of the other SNPs in the *RAGE* gene and have been most investigated for their association with diabetes and diabetic complications.[11] The restriction enzymes used for the digestion of PCR-amplified products for detecting these SNPs, restriction sites and the size of restriction-digested products for wild-type and mutant allele are summarized in Table 2. The nucleotide change caused by rs3134940, rs1800625, and rs2070600 results in the creation of a restriction site, whereas rs1800624 causes the deletion of the restriction site for the restriction enzymes, as mentioned in Table 2. A representative agarose gel image depicting DNA bands corresponding to undigested PCR-amplified products and restriction-digested products of different genotypes for the four SNPs is shown in Figure 2. The results of genotype distribution, allele

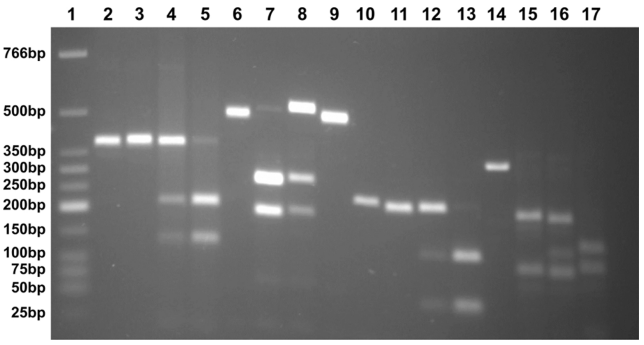

Figure 2. PCR-amplified and restriction-digested products for SNPs rs3134940, rs1800624, rs1800625, and rs2070600. Lane 1: Low-molecular-weight DNA ladder. Lane 2: PCR-amplified product for rs3134940. Lanes 3−5: Restriction digested products of wild-type (AA), heterozygous (AG), and homozygous mutant (GG) genotypes of rs3134940, respectively. Lane 6: PCR-amplified product for rs1800624. Lanes 7−9: Restriction digested products of wild-type (TT), heterozygous (TA), and homozygous mutant (AA) genotypes of rs1800624, respectively. Lane 10: PCR-amplified product of rs1800625. Lanes 11−13: Restriction digested products of wild-type (TT), heterozygous (TC), and homozygous mutant (CC) genotypes of rs1800625, respectively. Lane 14: PCR-amplified product of rs2070600. Lanes 15−17: Restriction digested products of wild-type (GG), heterozygous (GA), and homozygous mutant (AA) genotypes of rs2070600, respectively.

frequencies, and their association with type 2 diabetes and diabetic nephropathy were the same, as shown in Tables 4−5 and Tables S3 and S4. There was 99.75% agreement between nanopore and PCR-RFLP genotyping results, with only two discrepant cases out of 199 samples for the four *RAGE* SNPs detected by the two methods (Table S1).

3.5. Association of Diabetes-Risk-Associated SNPs with Various Clinical Parameters. *RAGE* SNPs showing significant association with type 2 diabetes were investigated for the association of carrier genotypes of these SNPs with AGEs (fructosamine and glycated albumin), inflammatory cytokine (TNF-α), MDA, insulin, HOMA-IR, CRP, and diabetes diagnosis markers (FBG and HbA_{1c}). Carrier genotypes of none of these SNPs were associated with any of these clinical and biochemical parameters by unpaired Student's t-test (Table S5). The result of logistic regression analysis for the association of type 2 diabetes-associated *RAGE* SNPs with clinical parameters is shown in Table S6. While blood urea, insulin, and CRP were positively associated with rs1800625, rs3134940, and rs3131300, MDA and HOMA-IR

https://doi.org/10.1021/acsomega.3c00297
ACS Omega XXXX, XXX, XXX−XXX

Table 6. Comparison of the Results of the Present Study with Previous Reports

SNP	findings of this study	previous supportive reports	previous contradictory reports
rs1800625	increased risk of type 2 diabetes	increased type 1 diabetes risk[45]	no association with diabetes mellitus[39] and type 2 diabetes[37,38,40]
	no association with diabetic nephropathy	no association with diabetic nephropathy (in dominant model)[38,41]	increased risk of diabetic nephropathy[46]
rs3134940	increased risk of type 2 diabetes		no association with diabetes[47] or type 2 diabetes[40]
	no association with diabetic nephropathy		increased risk of diabetic nephropathy[48] and decreased risk of diabetic nephropathy[34]
rs2070600	increased risk of type 2 diabetes	increased risk of diabetes[47] and type 1 diabetes[49]	no association with type 2 diabetes[37,50]
	no association with diabetic nephropathy	no association with diabetic nephropathy[46,48,51−53]	

were negatively associated. Similarly, HDL showed a negative association with rs2070600 and rs9391855.

4. DISCUSSION

Diabetes is a multifactorial disease, and genetics plays a role in developing diabetes and its complications. Among various genes associated with diabetes and its complications, the *RAGE* gene is a potential candidate known to be involved in the pathogenesis of diabetes and diabetic complications. AGE−RAGE signaling increases the expression of inflammatory cytokines and reactive oxygen species, which exacerbate the progression of diabetes and its complications. As a result, polymorphism in the *RAGE* gene may influence the outcomes of the AGE−RAGE interaction. In this study, we first detected all *RAGE* polymorphisms from the subjects by nanopore sequencing of the respective *RAGE* gene amplicons and studied their association with type 2 diabetes and diabetic nephropathy. PCR-RFLP was performed for four *RAGE* SNPs, i.e., rs3134940, rs1800624, rs1800625, and rs2070600, to assess the accuracy and utility of nanopore sequencing as a high-throughput method of SNP detection over the conventional PCR-RFLP method.

An overall comparison of the findings of this study with the previous reports of *RAGE* SNP association with diabetes and diabetic nephropathy is summarized in Table 6. Previous studies have reported contradictory results on the association of *RAGE* SNPs with diabetes and its complications.[11] In this study, the SNP rs1800625 was associated with an increased risk of type 2 diabetes but not diabetic nephropathy. While some reports conclude no association of rs1800625 with type 1 and type 2 diabetes,[37−40] diabetic nephropathy,[38,41] and diabetic retinopathy,[42−44] other studies report an increased risk of type 1 diabetes[45] and diabetic nephropathy.[46] The SNP rs1800625 is present in the promoter region of the *RAGE* gene. One in vitro study has illustrated a two-fold increase in the expression of the reporter gene caused by the mutant allele of rs1800625.[16] Thus, the increased expression of RAGE may lead to increased AGE−RAGE interaction and downstream signaling, which may promote the pathogenesis of diabetes and its complications.

The intronic SNP rs3134940 was in perfect linkage disequilibrium with rs1800625. Hence, it was associated with an increased risk of type 2 diabetes but not diabetic nephropathy. However, contradictory to our finding, previous studies have reported no association of rs3134940 with type 2 diabetes[40,47] and an increased[48] or decreased risk[34] of diabetic nephropathy. This SNP was also not associated with chronic kidney disease[54] and diabetic retinopathy.[42,55,56] During mRNA processing, introns are spliced from pre-mRNA; therefore, any SNPs in the intron region are least likely to affect the protein. The mechanism by which rs3134940 can increase the risk of diabetes or diabetic complications is unknown. It has been proposed by various groups that rs3134940 may affect the alternative splicing of RAGE mRNA involving the region between intron 7 and 9, which could affect the expression of endogenous secretory RAGE (esRAGE), one of the RAGE isoforms.[34,55−58] Unlike RAGE, esRAGE is not involved in AGE−RAGE signaling as it lacks intramembrane and cytoplasmic domains. Thus, esRAGE acts as a decoy receptor for AGEs, and the physiological level of esRAGE can affect the extent of AGE−RAGE signaling and the associated pathogenesis. However, no experimental evidence has shown the effect of rs3134940 on esRAGE production.

Compared to the SNPs rs1800625, a stronger association of rs2070600 with type 2 diabetes was observed, even though it was not associated with diabetic nephropathy. These results agreed with those of the previous studies, which reported that rs2070600 increases the risk of diabetes[47,49] but not diabetic nephropathy.[46,51−53] However, there are reports contradicting these results, which claim no association between rs2070600 and type 2 diabetes.[37,50] No literature has reported a clear association between rs2070600 and diabetic nephropathy. The non-synonymous replacement of glycine by serine at the 82nd position of RAGE caused by rs2070600 induces changes in the structure of the variable domain of RAGE,[15] which can potentially affect AGE−RAGE signaling. In vitro studies have elucidated that RAGE with rs2070600 has a higher binding affinity for amyloid-beta peptides (Aβ42) and prototypic S100/cangrulin, which upregulated inflammatory mediators.[59,60] Substitution of glycine with serine at the 82nd position of RAGE promotes N-linked glycosylation of adjacent asparagine residue at the 81st position, which may also affect ligand binding and further downstream signaling initiated by AGE−RAGE interaction.[61] Several studies have also found a significantly lower plasma sRAGE level in the subjects carrying rs2070600,[42,53,62,63] and the same has been elucidated using a cell culture model.[64] Decreased plasma sRAGE levels might fail to sufficiently clear the already elevated plasma AGEs in diabetics, resulting in increased AGE−RAGE signaling. In this study, sRAGE levels were not measured; hence, the role of this SNP in type 2 diabetes development via sRAGE remains obscure. The discrepancies in the results of *RAGE* SNP association with type 2 diabetes and diabetic nephropathy in this study and previous studies can be attributed to the different environments, lifestyles, genetics, ethnicity, and geography of the study population.

In this study, nanopore sequencing showed a high accuracy of 99.75% compared to the result of PCR-RFLP. In fact,

https://doi.org/10.1021/acsomega.3c00297
ACS Omega XXXX, XXX, XXX−XXX

several studies have reported even up to 100% concordance between the results of nanopore and Sanger sequencing, a gold standard approach.[65−68] The high accuracy of the current nanopore sequencing approaches makes it a rapid, cost-effective, and high-throughput approach that can be used for SNP detection, including in clinical diagnostics.[65]

This study reports two novel polymorphisms in our population at positions 32181834 and 32181132 of chromosome 6, which are located in intron 8 and 3′ UTR of the *RAGE* gene, respectively. These two SNPs were present at a very low frequency in our study population, and hence a large sample size would be required to sufficiently detect these novel polymorphisms and confidently check for their association with type 2 diabetes and diabetic nephropathy. We also found that none of the SNPs detected were associated with diabetic nephropathy, which could be due to the limited sample size of the diabetic nephropathy group; hence, a study involving a large population size is required.

Fructosamine and glycated albumin levels represent the extent of glycation, and a higher physiological level of AGEs is expected to promote both diabetes and diabetic complications.[1,13] In this study, both type 2 diabetes and diabetic nephropathy subjects had significantly higher levels of fructosamine, glycated albumin, FBG, and, HbA_{1c}. Yet, these parameters were not associated with the carrier genotypes of the SNPs associated with type 2 diabetes. Hence, the carrier genotypes of type 2 diabetes-associated SNPs may not be involved in the observed disease-specific elevation of these biochemical parameters. These findings are similar to a previous report that found no association between rs1800625 or rs2070600 and AGEs.[69] The level of AGEs can be reasonably expected to be associated with glycemic status, which is elevated in diabetes, rather than gene polymorphisms. The TNF-α levels increase upon AGE−RAGE signaling, followed by NF-κB activation.[1] No association between rs1800625 or rs2070600 and the TNF-α level was observed in this study. Thus, the carrier genotypes of rs1800625 and rs2070600 may not affect the TNF-α levels despite these SNPs being associated with type 2 diabetes. The TNF-α level was not associated with type 2 diabetes and diabetic nephropathy in this study. This result is the same as previously found[70] but contradictory to several other reports.[71−73] Further, the carrier genotypes of rs1800625 and rs2070600 were not associated with FBG and HbA_{1c} despite being associated with type 2 diabetes. Also, MDA (a marker for oxidative stress), insulin, HOMA-IR, and CRP were neither elevated in any disease groups nor associated with any type 2 diabetes-associated SNPs as analyzed by one-way ANOVA and unpaired Student's *t*-test, respectively. Logistic regression analysis revealed that rs1800625 might increase the fasting insulin level, and a higher fasting insulin level is linked to insulin resistance and type 2 diabetes.[74] In this study, HOMA-IR was found to be negatively associated with rs1800625, which could be due to the maintenance of blood glucose level in subjects with high insulin levels undergoing oral hypoglycemic drug treatment. However, recent studies suggest that hyperinsulinemia is a causal factor for glucose intolerance.[74] Therefore, hyperinsulinemia may predict the future risk of type 2 diabetes. CRP, an inflammatory marker, showed a weak positive association with rs1800625. Elevated CRP level is positively associated with the risk of type 2 diabetes development.[75−77] While MDA showed a weak negative association and blood urea showed a weak positive association with rs1800625 in logistic regression analysis, these results must be verified in a larger cohort to check if the association is due to polymorphism or by chance. Also, HDL was found to be negatively associated with rs2070600 in logistic regression analysis. The association results for rs3134940, rs3131300, and rs9391855 are the same as the corresponding SNPs in complete linkage disequilibrium (Table S6). Although we have found a weak association of SNPs with insulin and CRP in this study, SNPs are generally not used as diagnostic markers to detect insulin resistance in clinical settings compared to measuring insulin or CRP. In fact, the measurement of blood glucose is sufficient to diagnose diabetes. However, SNPs or other markers such as insulin or CRP could be helpful in predicting the risk of development of type 2 diabetes, and both of these parameters are associated with SNP rs1800625.

5. CONCLUSIONS

In this study, we used the Oxford Nanopore Technology-based DNA sequencing to detect the SNPs in the *RAGE* gene, which play a significant role in the progression of diabetes and its complications. The nanopore sequencing method detected 33 *RAGE* polymorphisms with high accuracy for SNP detection, as validated by PCR-RFLP. Therefore, the application of nanopore sequencing can be extended to identify disease-specific genetic variations in clinical settings. Five of the *RAGE* gene polymorphisms detected, i.e., rs1800625, rs3131300, rs3134940, rs2070600, and rs9391855, were associated with an increased type 2 diabetes risk. The usefulness of these five *RAGE* SNPs as type 2 diabetes risk prediction markers requires to be studied in a larger cohort, which would also facilitate the study of the less frequent *RAGE* SNPs for their association with type 2 diabetes and its complications.

■ ASSOCIATED CONTENT

Supporting Information

The Supporting Information is available free of charge at https://pubs.acs.org/doi/10.1021/acsomega.3c00297.

PCR amplification of the *RAGE* gene; linkage disequilibrium map of *RAGE* SNPs; result of the nanopore, PCR-RFLP, and Sanger sequencing for verification of the discrepant results between nanopore and PCR-RFLP; *RAGE* SNPs in perfect linkage disequilibrium; allele frequency of *RAGE* polymorphisms in healthy, DM and DN, and DM + DN groups; association of mutated alleles of *RAGE* polymorphisms with type 2 diabetes and diabetic nephropathy; association of type 2 diabetes-associated *RAGE* SNPs with AGEs, TNF-α, diabetes diagnosis markers, MDA, insulin, HOMA IR, and CRP; logistic regression analysis results for clinical parameters and genetic variants (SNPs) (PDF)

■ AUTHOR INFORMATION

Corresponding Authors

Mahesh J. Kulkarni − *Biochemical Sciences Division, CSIR-National Chemical Laboratory, Pune 411008, India; Academy of Scientific and Innovative Research (AcSIR), Ghaziabad 201002, India;* orcid.org/0000-0003-3932-9092; Email: mj.kulkarni@ncl.res.in

Dhanasekaran Shanmugam − *Biochemical Sciences Division, CSIR-National Chemical Laboratory, Pune 411008, India; Academy of Scientific and Innovative Research (AcSIR), Ghaziabad 201002, India*; Email: d.shanmugam@ncl.res.in

https://doi.org/10.1021/acsomega.3c00297
ACS Omega XXXX, XXX, XXX−XXX

Abdulrahaman A. Momin − *Department of Biochemistry, Bharati Vidyapeeth (DTU) Medical College, Pune 411043, India*; Email: rahaman.momin@gmail.com

Authors

Arvindkumar H. Chaurasiya − *Biochemical Sciences Division, CSIR-National Chemical Laboratory, Pune 411008, India; Academy of Scientific and Innovative Research (AcSIR), Ghaziabad 201002, India*

Ajinkya A. Khilari − *Biochemical Sciences Division, CSIR-National Chemical Laboratory, Pune 411008, India; Academy of Scientific and Innovative Research (AcSIR), Ghaziabad 201002, India*

Rubina Kazi − *Biochemical Sciences Division, CSIR-National Chemical Laboratory, Pune 411008, India*

Meera R. Jaiswal − *Biochemical Sciences Division, CSIR-National Chemical Laboratory, Pune 411008, India; Academy of Scientific and Innovative Research (AcSIR), Ghaziabad 201002, India*

Gouri M. Bhoite − *Department of Biochemistry, Bharati Vidyapeeth (DTU) Dental College, Pune 411043, India*

Meghana K. Padwal − *Department of Biochemistry, Bharati Vidyapeeth (DTU) Medical College, Pune 411043, India*

Complete contact information is available at: https://pubs.acs.org/10.1021/acsomega.3c00297

Author Contributions

Conceptualization: A.A.M., M.J.K., and D.S.; formal analysis: A.H.C., A.A.K., G.M.B., M.K.P., and A.A.M.; investigation: A.H.C., A.A.K., R.K., and M.R.J.; methodology: A.A.M. and D.S.; resources: A.A.M., D.S., and M.J.K.; data curation: A.H.C., A.A.K., and M.J.K.; software: A.A.K.; supervision: D.S. and M.J.K.; writing—original draft: A.H.C. and M.J.K.; writing—review and editing: M.J.K. and D.S.

Notes

The authors declare no competing financial interest.

The nanopore sequencing data have been deposited in the Sequence Read Archive at NCBI (http://www.ncbi.nlm.nih.gov/sra) under the BioProject accession number PRJNA904121. The bash script used to analyze raw data generated by nanopore sequencing can be accessed through the GitHub link https://github.com/ajinkyakhilari/ampvar.

■ ACKNOWLEDGMENTS

The authors thank all of the subjects participating in the study. A.H.C., A.A.K., and R.K. thank the University Grants Commission, Department of Biotechnology, and Council of Scientific and Industrial Research, respectively, for the fellowship. The authors would also like to thank Dr. Mahesh S. Dharne for the Sanger sequencing.

■ REFERENCES

(1) Singh, V. P.; Bali, A.; Singh, N.; Jaggi, A. S. Advanced glycation end products and diabetic complications. *Korean J. Physiol. Pharmacol.* **2014**, *18*, 1−14.

(2) Gheith, O.; Farouk, N.; Nampoory, N.; Halim, M. A.; Al-Otaibi, T. Diabetic kidney disease: world wide difference of prevalence and risk factors. *J. Nephropharmacol.* **2016**, *5*, 49−56.

(3) Aldukhayel, A. Prevalence of diabetic nephropathy among Type 2 diabetic patients in some of the Arab countries. *Int. J. Health Sci.* **2017**, *11*, 1−4.

(4) Yuan, C. M.; Nee, R.; Ceckowski, K. A.; Knight, K. R.; Abbott, K. C. Diabetic nephropathy as the cause of end-stage kidney disease reported on the medical evidence form CMS2728 at a single center. *Clin. Kidney J.* **2017**, *10*, 257−262.

(5) Satirapoj, B.; Adler, S. G. Comprehensive approach to diabetic nephropathy. *Kidney Res. Clin. Pract.* **2014**, *33*, 121−131.

(6) Adeghate, E.; Schattner, P.; Dunn, E. An update on the etiology and epidemiology of diabetes mellitus. *Ann. N.Y. Acad. Sci.* **2006**, *1084*, 1−29.

(7) Murea, M.; Ma, L.; Freedman, B. I. Genetic and environmental factors associated with type 2 diabetes and diabetic vascular complications. *Rev. Diabet. Stud.* **2012**, *9*, 6−22.

(8) Mambiya, M.; Shang, M.; Wang, Y.; Li, Q.; Liu, S.; Yang, L.; Zhang, Q.; Zhang, K.; Liu, M.; Nie, F.; Zeng, F.; Liu, W. The Play of Genes and Non-genetic Factors on Type 2 Diabetes. *Front. Public Health* **2019**, *7*, 349.

(9) Singh, S. The genetics of type 2 diabetes mellitus: a review. *J. Sci. Res.* **2011**, *55*, 35−48.

(10) Doria, A. Genetics of diabetes complications. *Curr. Diabetes Rep.* **2010**, *10*, 467−475.

(11) Serveaux-Dancer, M.; Jabaudon, M.; Creveaux, I.; Belville, C.; Blondonnet, R.; Gross, C.; Constantin, J. M.; Blanchon, L.; Sapin, V. Pathological Implications of Receptor for Advanced Glycation End-Product (AGER) Gene Polymorphism. *Dis. Markers* **2019**, *2019*, 2067353.

(12) Perez-Alcantara, M.; Honoré, C.; Wesolowska-Andersen, A.; Gloyn, A. L.; McCarthy, M. I.; Hansson, M.; Beer, N. L.; van de Bunt, M. Patterns of differential gene expression in a cellular model of human islet development, and relationship to type 2 diabetes predisposition. *Diabetologia* **2018**, *61*, 1614−1622.

(13) Xue, J.; Rai, V.; Singer, D.; Chabierski, S.; Xie, J.; Reverdatto, S.; Burz, D. S.; Schmidt, A. M.; Hoffmann, R.; Shekhtman, A. Advanced glycation end product recognition by the receptor for AGEs. *Structure* **2011**, *19*, 722−732.

(14) Vlassara, H.; Uribarri, J. Advanced glycation end products (AGE) and diabetes: cause, effect, or both? *Curr. Diabetes Rep.* **2014**, *14*, 453.

(15) Xie, J.; Reverdatto, S.; Frolov, A.; Hoffmann, R.; Burz, D. S.; Shekhtman, A. Structural basis for pattern recognition by the receptor for advanced glycation end products (RAGE). *J. Biol. Chem.* **2008**, *283*, 27255−27269.

(16) Hudson, B. I.; Stickland, M. H.; Futers, T. S.; Grant, P. J. Effects of novel polymorphisms in the RAGE gene on transcriptional regulation and their association with diabetic retinopathy. *Diabetes* **2001**, *50*, 1505−1511.

(17) Yang, W.; Kang, X.; Yang, Q.; Lin, Y.; Fang, M. Review on the development of genotyping methods for assessing farm animal diversity. *J. Anim. Sci. Biotechnol.* **2013**, *4*, 2.

(18) Athanasopoulou, K.; Boti, M. A.; Adamopoulos, P. G.; Skourou, P. C.; Scorilas, A. Third-Generation Sequencing: The Spearhead towards the Radical Transformation of Modern Genomics. *Life* **2021**, *12*, 30.

(19) Rhee, M.; Burns, M. A. Nanopore sequencing technology: nanopore preparations. *Trends Biotechnol.* **2007**, *25*, 174−181.

(20) Kumar, S.; Banks, T. W.; Cloutier, S. SNP Discovery through Next-Generation Sequencing and Its Applications. *Int. J. Plant Genom.* **2012**, *2012*, 831460.

(21) Ramachandran, A. Know the signs and symptoms of diabetes. *Indian J. Med. Res.* **2014**, *140*, 579−581.

(22) The Expert Committee on the Diagnosis and Classification of Diabetes Mellitus. Report of the expert committee on the diagnosis and classification of diabetes mellitus. *Diabetes Care* **2003**, *26*, S5−S20.

(23) Horáková, D.; Štěpánek, L.; Janout, V.; Janoutová, J.; Pastucha, D.; Kollárová, H.; Petráková, A.; Štěpánek, L.; Husár, R.; Martiník, K. Optimal Homeostasis Model Assessment of Insulin Resistance (HOMA-IR) Cut-Offs: A Cross-Sectional Study in the Czech Population. *Medicina* **2019**, *55*, 158.

(24) De Coster, W.; D'Hert, S.; Schultz, D. T.; Cruts, M.; Van Broeckhoven, C. NanoPack: visualizing and processing long-read sequencing data. *Bioinformatics* **2018**, *34*, 2666−2669.

(25) Li, H. Minimap2: pairwise alignment for nucleotide sequences. *Bioinformatics* **2018**, *34*, 3094−3100.
(26) Li, H.; Handsaker, B.; Wysoker, A.; Fennell, T.; Ruan, J.; Homer, N.; Marth, G.; Abecasis, G.; Durbin, R. The Sequence Alignment/Map format and SAMtools. *Bioinformatics* **2009**, *25*, 2078−2079.
(27) Loman, N. J.; Quick, J.; Simpson, J. T. A complete bacterial genome assembled de novo using only nanopore sequencing data. *Nat. Methods* **2015**, *12*, 733−735.
(28) Koren, S.; Walenz, B. P.; Berlin, K.; Miller, J. R.; Bergman, N. H.; Phillippy, A. M. Canu: scalable and accurate long-read assembly via adaptive k-mer weighting and repeat separation. *Genome Res.* **2017**, *27*, 722−736.
(29) Vaser, R.; Sović, I.; Nagarajan, N.; Šikić, M. Fast and accurate de novo genome assembly from long uncorrected reads. *Genome Res.* **2017**, *27*, 737−746.
(30) Lee, J. Y.; Kong, M.; Oh, J.; Lim, J.; Chung, S. H.; Kim, J. M.; Kim, J. S.; Kim, K. H.; Yoo, J. C.; Kwak, W. Comparative evaluation of Nanopore polishing tools for microbial genome assembly and polishing strategies for downstream analysis. *Sci. Rep.* **2021**, *11*, 20740.
(31) Cingolani, P.; Platts, A.; Wang, L. L.; Coon, M.; Nguyen, T.; Wang, L.; Land, S. J.; Lu, X.; Ruden, D. M. A program for annotating and predicting the effects of single nucleotide polymorphisms, SnpEff: SNPs in the genome of Drosophila melanogaster strain w1118; iso-2; iso-3. *Fly* **2012**, *6*, 80−92.
(32) Afgan, E.; Baker, D.; Batut, B.; van den Beek, M.; Bouvier, D.; Cech, M.; Chilton, J.; Clements, D.; Coraor, N.; Grüning, B. A.; Guerler, A.; Hillman-Jackson, J.; Hiltemann, S.; Jalili, V.; Rasche, H.; Soranzo, N.; Goecks, J.; Taylor, J.; Nekrutenko, A.; Blankenberg, D. The Galaxy platform for accessible, reproducible and collaborative biomedical analyses: 2018 update. *Nucleic Acids Res.* **2018**, *46*, W537−w544.
(33) Solé, X.; Guinó, E.; Valls, J.; Iniesta, R.; Moreno, V. SNPStats: a web tool for the analysis of association studies. *Bioinformatics* **2006**, *22*, 1928−1929.
(34) Cai, W.; Li, J.; Xu, J. X.; Liu, Y.; Zhang, W.; Xiao, J. R.; Zhu, L. Y.; Liu, J. Y. Association of 2184AG Polymorphism in the RAGE Gene with Diabetic Nephropathy in Chinese Patients with Type 2 Diabetes. *J. Diabetes Res.* **2015**, *2015*, 310237.
(35) Yang, H. Y.; Chuang, S. Y.; Fang, W. H.; Huang, G. S.; Wang, C. C.; Huang, Y. Y.; Chu, M. Y.; Lin, C.; Su, W.; Chen, C. Y.; Yang, Y. T.; Su, S. L. Effect of RAGE polymorphisms on susceptibility to and severity of osteoarthritis in a Han Chinese population: a case-control study. *Genet. Mol. Res.* **2015**, *14*, 11362−11370.
(36) Kalousová, M.; Jáchymová, M.; Mestek, O.; Hodková, M.; Kazderová, M.; Tesar, V.; Zima, T. Receptor for advanced glycation end products–soluble form and gene polymorphisms in chronic haemodialysis patients. *Nephrol. Dial. Transplant.* **2007**, *22*, 2020−2026.
(37) Goulart, A. C.; Germer, S.; Rexrode, K. M.; Martin, M.; Zee, R. Y. Polymorphisms in advanced glycosylation end product-specific receptor (AGER) gene, insulin resistance, and type 2 diabetes mellitus. *Clin. Chim. Acta* **2008**, *398*, 95−98.
(38) Kang, P.; Tian, C.; Jia, C. Association of RAGE gene polymorphisms with type 2 diabetes mellitus, diabetic retinopathy and diabetic nephropathy. *Gene* **2012**, *500*, 1−9.
(39) Niu, W.; Qi, Y.; Wu, Z.; Liu, Y.; Zhu, D.; Jin, W. A meta-analysis of receptor for advanced glycation end products gene: four well-evaluated polymorphisms with diabetes mellitus. *Mol. Cell. Endocrinol.* **2012**, *358*, 9−17.
(40) Cheng, H.; Zhu, W.; Zhu, M.; Sun, Y.; Sun, X.; Jia, D.; Yang, C.; Yu, H.; Zhang, C. Susceptibility of six polymorphisms in the receptor for advanced glycation end products to type 2 diabetes: a systematic review and meta-analysis. *Endocr. J.* **2021**, *68*, 993−1010.
(41) Shi, Z.; Lu, W.; Xie, G. Association between the RAGE gene -374T/A, -429T/C polymorphisms and diabetic nephropathy: a meta-analysis. *Ren. Fail.* **2015**, *37*, 751−756.
(42) Yang, L.; Wu, Q.; Li, Y.; Fan, X.; Hao, Y.; Sun, H.; Cui, Y.; Han, L. Association of the receptor for advanced glycation end products gene polymorphisms and circulating RAGE levels with diabetic retinopathy in the Chinese population. *J. Diabetes Res.* **2013**, *2013*, 264579.
(43) Ramprasad, S.; Radha, V.; Mathias, R. A.; Majumder, P. P.; Rao, M. R.; Rema, M. Rage gene promoter polymorphisms and diabetic retinopathy in a clinic-based population from South India. *Eye* **2007**, *21*, 395−401.
(44) Balasubbu, S.; Sundaresan, P.; Rajendran, A.; Ramasamy, K.; Govindarajan, G.; Perumalsamy, N.; Hejtmancik, J. F. Association analysis of nine candidate gene polymorphisms in Indian patients with type 2 diabetic retinopathy. *BMC Med. Genet.* **2010**, *11*, 158.
(45) Picheth, G.; Heidemann, M.; Pedrosa, F. O.; Chautard-Freire-Maia, E. A.; Costantini, C. O.; da Rocha Martinez, T. L.; de Souza, E. M. The -429 T>C polymorphism of the receptor for advanced glycation end products (RAGE) is associated with type 1 diabetes in a Brazilian population. *Clin. Chim. Acta* **2007**, *383*, 163−164.
(46) Zhang, Y.; Jia, N.; Hu, F.; Fan, N.; Guo, X.; Du, H.; Mei, C.; Gao, C. Association of single-nucleotide polymorphisms in the RAGE gene and its gene- environment interactions with diabetic nephropathy in Chinese patients with type 2 diabetes. *Oncotarget* **2017**, *8*, 96885−96892.
(47) Kanková, K.; Márová, I.; Záhejský, J.; Muzík, J.; Stejskalová, A.; Znojil, V.; Vácha, J. Polymorphisms 1704G/T and 2184A/G in the RAGE gene are associated with antioxidant status. *Metabolism* **2001**, *50*, 1152−1160.
(48) Blech, I.; Katzenellenbogen, M.; Katzenellenbogen, A.; Wainstein, J.; Rubinstein, A.; Harman-Boehm, I.; Cohen, J.; Pollin, T. I.; Glaser, B. Predicting diabetic nephropathy using a multifactorial genetic model. *PLoS One* **2011**, *6*, No. e18743.
(49) Forbes, J. M.; Söderlund, J.; Yap, F. Y.; Knip, M.; Andrikopoulos, S.; Ilonen, J.; Simell, O.; Veijola, R.; Sourris, K. C.; Coughlan, M. T.; Forsblom, C.; Slattery, R.; Grey, S. T.; Wessman, M.; Yamamoto, H.; Bierhaus, A.; Cooper, M. E.; Groop, P. H. Receptor for advanced glycation end-products (RAGE) provides a link between genetic susceptibility and environmental factors in type 1 diabetes. *Diabetologia* **2011**, *54*, 1032−1042.
(50) Zhang, H. M.; Chen, L. L.; Wang, L.; Liao, Y. F.; Wu, Z. H.; Ye, F.; Xu, S.; Yi, L. L. Association of 1704G/T and G82S polymorphisms in the receptor for advanced glycation end products gene with diabetic retinopathy in Chinese population. *J. Endocrinol. Invest.* **2009**, *32*, 258−262.
(51) Yoshioka, K.; Yoshida, T.; Takakura, Y.; Umekawa, T.; Kogure, A.; Toda, H.; Yoshikawa, T. Association study of G1704T and G82S polymorphisms of RAGE gene for microalbuminuria in Japanese type 2 diabetic patients. *Metabolism* **2005**, *54*, 488−491.
(52) Poirier, O.; Nicaud, V.; Vionnet, N.; Raoux, S.; Tarnow, L.; Vlassara, H.; Parving, H. H.; Cambien, F. Polymorphism Screening of Four Genes Encoding Advanced Glycation End-Product Putative Receptors. *Diabetes* **2001**, *50*, 1214−1218.
(53) Lim, S. C.; Dorajoo, R.; Zhang, X.; Wang, L.; Ang, S. F.; Tan, C. S. H.; Yeoh, L. Y.; Ng, X. W.; Li, N.; Su, C.; Liu, S.; Wong, M. D. S.; Low, K. M. S.; Yao, A. O.; Babitha, J.; Fun, S.; Zhou, S.; Lee, S. B. M.; Tang, W. E.; Tavintharan, S.; Sum, C. F.; Liu, J. J. Genetic variants in the receptor for advanced glycation end products (RAGE) gene were associated with circulating soluble RAGE level but not with renal function among Asians with type 2 diabetes: a genome-wide association study. *Nephrol. Dial. Transplant.* **2016**, *32*, 1697−1704.
(54) Wong, F. N.; Chua, K. H.; Kuppusamy, U. R.; Wong, C. M.; Lim, S. K.; Tan, J. A. Association of the receptor for advanced glycation end-products (RAGE) gene polymorphisms in Malaysian patients with chronic kidney disease. *PeerJ* **2016**, *4*, No. e1908.
(55) Li, J.; Cai, W.; Zhang, W.; Zhu, W. F.; Liu, Y.; Yue, L. X.; Zhu, L. Y.; Xiao, J. R.; Liu, J. Y.; Xu, J. X. Polymorphism 2184A/G in the AGER gene is not associated with diabetic retinopathy in Han Chinese patients with type 2 diabetes. *J. Int. Med. Res.* **2016**, *44*, 520−528.

https://doi.org/10.1021/acsomega.3c00297
ACS Omega XXXX, XXX, XXX−XXX

(56) Ng, Z. X.; Kuppusamy, U. R.; Poh, R.; Tajunisah, I.; Koay, A. C.; Fong, K. C.; Chua, K. H. Lack of association between Gly82Ser, 1704G/T and 2184A/G of RAGE gene polymorphisms and retinopathy susceptibility in Malaysian diabetic patients. *Genet. Mol. Res.* **2012**, *11*, 455−461.
(57) Kanková, K.; Stejskalová, A.; Hertlová, M.; Znojil, V. Haplotype analysis of the RAGE gene: identification of a haplotype marker for diabetic nephropathy in type 2 diabetes mellitus. *Nephrol. Dial. Transplant.* **2005**, *20*, 1093−1102.
(58) Chocholatý, M.; Jáchymová, M.; Schmidt, M.; Havlová, K.; Křepelová, A.; Zima, T.; Babjuk, M.; Kalousová, M. Polymorphisms of the receptor for advanced glycation end-products and glyoxalase I in patients with renal cancer. *Tumour Biol.* **2015**, *36*, 2121−2126.
(59) C, R. C.; Lukose, B.; Rani, P. G82S RAGE polymorphism influences amyloid-RAGE interactions relevant in Alzheimer's disease pathology. *PLoS One* **2020**, *15*, No. e0225487.
(60) Hofmann, M. A.; Drury, S.; Hudson, B. I.; Gleason, M. R.; Qu, W.; Lu, Y.; Lalla, E.; Chitnis, S.; Monteiro, J.; Stickland, M. H.; Bucciarelli, L. G.; Moser, B.; Moxley, G.; Itescu, S.; Grant, P. J.; Gregersen, P. K.; Stern, D. M.; Schmidt, A. M. RAGE and arthritis: the G82S polymorphism amplifies the inflammatory response. *Gene Immun.* **2002**, *3*, 123−135.
(61) Park, S. J.; Kleffmann, T.; Hessian, P. A. The G82S polymorphism promotes glycosylation of the receptor for advanced glycation end products (RAGE) at asparagine 81: comparison of wild-type rage with the G82S polymorphic variant. *J. Biol. Chem.* **2011**, *286*, 21384−21392.
(62) Peng, W. H.; Lu, L.; Wang, L. J.; Yan, X. X.; Chen, Q. J.; Zhang, Q.; Zhang, R. Y.; Shen, W. F. RAGE gene polymorphisms are associated with circulating levels of endogenous secretory RAGE but not with coronary artery disease in Chinese patients with type 2 diabetes mellitus. *Arch. Med. Res.* **2009**, *40*, 393−398.
(63) Maruthur, N. M.; Li, M.; Halushka, M. K.; Astor, B. C.; Pankow, J. S.; Boerwinkle, E.; Coresh, J.; Selvin, E.; Kao, W. H. Genetics of Plasma Soluble Receptor for Advanced Glycation End-Products and Cardiovascular Outcomes in a Community-based Population: Results from the Atherosclerosis Risk in Communities Study. *PLoS One* **2015**, *10*, No. e0128452.
(64) Miller, S.; Henry, A. P.; Hodge, E.; Kheirallah, A. K.; Billington, C. K.; Rimington, T. L.; Bhaker, S. K.; Obeidat, M.; Melén, E.; Merid, S. K.; Swan, C.; Gowland, C.; Nelson, C. P.; Stewart, C. E.; Bolton, C. E.; Kilty, I.; Malarstig, A.; Parker, S. G.; Moffatt, M. F.; Wardlaw, A. J.; Hall, I. P.; Sayers, I. The Ser82 RAGE Variant Affects Lung Function and Serum RAGE in Smokers and sRAGE Production In Vitro. *PLoS One* **2016**, *11*, No. e0164041.
(65) Schmidt, J.; Berghaus, S.; Blessing, F.; Herbeck, H.; Blessing, J.; Schierack, P.; Rödiger, S.; Roggenbuck, D.; Wenzel, F. Genotyping of familial Mediterranean fever gene (MEFV)-Single nucleotide polymorphism-Comparison of Nanopore with conventional Sanger sequencing. *PLoS One* **2022**, *17*, No. e0265622.
(66) Matern, B. M.; Olieslagers, T. I.; Groeneweg, M.; Duygu, B.; Wieten, L.; Tilanus, M. G. J.; Voorter, C. E. M. Long-Read Nanopore Sequencing Validated for Human Leukocyte Antigen Class I Typing in Routine Diagnostics. *J. Mol. Diagn.* **2020**, *22*, 912−919.
(67) Crossley, B. M.; Rejmanek, D.; Baroch, J.; Stanton, J. B.; Young, K. T.; Killian, M. L.; Torchetti, M. K.; Hietala, S. K. Nanopore sequencing as a rapid tool for identification and pathotyping of avian influenza A viruses. *J. Vet. Diagn. Invest.* **2021**, *33*, 253−260.
(68) Watson, C. M.; Crinnion, L. A.; Lindsay, H.; Mitchell, R.; Camm, N.; Robinson, R.; Joyce, C.; Tanteles, G. A.; Halloran, D. J. O.; Pena, S. D. J.; Carr, I. M.; Bonthron, D. T. Assessing the utility of long-read nanopore sequencing for rapid and efficient characterization of mobile element insertions. *Lab. Invest.* **2021**, *101*, 442−449.
(69) Gaens, K. H.; Ferreira, I.; van der Kallen, C. J.; van Greevenbroek, M. M.; Blaak, E. E.; Feskens, E. J.; Dekker, J. M.; Nijpels, G.; Heine, R. J.; t Hart, L. M.; de Groot, P. G.; Stehouwer, C. D.; Schalkwijk, C. G. Association of polymorphism in the receptor for advanced glycation end products (RAGE) gene with circulating RAGE levels. *J. Clin. Endocrinol. Metab.* **2009**, *94*, 5174−5180.
(70) Lampropoulou, I. T.; Stangou, M.; Papagianni, A.; Didangelos, T.; Iliadis, F.; Efstratiadis, G. TNF-$\alpha$and Microalbuminuria in Patients with Type 2 Diabetes Mellitus. *J. Diabetes Res.* **2014**, *2014*, 394206.
(71) Navarro, J. F.; Mora-Fernández, C. The role of TNF-alpha in diabetic nephropathy: pathogenic and therapeutic implications. *Cytokine Growth Factor Rev.* **2006**, *17*, 441−450.
(72) Chen, Y. L.; Qiao, Y. C.; Xu, Y.; Ling, W.; Pan, Y. H.; Huang, Y. C.; Geng, L. J.; Zhao, H. L.; Zhang, X. X. Serum TNF-α concentrations in type 2 diabetes mellitus patients and diabetic nephropathy patients: A systematic review and meta-analysis. *Immunol. Lett.* **2017**, *186*, 52−58.
(73) Donate-Correa, J.; Martín-Núñez, E.; Muros-de-Fuentes, M.; Mora-Fernández, C.; Navarro-González, J. F. Inflammatory cytokines in diabetic nephropathy. *J. Diabetes Res.* **2015**, *2015*, 948417.
(74) Janssen, J. Hyperinsulinemia and Its Pivotal Role in Aging, Obesity, Type 2 Diabetes, Cardiovascular Disease and Cancer. *Int. J. Mol. Sci.* **2021**, *22*, 7797.
(75) Stanimirovic, J.; Radovanovic, J.; Banjac, K.; Obradovic, M.; Essack, M.; Zafirovic, S.; Gluvic, Z.; Gojobori, T.; Isenovic, E. R. Role of C-Reactive Protein in Diabetic Inflammation. *Mediat. Inflamm.* **2022**, *2022*, 3706508.
(76) Kanmani, S.; Kwon, M.; Shin, M. K.; Kim, M. K. Association of C-Reactive Protein with Risk of Developing Type 2 Diabetes Mellitus, and Role of Obesity and Hypertension: A Large Population-Based Korean Cohort Study. *Sci. Rep.* **2019**, *9*, 4573.
(77) Cheng, L.; Zhuang, H.; Yang, S.; Jiang, H.; Wang, S.; Zhang, J. Exposing the Causal Effect of C-Reactive Protein on the Risk of Type 2 Diabetes Mellitus: A Mendelian Randomization Study. *Front. Genet.* **2018**, *9*, 657.

https://doi.org/10.1021/acsomega.3c00297
ACS Omega XXXX, XXX, XXX−XXX